UNIVERSIDADE FEDERAL DO RIO GRANDE DO SUL
ESCOLA DE ENGENHARIA
PROGRAMA DE PÓS-GRADUAÇÃO EM ENGENHARIA ELÉTRICA

**LUCIANO GONÇALVES MOREIRA**

# EVENT-TRIGGERED CONTROL FOR RATIONAL AND LUR'E TYPE NONLINEAR SYSTEMS

Porto Alegre
2018

**LUCIANO GONÇALVES MOREIRA**

# EVENT-TRIGGERED CONTROL FOR RATIONAL AND LUR'E TYPE NONLINEAR SYSTEMS

Thesis presented to Programa de Pós-Graduação em Engenharia Elétrica of Universidade Federal do Rio Grande do Sul in partial fulfillment of the requirements for the degree of Doctor in Electrical Engineering.

Area: Control and Automation

ADVISOR: Prof. Dr. João Manoel Gomes da Silva Jr.

Porto Alegre
2018

**LUCIANO GONÇALVES MOREIRA**

# EVENT-TRIGGERED CONTROL FOR RATIONAL AND LUR'E TYPE NONLINEAR SYSTEMS

This thesis was considered adequate for the awarding of the degree of Doctor in Electrical Engineering and approved in its final form by the Advisor and the Examination Committee.

Advisor: _____
Prof. Dr. João Manoel Gomes da Silva Jr., PPGEE - UFRGS
Docteur de l'Université Paul Sabatier – Toulouse, France

Examination Committee:

Prof. Dr. Reinaldo Martinez Palhares, DELT - UFMG
Doutor pela Universidade Estadual de Campinas – Campinas, Brasil

Prof. Dr. Eugênio de Bona Castelan Neto, DAS - UFSC
Docteur de l'Université Paul Sabatier – Toulouse, France

Prof. Dr. Alexandre Sanfelici Bazanella, PPGEE - UFRGS
Doutor pela Universidade Federal de Santa Catarina – Florianópolis, Brasil

Prof. Dr. Jeferson Vieira Flores, PPGEE - UFRGS
Doutor pela Universidade Federal do Rio Grande do Sul – Porto Alegre, Brasil

Prof. Dr. Aurélio Tergonlina Salton, DELAE - UFRGS
PhD by The University of Newcastle Australia – Newcastle, Australia

Head of PPGEE: _____
Prof. Dr. João Manoel Gomes da Silva Jr.

Porto Alegre, December 2018.

# DEDICATION

Aos meus amores: Cláudia e João Paulo.

To the loves of my life: Cláudia and João Paulo.

# ACKNOWLEDGMENTS

*À minha família, pela paciência, compreensão pela ausência (mesmo nos momentos em que eu estava perto, mas indisponível, concentrado no trabalho), pelos cafés e lanches trazidos na minha mesa de trabalho, pelos beijos e abraços nos momentos delicados e pelo cinto apertado ao longo dos anos do doutorado.*

*Ao meu orientador, Prof. Dr. João Manoel Gomes da Silva Jr., pelo seu excelente trabalho, pela sua dedicação, conselhos, revisões cuidadosas e indicação de rumos para o trabalho.*

To my foreign advisor Dr. Sophie Tarbouriech for the invaluable help given, specially during the visiting period at LAAS-CNRS.

*Aos professores do programa, em especial ao Prof. Dr. Alexandre Sanfelice Bazanella, de quem fui aluno em tantas disciplinas.*

*Aos colegas de curso, em especial aos mais próximos: Charles Lorenzini, "chefe do laboratório"; Leonardo Groff e Alessandra Palmeira.*

Also to the good friends I made in France and, specially to Alexandre Seuret, for his invaluable insights and suggestions and to Matteo Cocetti, from whom I learned a lot and who made all moments happier with his sympathy.

*Ao povo brasileiro que, através de seus impostos e das agências de fomento, torna possível a existência deste tipo de trabalho, tanto pela concessão de bolsas de estudo quanto pela manutenção da estrutura física e humana das universidades públicas. Em particular, este trabalho recebeu o apoio de bolsas da CAPES de doutorado durante parte de sua execução e do Programa de Doutorado Sanduíche no Exterior.*

# ABSTRACT

In the present work, the design of event-triggered controllers for two classes of nonlinear systems is addressed: rational systems and Lur'e type systems. Lyapunov theory techniques are used in both cases to derive asymptotic stability conditions in the form of linear matrix inequalities that are then used in convex optimization problems as means of computing the control system parameters aiming at a reduction of the number of events generated.

In the context of rational systems, state-feedback control is considered and differential-algebraic representations are used as means to obtain tractable stability conditions. An event-triggering strategy which uses weighting matrices to strive for less events is proposed and then it is proven that this strategy does not lead to Zeno behavior.

In the case of Lur'e systems, observer-based state-feedback is addressed with event generators that have access only to the system output and observed state, but it imposes the need of a dwell-time, i.e. a time interval after each event where the trigger condition is not evaluated, to cope with Zeno behavior. Two distinct approaches, exact time-discretization and looped-functional techniques, are considered to ensure asymptotic stability in the presence of the dwell-time.

For both system classes, emulation design and co-design are addressed. In the emulation design context, the control law (and the observer gains, when appropriate) are given and the task is to compute the event generator parameters. In the co-design context, the event generator and the control law or the observer can be simultaneously designed.

Numerical examples are presented to illustrate the application of the proposed methods.

**Keywords: Network control, event-triggered control, nonlinear systems, Lur'e systems.**

# RESUMO

Neste trabalho é abordado o projeto de controladores baseados em eventos para duas classes de sistemas não lineares: sistemas racionais e sistemas tipo Lur'e. Técnicas da teoria de Lyapunov são usadas em ambos os casos para derivar condições de estabilidade assintótica na forma de inequações matriciais lineares. Tais condições são então utilizadas em problemas de otimização convexa como meio de calcular os parâmetros do sistema de controle, visando uma redução no número de eventos gerados.

No contexto de sistemas racionais, realimentação de estados é considerada e representações algébrico-diferenciais são usadas como meio de obter condições de estabilidade tratáveis computacionalmente. Uma estratégia de disparo de eventos que usa uma medida de erro ponderado através de matrizes definidas positivas é proposta e é demonstrado que tal estratégia não gera comportamento de Zenão.

No caso de sistemas tipo Lur'e, considera-se o caso de controladores com restrições de informações, a saber, com acesso apenas às saídas do sistema. Um observador de estados é então utilizado para recuperar a informação faltante. Neste contexto, é necessária a introdução de um tempo de espera (*dwell time*, em inglês) para garantir a inexistência de comportamento de Zenão. Todavia, a introdução do tempo de espera apresenta um desafio adicional na garantia de estabilidade que é tratado neste trabalho considerando duas técnicas possíveis: a discretização exata do sistema e o uso de *looped-functionals* (funcionais em laço, em uma tradução livre).

Para ambas classes de sistemas, são tratados os problemas de projeto por emulação e *co-design* (projeto simultâneo, em uma tradução livre). No projeto por emulação, a lei de controle (e os ganhos do observador, quando apropriado) são dados *a priori* e a tarefa é projetar os parâmetros do gerador de eventos. No caso do *co-design*, o gerador de eventos e a lei de controle ou o observador são projetados simultaneamente.

Exemplos numéricos são usados para ilustrar a aplicação dos métodos propostos.

**Palavras-chave: Controle em rede, controle baseado em eventos (*event-triggered control*), sistemas não lineares, sistemas tipo Lur'e.**

# CONTENTS

# LIST OF FIGURES

# LIST OF TABLES

# LIST OF ABBREVIATIONS

| | |
|---|---|
| DAR | Differential Algebraic Representation. |
| DC | Direct Current. |
| ISS | Input-to-State Stable. |
| LMI | Linear Matrix Inequality. |
| NCS | Network Control System. |
| RA | Region of Attraction. |
| RAS | Region of Asymptotic Stability. |
| ZOH | Zero-order hold. |

# LIST OF SYMBOLS

| | |
|---|---|
| $\mathbb{R}$ | The set of real numbers. |
| $\mathbb{R}^+$ | Real numbers greater than zero. |
| $\mathbb{N}$ | Natural numbers, including the zero. |
| $\|\| \cdot \|\|$ | Euclidean norm. |
| $I$ | Identity matrix. |
| $0$ | Null-matrix or the scalar zero. |
| $A', v'$ | Transpose of matrix $A$ or the vector $v$, respectively. |
| $\mathrm{diag}\, X, Y$ | Block-diagonal matrix made from blocks $X$ and $Y$. |
| $A_{(i)}, v_{(i)}$ | i-th row of matrix $A$ or vector $v$, respectively. |
| $*$ | Symmetric block within a matrix. |
| $\mathrm{He}\{A\}$ | Sum with transpose: $\mathrm{He}\{A\} = A + A'$. |
| $\mathrm{tr}(A)$ | Trace of matrix $A$. |
| $\mathbb{F}^n_{[0,T]}$ | Denotes, for a given positive scalar $T$, the set of continuous functions from the interval $[0, T]$ into $\mathbb{R}^n$. |
| $\mathrm{Ver}(\mathcal{B})$ | Denotes the vertices of a polytope $\mathcal{B}$. |

# 1 INTRODUCTION

The technical advances and the popularization of digital communication networks that took place in the last decades have introduced innovations in many fields of science and technology, as well as in our daily activities. As examples of this revolution, we can cite the appearance of smart sensors, which transmit data through digital networks (e.g. bluetooth, Wi-Fi, etc.) and the mobile phone communications that currently are carried almost entirely over digital communication networks.

These advances also spread to the automatic control field, leading to what is called Networked Control Systems (NCS). In such systems, part of the communication among their components (controller, plant, sensors, actuators) take place over a shared generic digital communication network. This paradigm allows the reduction of the cost of the system and also increases its flexibility, as pointed, for instance, in HESPANHA; NAGHSHTABRIZI; XU (2007); POSTOYAN et al. (2015); GHIGGI et al. (2015). In this context of shared network, bandwidth and energy consumption (in wireless systems) become important issues (DONKERS; HEEMELS, 2012; ABDELRAHIM et al., 2016). Bandwidth consumption can be reduced if one brings down the number of transmissions over the network. At the same time, since a significant part of the energy consumption in wireless systems is due to the data transmissions (TIBERI; LINDBERG; ISAKSSON, 2012; GOMES DA SILVA JR.; LAGES; SBARBARO, 2014), one can reduce the energy consumption in these systems by reducing the number of transmissions. Such considerations lead to the research of control techniques that need fewer control updates than the traditional periodic sampling mechanisms usually applied in the digital control field. Besides the advantages mentioned for NCS, the use of techniques that lead to fewer control updates are also suitable for systems where actuator fatigue is important.

With these objectives in mind, there exist in the literature some aperiodic sampling techniques where the transmission of the sensors data and the update of the control signal occur only at instants determined by variations in the state and/or outputs of the systems. In particular, there exist the event-triggered and the self-triggered control approaches. In the event-triggered control, an event generator continuously monitors the state and/or the outputs of the system and triggers the sampling, transmission and update of the control signal when a criterion based on the value of the state and/or outputs is verified (HESPANHA; NAGHSHTABRIZI; XU, 2007; HEEMELS; JOHANSSON; TABUADA, 2012). On the other hand, in the self-triggered control, each time an event occurs, the event generator calculates the next event instant, based on the information available about the current state and the system dynamics (HEEMELS; JOHANSSON; TABUADA, 2012).

Considering the number of publications, the literature has favored the event-triggered control approach so far. Possible reasons for this preference are the facts that event-

triggered systems can be computationally less demanding and handle non-modeled dynamics better than self-triggered ones. Event-triggered control systems can have linear complexity with respect to the order of the closed-loop system, i.e. the sum of the orders of the plant and of the controller, as in the schema proposed in (MOREIRA et al., 2016) and in (MOREIRA; GROFF; GOMES DA SILVA JR., 2016a), while self-triggered systems have at least quadratic complexity, as in (HEEMELS; JOHANSSON; TABUADA, 2012). Furthermore, since the self-triggered systems operate in completely open-loop between events, without even monitoring the state or outputs of the system, it is harder to accommodate for disturbances. For these reasons, the present work addresses event-triggered control.

Most of the literature on event-triggered control addresses linear systems and only during the last few years there has been an increase in the number of works addressing nonlinear plants. Besides that, the majority of works both for linear and nonlinear cases address the stability analysis, but do not present constructive methods that allow to compute the parameters of the control law and/or the event generator parameters, i.e. to treat the synthesis problem. The exceptions, treating the synthesis, are (GOMES DA SILVA JR.; LAGES; SBARBARO, 2014; SBARBARO; TARBOURIECH; GOMES DA SILVA JR., 2014; TARBOURIECH et al., 2016; GROFF et al., 2016; MOREIRA et al., 2016) considering the linear case and (TARBOURIECH et al., 2017; ARANDA-ESCOLÁSTICO et al., 2017; ZHANG; HAN, 2017; MOREIRA et al., 2017a,b) addressing some classes of nonlinear systems.

Therefore, the research of constructive methodologies for event-triggered control considering continuous-time nonlinear systems is still an open field. The present work addresses precisely that, presenting a design methodology for some classes of nonlinear systems.

The first class of nonlinear systems that is addressed is the rational one. Many processes of interest can be modeled as rational systems. For instance, brushless DC motors, when modeled by the Lorenz equation (HEMATI, 1994); biological systems like gen expression, metabolic networks and enzymatic reactions (WU; MU, 2009; NĚMCOVÁ, 2010); bioreactors (CAMPESTRINI et al., 2014; ANTONELLI et al., 2003); systems in Economy, Physics and Engineering fields (NĚMCOVÁ, 2010); DC-DC converters (SIRA-RAMÍREZ; SILVA-ORTIGOZA, 2006; JAVAID; DUJIĆ, 2015). Moreover, by noting that polynomial systems are a subclass of rational ones, truncated Taylor series expansion can be applied to derive accurate approximations of general smooth nonlinear systems.

The second class of nonlinear systems addressed are the Lur'e systems, i.e. systems composed by the feedback connection of a linear system and a sector-bounded nonlinearity. Two cases are considered: nonlinearities that depend on the system input and nonlinearities that depend on the system state. In the first case one can include linear plants subject to actuator saturation (TARBOURIECH et al., 2011; ZACCARIAN; TEEL, 2011; TURNER; HERRMANN, 2014); quantization of the control input (DE SOUZA; COUTINHO; FU, 2010; FU; XIE, 2005) and backlash, for instance. In the case of sector-bound nonlinearities that depend on the state, many nonlinearities can be addressed, such as piecewise linear, odd-degree polynomial and trigonometric ones.

Hence, the following general goal is defined for the present work:

- Propose an event-triggered control design methodology for the following classes of nonlinear systems: rational and Lur'e type systems.

And, from this general goal, the following specific goals are considered:

- Propose a systematic methodology allowing the synthesis of the parameters of the event generator considering a given control law that stabilizes the system when implemented in continuous-time, i.e. by direct connection between the controller and the plant. This is referred as emulation design.
- When possible, address also the co-design of the event-trigger and other parameters of the control system. For instance, design simultaneously the event generator and the control law and/or observer parameters.
- In the cases where only local (regional) stabilization is possible, explicitly characterize a set of initial conditions where the asymptotic stability is guaranteed.
- Compute the control system parameters through convex optimization problems based on linear matrix inequalities.

This thesis is structured as follows:

In Chapter 2, the paradigm of event-triggered control is presented, detailing its characteristics like typical topologies, Zeno behavior and triggering conditions (i.e. strategies to determine the trigger instants). This chapter also completes the bibliographical review started at the Introduction.

Chapters 3 to 5 address rational systems. In Chapter 3, the specific problem for rational systems is formulated, stating the characteristics of the system being considered, the mathematical tools used in the derivation of stability conditions and the trigger condition proposed. Besides that, in this chapter we present a proof that the proposed trigger condition does not lead to the occurrence of Zeno behavior. The chapters that follow, Chapter 4 and Chapter 5, address the design in the emulation and co-design contexts, respectively, including numerical examples to illustrate each of the methods.

Chapters 6 and 7 address Lur'e type systems, considering controllers and event-generators that have access only to the plant outputs and the use of nonlinear observers to recover the missing information. Chapter 6 addresses Lur'e systems with sector-bound nonlinearities that depend only on the plant input, while Chapter 7 considers Lur'e systems where the nonlinearity is also sector-bounded but depends on the plant state.

The thesis ends with a final remarks chapter containing the conclusions and the perspectives of future work.

# 2 EVENT-TRIGGERED CONTROL

The event-triggered control paradigm consists in transmitting data among the elements of the system only when a trigger condition is verified (HESPANHA; NAGHSHTABRIZI; XU, 2007; HEEMELS; JOHANSSON; TABUADA, 2012). As stated in Chapter 1, the main applications of this paradigm are in Networked Control Systems, where it is interesting to reduce the data exchange among the elements that are connected via generic shared communication networks (HESPANHA; NAGHSHTABRIZI; XU, 2007) and in systems subject to actuator fatigue, where it is interesting to avoid frequent changes in the control action.

## 2.1 Topologies

A typical topology for event-triggered control systems, presented e.g. in (HEEMELS; JOHANSSON; TABUADA, 2012; KIENER; LEHMANN; JOHANSSON, 2014; LEHMANN; LUNZE, 2011; LEHMANN; KIENER; JOHANSSON, 2012; SBARBARO; TARBOURIECH; GOMES DA SILVA JR., 2014; TARBOURIECH et al., 2016), is depicted in Figure 2.1. A static or dynamic controller receives information from the plant output (or, possibly its complete state) at instants defined by the event generator. Plant and controller are in different nodes of a generic data communication network, represented by the double lines in the figure. The event generator monitors the state of the plant continuously, i.e. in continuous-time, and based on this information, determines when a new sample needs to be sent to the controller, causing an update of the control signal. Between events, a zero-order hold keeps the signal applied to the controller input constant.

In this case, the closed-loop system can be represented by:

$$\begin{cases} \dot{x}_p(t) = f_p(x_p(t),u(t)) \\ y(t) = g_p(x_p(t)) \\ \dot{x}_c(t) = f_c(x_c(t),y(t_k)) \\ u(t) = g_c(x_c(t)) \end{cases} \tag{2.1}$$

where $x_p \in \mathbb{R}^n$ is the plant state vector, $x_c \in \mathbb{R}^{n_c}$ is the controller state vector, $u \in \mathbb{R}^m$ is the plant's inputs vector, $y \in \mathbb{R}^p$ is the outputs vector, $t_k \in \mathbb{R}, k \in \mathbb{N}$ are the event instants, $f_p$, $g_p$, $f_c$ and $g_c$ are generic matrix functions of appropriate dimensions.

A slight variation of this topology, shown in Figure 2.2, includes the transmission of the control signal via a generic network. In this case, the update of the control signal takes place at the same time as the controller input and the control signal is kept constant between two events by a zero-order hold located at the plant input. This topology

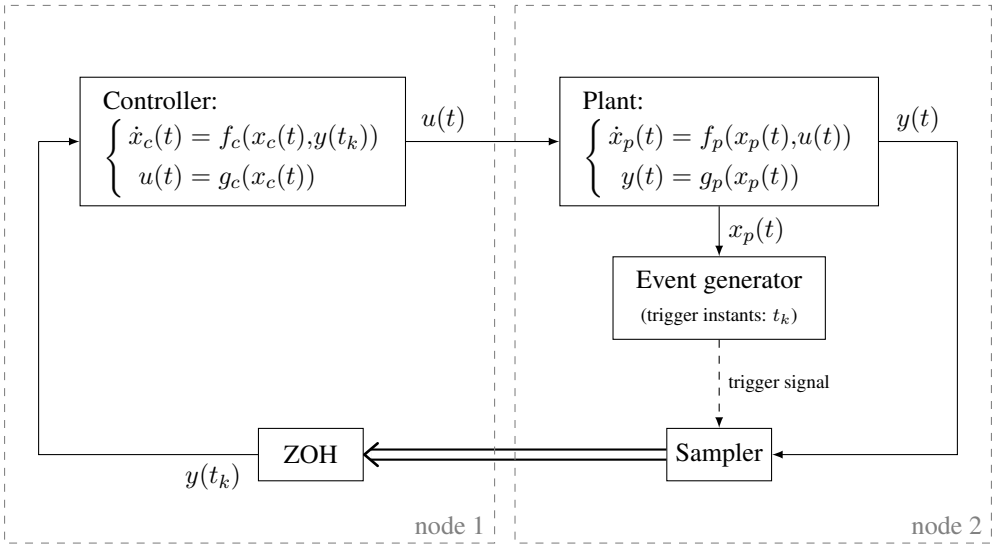


Figure 2.1: Event-triggered control topology with dedicated link for the control signal.

is considered e.g. em (ABDELRAHIM et al., 2014a, 2016; AL-AREQI; GÖRGES; LIU, 2015; DONKERS; HEEMELS, 2012; HEEMELS; JOHANSSON; TABUADA, 2012; GOMES DA SILVA JR.; LAGES; SBARBARO, 2014; REIMANN et al., 2015; TALLAPRAGADA; CHOPRA, 2012).

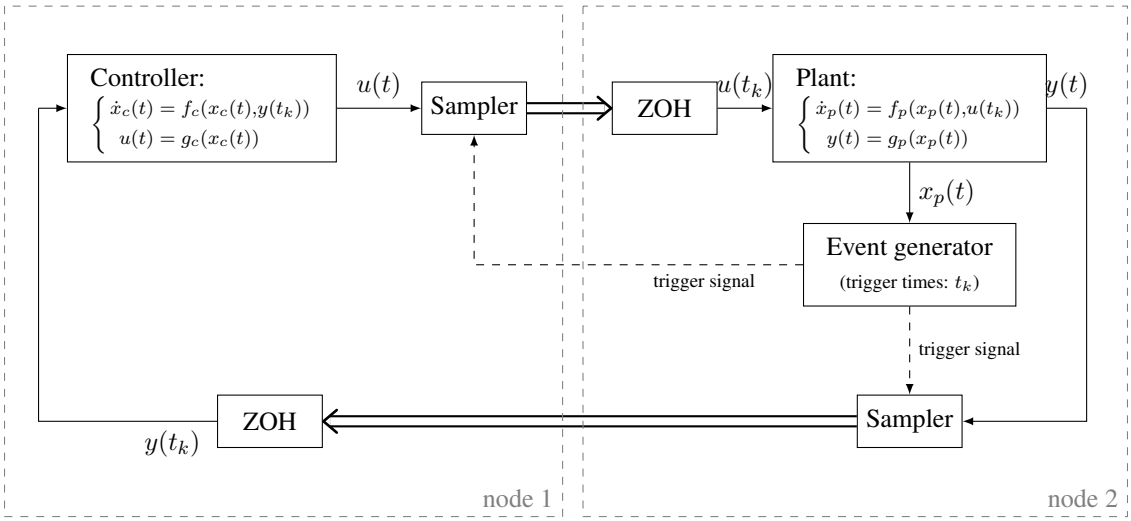


Figure 2.2: Event-triggered control topology without dedicated links between nodes.

In this case, the closed-loop system can be represented by:

$$\begin{cases} \dot{x}_p(t) = f_p(x_p(t),u(t_k)) \\ y(t) = g_p(x_p(t)) \\ \dot{x}_c(t) = f_c(x_c(t),y(t_k)) \\ u(t) = g_c(x_c(t)) \end{cases} \tag{2.2}$$

One should note that in the case of a static controller, the closed-loop representations of both topologies are equivalent.

Other variations in the topologies include:

- The event generator monitoring only the plant outputs or the plant inputs and outputs.
- The plant outputs being continuously transmitted to the controller, but the control action being transmitted (or updated) only at the event instants.

## 2.2 Zeno behavior

One of the challenges in designing event-triggered control systems is to ensure that the event generator does not lead to Zeno behavior. Zeno behavior (HEEMELS; JOHANSSON; TABUADA, 2012) is the occurrence of infinitely many events at the same instant, i.e. without a time interval between them, or the occurrence of inter-event times that tend to zero as the time goes to infinity or, in even more pathological cases, as the time goes to some finite instant (which characterizes the existence of a finite accumulation point in the event instants sequence). Therefore, we can formally define the occurrence of Zeno behavior as follows.

**Definition 1.** *A sequence of event instants $\{t_k\}_{k\in\mathbb{N}}$ presents Zeno behavior if at least one of the following conditions is verified:*

*(i)* $t_{k+1} - t_k = 0 \quad$ *for some* $k$.

*(ii)* $\lim_{k\to\infty} t_{k+1} - t_k = 0$.

Note that the existence of a finite accumulation point is characterized by condition *(ii)* in Definition 1.

The occurrence of Zeno behavior renders the control system useless since the transmissions of the signals would eventually use all the network bandwidth. Two methods to cope with this problem are found in the literature, both based on the fact that the existence of a positive scalar $\epsilon$ such that $t_{k+1} - t_k \geq \epsilon$, $\forall k \in \mathbb{N}$ is a sufficient condition for ensuring that Zeno behavior does not happen:

1. Proving that the event-trigger mechanism ensures the existence of $\epsilon > 0$ such that $t_{k+1} - t_k \geq \epsilon$, $\forall k \in \mathbb{N}$. In this case, it is said that the event-trigger mechanism has a guaranteed minimum inter-event interval $\epsilon$. This is done for example in (TABUADA, 2007) and (MOREIRA et al., 2017a).

2. The use of a dwell-time to impose a minimum inter-event interval (MAZO; ANTA; TABUADA, 2010). The dwell-time is a time interval defined at design time such that, when an event occurs, the trigger condition is not re-evaluated until the dwell-time has elapsed (see, for instance MAZO; ANTA; TABUADA (2010) for details). Hence, an explicit minimum inter-event time is forced and Zeno behavior is avoided. The main challenge in this case is to ensure the asymptotic stability in the presence of the dwell-time. This technique is used for instance in (ABDELRAHIM et al., 2016) and (TARBOURIECH et al., 2017).

## 2.3 Stability

Besides ensuring that there is no Zeno behavior, one needs to design the trigger conditions such that the closed-loop equilibrium point of interest is stable under the aperiodic

control updating introduced by the event-triggered control strategy. In this thesis, we assume, without loss of generality, that the origin is the equilibrium of interest. The aperiodic update of the control signal renders impossible to use the traditional discretization and $Z$ transform techniques in the analysis (GHIGGI et al., 2015). For this reason, more elaborated techniques based on the Lyapunov theory (KHALIL, 1996), hybrid systems framework (GOEBEL; SANFELICE; TEEL, 2012) and, more recently, time-delay systems theory (FRIDMAN, 2014) have been employed.

Lyapunov theory techniques consider a stability criterion like the one presented in Appendix A, Theorem A.1. One chooses a Lyapunov candidate function, i.e. a positive-definite function $V(x)$ (which means one that satisfies (A.1) of Theorem A.1) and design an event generator that ensures the negativity of the time derivative of the Lyapunov candidate (which means, ensuring satisfaction of (A.2) of Theorem A.1). Among the works that use this technique one can cite (TABUADA, 2007; HEEMELS; DONKERS; TEEL, 2011; HEEMELS; JOHANSSON; TABUADA, 2012; DONKERS; HEEMELS, 2012; TALLAPRAGADA; CHOPRA, 2014; LIU; JIANG, 2015; GOMES DA SILVA JR.; LAGES; SBARBARO, 2014; SBARBARO; TARBOURIECH; GOMES DA SILVA JR., 2014; TARBOURIECH et al., 2016; GROFF et al., 2016; MOREIRA et al., 2016, 2017a,b). In some of them, *a priori* knowledge of a Lyapunov function for the system is required, constituting a serious drawback when the synthesis problem is considered.

Hybrid systems, as defined in (GOEBEL; SANFELICE; TEEL, 2012), are those that feature both continuous and instantaneous changes in their state. Therefore, they show characteristics of both continuous- and discrete-time dynamical systems. In (GOEBEL; SANFELICE; TEEL, 2012), a formal framework for the analysis of such systems is defined, including specific stability conditions for them. As examples of papers considering event-triggered control and employing these techniques one can cite (ABDELRAHIM et al., 2015, 2016; POSTOYAN et al., 2015). It should be noticed that the stability conditions for hybrid systems are based on Lyapunov theory and that the results shown in the mentioned papers feature event generators that do not effectively postpone the events with respect to the minimum inter-event time explicitly imposed in the triggering strategy, i.e., many events are separated only by the minimum inter-event time. Therefore, although the hybrid systems formalism can be seen as a natural framework to model event-triggered control systems, its efficacy has not been demonstrated until now.

The time-delay approach models the sampled control as a time-delayed signal with a varying delay that increases linearly over the sampling interval with a unitary time-derivative and is reset to zero at the next sampling instant. Then Lyapunov-Krasowskii functionals (FRIDMAN, 2014) or looped-functionals (BRIAT; SEURET, 2012; SEURET, 2012) are used to derive stability conditions. Since this approach, when directly applied, is suitable for addressing discrete-time systems, it can be directly applied to obtain stability conditions solely in the context of periodic event-triggered control (PETC), i.e. event-triggered control systems where the triggering condition is evaluated only in a periodical fashion. It is considered for instance in (ARANDA-ESCOLÁSTICO et al., 2017) to derive sum-of-squares (SOS) conditions that guarantee the global asymptotic stability of a class of nonlinear PETC systems. Nevertheless, in the context of continuous-time event-triggered control, time-delay techniques can be of great value to address the stability in the presence of dwell time in the trigger conditions, as will be seen in Part II of this thesis. In such cases, the time-delay approach can be combined with the Lyapunov theory techniques.

## 2.4 Triggering strategies

In this section, the different triggering strategies found in the literature are presented.

### 2.4.1 Absolute error threshold

The simplest idea of triggering strategy is to generate an event when the norm of the difference between the current and the last sampled state values reaches a threshold. This strategy can be summarized as follows:

**Algorithm 1** Absolute error threshold trigger

**if** $||x(t) - x(t_k)|| \geq \epsilon_{abs}$ **then**
  Generate an event;
  $t_k = t$;
**end if**

The term $\epsilon_{abs} \in \mathbb{R}^+$ is the chosen threshold and it is the only design parameter available in this case.

To simplify the analysis, it is very common in the event-triggered control field to define the sampling error signal $\delta(t)$ as follows:

$$\delta(t) \triangleq x(t_k) - x(t) \tag{2.3}$$

Considering this definition, the Algorithm 1 can be rewritten as:

**Algorithm 2** Absolute error threshold trigger – using $\delta(t)$

**if** $||\delta(t)|| \geq \epsilon_{abs}$ **then**
  Generate an event;
  $t_k = t$;
**end if**

An extension to the absolute error threshold strategy consists in applying different weights to the error in each state variable (and their cross-products), leading to:

**Algorithm 3** Weighted absolute error threshold trigger

**if** $\delta'(t)Q_\delta\delta(t) \geq 1$ **then**
  Generate an event;
  $t_k = t$;
**end if**
$Q_\delta \in \mathbb{R}^{n\times n}$ is a symmetric positive-definite matrix.

In this case, $Q_\delta$ is the design parameter. Since it is a matrix, this strategy has more degrees of freedom than the one defined by Algorithm 2.

These strategies are used, for instance in (DURAND; MARCHAND, 2009a,b; TIBERI; ARAUJO; JOHANSSON, 2012; LEHMANN; KIENER; JOHANSSON, 2012; KIENER; LEHMANN; JOHANSSON, 2014). Since there is no normalization of the error norm with respect to the state norm, as the state approaches the origin, the error norm becomes small and the event generator stops triggering. This means that, after this point, the system operates in open-loop. If it is open-loop stable, it will converge to the origin at

the open-loop convergence rate. However, if it is open-loop unstable, operating in open-loop will make the norm of the state increase again until the error threshold is reached and a new event is generated. This process will repeat indefinitely leading to a limit cycle or to chaotic behavior. Thus, these strategies do not allow asymptotic stability with open-loop unstable systems. Moreover, for open-loop stable systems, the trajectories can converge to a point different of the origin, although close to it.

Modifications to avoid these problems are presented, for instance, in (TIBERI; ARAUJO; JOHANSSON, 2012), which includes a filter before the event generator to avoid the open-loop operation. Unfortunately, the proposed modification is only suitable for first-order open-loop stable linear systems. Hence, it regards only a small class of systems.

### 2.4.2 Relative error threshold

One alternative to achieve asymptotic stability of the origin is to normalize the sampling error norm to the current state norm, leading to the relative error threshold strategy, defined as follows:

**Algorithm 4** Relative error threshold trigger

**if** $\frac{||\delta(t)||}{||x(t)||} \geq \sigma_0$ **then**
  Generate an event;
  $t_k = t$;
**end if**

This strategy has been proposed in (TABUADA, 2007), which demonstrates that it ensures asymptotic stability and absence of Zeno behavior for a broad class of systems. The term $\sigma_0 \in \mathbb{R}^+$ is the design parameter and its value can be chosen in an interval that depends on the dynamics of the system. The greater the value of $\sigma_0$, the more the error can grow before a new event occurs. Hence, one expects less events for larger values of $\sigma_0$. One should also note that the trigger condition can be rewritten as $||\delta(t)|| \geq \sigma_0||x(t)||$ or as $||\delta(t)|| - \sigma_0||x(t)|| \geq 0$.

### 2.4.3 Weighted relative error threshold

The trigger condition described by Algorithm 4 can be further extended by considering weights for the different variables, leading to the following strategy:

**Algorithm 5** Weighted relative error threshold trigger

**if** $\delta'(t)Q_\delta\delta(t) - x'(t)Q_x x(t) > 0$ **then**
  Generate an event;
  $t_k = t$;
**end if**

In this case, matrices $Q_\delta$ and $Q_x$ are the design parameters. They are symmetric positive-definite $n \times n$ matrices and act as weights in the relative error measurement. The relation between these matrices has a role similar to that of $\sigma_0$ in Algorithm 4, in the sense that the "larger" $Q_x$ and the "smaller" $Q_\delta$, the more the current state can deviate from the last sampled one before a new event is generated. To illustrate this fact, note that letting $Q_x = \sigma I$ and $Q_\delta = \mu I$, one retrieves the trigger condition from Algorithm 4

with $\sigma_0 = \sigma/\mu$. That is, the strategy described by Algorithm 5 is indeed a generalization of Algorithm 4. Therefore, one can expect that it allows to achieve less events than with Algorithm 4.

This strategy has been introduced as part of the author's research and it is used for instance in (MOREIRA et al., 2016, 2017a; MOREIRA; GROFF; GOMES DA SILVA JR., 2016a; MOREIRA et al., 2017b).

### 2.4.4 Extensions to the trigger criteria

Many variations and extensions of the trigger criteria presented in the previous sections can be considered, as for instance: the inclusion of filters before or after the measurements (TIBERI; LINDBERG; ISAKSSON, 2012; GIRARD, 2015); the use of only part of the system state and/or the use of the control input signals; the use of only the output signals (ABDELRAHIM et al., 2016; MOREIRA et al., 2017b; TARBOURIECH et al., 2017); the inclusion of artificial variables (POSTOYAN et al., 2015) or combinations of these ideas. These variations generally aim at further reducing the number of events or to broaden the applicability of the techniques (in the case of only the output signals, for instance).

## 2.5 Emulation design and co-design

With respect to the design tasks, there are two approaches in the literature: emulation design and co-design.

In the emulation design context, one starts with a stabilizing controller previously designed considering a continuous-time implementation, i.e., without sampling or event-trigger mechanisms. Then the design task is to synthesize only the event-trigger condition so that the event-triggered implementation of the closed-loop is stable. Among works addressing this approach one can cite (TABUADA, 2007; DONKERS; HEEMELS, 2012; POSTOYAN et al., 2013; BESCHI et al., 2014; ARANDA-ESCOLASTICO; GUINALDO; DORMIDO, 2015; ABDELRAHIM et al., 2016; POSTOYAN et al., 2015; SEURET et al., 2013; MOREIRA et al., 2016).

In the co-design context, the trigger function and the control law parameters are designed simultaneously. Doing so, one expects to achieve a better result in terms of the number of events generated, since those parameters can all be included as variables in the same optimization problem, allowing more degrees of freedom and leading to the choice of the values of all of them that optimize the objective function. There is also the simplicity advantage: the designer needs to execute less steps and does not need to use different mathematical tools to compute each part of the system. Among the papers addressing the co-design of control law and trigger condition, one can cite (LI; XU, 2011; ABDELRAHIM et al., 2014a; WU; REIMANN; LIU, 2014; AL-AREQI; GÖRGES; LIU, 2015). Since just a few papers available in the event-trigger control literature consider the use of observers [1], the term co-design is usually employed to the method of designing the trigger condition and the control law simultaneously. But when observers are considered, co-design can mean that the trigger condition and any other of the parameters of the system, like the control law and/or the observer gains, are designed concomitantly.

[1] For instance, (SBARBARO; TARBOURIECH; GOMES DA SILVA JR., 2014; SELIVANOV; FRIDMAN, 2016; GROFF et al., 2016; TARBOURIECH et al., 2017) use observers, but all of them address only emulation design.

## 2.6 Linear plants

The literature on event-triggered control addressing linear plants is vast. One can cite the following papers considering static state-feedback control laws: (HEEMELS; JOHANSSON; TABUADA, 2012), which presents a comprehensive research of event-triggered control techniques for this class of systems. (ARANDA-ESCOLASTICO; GUINALDO; DORMIDO, 2015), which considers a relative error threshold trigger criterion and an event generator that monitors the system in a periodic fashion instead of continuously, resulting in what is know as periodic event-triggered control. (SBARBARO; TARBOURIECH; GOMES DA SILVA JR., 2014) and (GROFF et al., 2016) address the use of state observers, the last one considering discrete-time systems, i.e. a periodic implementation of event-triggered control.

Output-feedback is addressed, for instance in (DONKERS; HEEMELS, 2012) considering decentralized event generators based on a relative error threshold criterion. In particular, stability and $\mathcal{L}_\infty$ performance analysis are provided for a system composed by a set of nodes. Each node has its own set of state variables and its own event generator, responsible for determining, based on its knowledge of local variables, when its data should be broadcast to the other nodes.

Proportional-Integral (PI) event-triggered controllers are considered in (TIBERI; ARAUJO; JOHANSSON, 2012) and in (BESCHI et al., 2014), for first order linear plants and in (GOMES DA SILVA JR.; LAGES; SBARBARO, 2014) for linear plants of higher order. In (DURAND; MARCHAND, 2009a,b), an absolute error trigger criterion is considered and simulations are presented to illustrate the applicability of their method. However, it should be noticed that these last two references do not show any proof of stability of the designed closed-loop system.

## 2.7 Nonlinear plants

In the context of nonlinear plants, (TABUADA, 2007) presents stability conditions for an event-triggering strategy based on Lyapunov functions and a generic static state-feedback control law (which can be linear or nonlinear as long as it is Lipschitz in compacts). It assumes knowledge of a Lyapunov function certificating input-to-state stability (ISS) [2] of the continuous-time closed-loop implementation with respect to the sampling error. Therefore, the results are not constructive and cannot be applied to systematically design the parameters of the event-trigger criterion. Nevertheless, this reference provides important insights in the analysis context.

Output feedback and event generators that access only the outputs of the system are addressed in (ABDELRAHIM et al., 2014b, 2016, 2015), which use the hybrid system formalism from (GOEBEL; SANFELICE; TEEL, 2012) and dwell-time techniques. It is assumed in these papers that the closed-loop systems at hand are $\mathcal{L}_2$-gain stable with respect to the sampling error and that the dynamics of this error grows exponentially. Unfortunately, these assumptions are not applicable to all classes of nonlinear systems. Moreover, the event generators presented in these references do not effectively postpone the events with respect to the minimum inter-event time explicitly imposed in the triggering strategy by the dwell time, i.e., many events are separated only by the minimum inter-event time, which translates into a large number of events.

[2] Details on ISS Lyapunov functions can be found in the original paper (TABUADA, 2007) and in (KHALIL, 1996).

In (BORGERS; HEEMELS, 2014), a study of the properties of the minimum inter-event time is presented considering systems with absolute and relative error threshold triggering strategies. It also takes into account external disturbances and measurement errors. No constructive conditions allowing the synthesis are presented.

Linear plants subject to input saturation are addressed e.g. in (WU; REIMANN; LIU, 2014) which considers an absolute error threshold trigger condition. In this work, the plant is discretized and LMI stability conditions are derived. Authors aim at maximizing the region of attraction of the closed-loop system instead of minimizing the number of events. Since it considers exact discretization of the system, the method is suitable only to periodic event-triggered control implementations. In (MOREIRA; GROFF; GOMES DA SILVA JR., 2016a), convex optimization problems are proposed as means to design the event-triggered control system in both the emulation and the co-design contexts considering linear plants subject to input saturation and a weighted relative error threshold trigger condition.

PI controllers for linear plants subject to saturation of the control input are addressed in (LEHMANN; JOHANSSON, 2012) and (LEHMANN; KIENER; JOHANSSON, 2012), which consider the use of anti-windup techniques to mitigate the effects of saturation; in (MOREIRA et al., 2016), which uses Lyapunov theory techniques and proposes convex optimization problems as means to compute the event-trigger parameters and in (MOREIRA et al., 2017b), which includes triggering strategies with limited information, i.e. accessing only the system outputs.

Also on nonlinear systems, (POSTOYAN et al., 2015) proposes the hybrid systems formalism from (GOEBEL; SANFELICE; TEEL, 2012) as a general tool for the stability analysis of event-triggered control systems. More recently, (TARBOURIECH et al., 2017) addresses the emulation design for plants subject to sector-bounded input nonlinearities considering triggering strategies with limited information and a state observer. In (ARANDA-ESCOLÁSTICO et al., 2017), stability conditions for discrete-time polynomial plants are derived using a time-delay approach. The method is suitable only for discrete-time systems, i.e. periodic event-trigger implementations.

## 2.8 Conclusion

In this chapter a bibliographical review on event-triggered control was presented. It summarized the characteristics of this control paradigm and the main results from the literature. The works mentioned, with the exception of (GOMES DA SILVA JR.; LAGES; SBARBARO, 2014), (SBARBARO; TARBOURIECH; GOMES DA SILVA JR., 2014), (GROFF et al., 2016) (these considering linear systems) and (MOREIRA et al., 2016), (MOREIRA; GROFF; GOMES DA SILVA JR., 2016a), (MOREIRA et al., 2017b), (TARBOURIECH et al., 2017) and (ARANDA-ESCOLÁSTICO et al., 2017) (these considering nonlinear systems) do not present constructive methods that allow the synthesis of the event-triggered controller neither in an emulation nor in a co-design context. It can also be observed that the literature addressing the co-design is scarce, specially for nonlinear systems.

In the next chapters we will address part of these gaps considering rational and Lur'e type systems.

# Part I

# Rational systems

# 3 PROBLEM FORMULATION

In this chapter, we state the problem of event-triggered control for rational systems considered in this thesis. We start presenting some preliminary concepts. Then we introduce the system, the topology and the type of event generator considered. In the sequence, it follows a demonstration that Zeno behavior does not occur with this event-trigger schema. Then the problem to be addressed is formally presented.

## 3.1 Preliminaries

Here we present some basic concepts on rational systems, differential-algebraic representations and annihilators that will be used in the sequel. Besides those, some other usual concepts from dynamical systems, like region of attraction (RA) and region of asymptotic stability (RAS) will be employed. These are recalled in Appendix A.

### 3.1.1 Rational systems

Rational systems are those that can be generically represented by the following equation:

$$\dot{x}(t) = f(x(t)) \tag{3.1}$$

where $x(t) \in \mathbb{R}^n$ is the system state and $f : \mathcal{D} \subset \mathbb{R}^n \to \mathbb{R}^n$ is a rational function of the state satisfying the usual conditions of existence and uniqueness of solutions in a region of interest $x \in \mathcal{B}_x \subset \mathcal{D}$ of the state space. The set $\mathcal{D}$ is the domain of $f$.

As pointed out in the Introduction, the class of rational systems encompasses the polynomial systems and therefore, methods suitable for rational systems can also be used for general nonlinear systems by considering truncated high-order Taylor series approximations, which are polynomial.

### 3.1.2 Differential-algebraic representations

To obtain tractable stability conditions in the form of LMIs, that can be conveniently cast into convex optimization problems as means to compute the event-triggered control system parameters, thus providing a systematic design method, we will use differential-algebraic representations (DAR) introduced in (TROFINO, 2000). Alternative representations for rational systems that could be used include linear fractional representations (LFR), as can be seen e.g. in (GHAOUI; SCORLETTI, 1996), quasi-linear parameter-varying (quasi-LPV) (PALMEIRA; GOMES DA SILVA JR.; FLORES, 2018) and Takagi-Sugeno (T-S) fuzzy systems (GAO; CHEN, 2007). The main advantage of the DAR is that it tends to be less conservative than the alternatives mentioned in this paragraph, since it takes into account the coupling between the state and the auxiliary variables used to model

nonlinear terms (COUTINHO; GOMES DA SILVA JR., 2010; GOMES DA SILVA JR. et al., 2014).

In particular, for rational systems it is always possible to obtain a DAR in the form (COUTINHO et al., 2004; TROFINO, 2000):

$$\begin{cases} \dot{x} = A_1(x)x + A_2(x)\xi(x) \\ 0 = \Omega_1(x)x + \Omega_2(x)\xi(x) \end{cases} \tag{3.2}$$

where $\xi(x) \in \mathbb{R}^q$ is an auxiliary vector containing the polynomial and rational terms of $f(x)$; $A_1(x) \in \mathbb{R}^{n\times n}$, $A_2(x) \in \mathbb{R}^{n\times q}$, $\Omega_1(x) \in \mathbb{R}^{q\times n}$, $\Omega_2(x) \in \mathbb{R}^{q\times q}$ are matrix functions affine with respect to $x$. It is assumed that the original equation $\dot{x}(t) = f(x(t))$ can be recovered by the eliminating $\xi(x)$ which implies that $\Omega_2(x)$ is supposed to be full column rank for all $x$ of interest, i.e. $\forall x \in \mathcal{B}_x$. Notice that this representation is valid only in the region of interest $\mathcal{B}_x$. The time dependency of $x$ was omitted to simplify notation.

As an example of DAR, consider the following scalar system:

$$\dot{x} = x + \frac{-x + 2x^3}{1 + x^2} \tag{3.3}$$

A possible DAR for (3.3) is given by (3.2) with:

$$\xi = \frac{1}{1+x^2}\begin{bmatrix} x \\ x^2 \end{bmatrix}$$

$$A_1 = 1,\ A_2 = \begin{bmatrix} -1 & 2x \end{bmatrix},\ \Omega_1 = \begin{bmatrix} 1 \\ 0 \end{bmatrix} \text{ and } \Omega_2 = \begin{bmatrix} -1 & -x \\ x & -1 \end{bmatrix}$$

As it will be clear in chapters 4 and 5, the DAR will allow the formulation of stability conditions in an LMI framework and therefore the use of convex optimization to design the trigger function parameters.

The choice of $\xi(x)$, $A_1(x), A_2(x), \Omega_1(x), \Omega_2(x)$ is not unique and different choices can lead to different results (COUTINHO et al., 2004; TROFINO, 2000). In the scope of this thesis, different decompositions may lead to more or less events being generated. It is possible to reduce the conservatism and the impact of different choices of DAR using the concept of linear and affine annihilators (COUTINHO et al., 2004).

### 3.1.3 Annihilators

A matrix function $\mathscr{N}(x)$ is a linear (affine) annihilator if it is linear (affine) with respect to $x$ and $\mathscr{N}(x)\,x = 0$ for all $x$ of interest (TROFINO, 2000; COUTINHO et al., 2004). In this thesis we will use the following annihilator (presented, e.g. in (TROFINO, 2000)) as a base for extended ones which will be introduced later:

$$\mathscr{N}_0(x) = \begin{bmatrix} x_{(2)} & -x_{(1)} & 0 & \cdots & 0 & 0 \\ 0 & x_{(3)} & -x_{(2)} & \cdots & 0 & 0 \\ \vdots & \vdots & \vdots & \ddots & \vdots & \vdots \\ 0 & \cdots & 0 & \cdots & x_{(n)} & -x_{(n-1)} \end{bmatrix} \tag{3.4}$$

Notice that, by construction, $\mathscr{N}_0(x)x = 0$. These annihilators will be used to reduce potential conservatism associated to the state-dependent stability conditions that will be derived in the sequel. Since a rational system admits several different DARs by choosing different matrices $A_1(x), A_2(x), \Omega_1(x), \Omega_2(x)$, different results can be obtained from different choices of these matrices. The linear and affine annihilators can be used to mitigate this problem.

## 3.2 Controlled system

A controlled version of system (3.1) considering a state-feedback control law can be represented by the following equation:

$$\begin{cases} \dot{x}(t) = f(x(t)) + g(x(t))u(t) \\ u(t) = Kx(t) \end{cases} \tag{3.5}$$

where $x(t) \in \mathbb{R}^n$ is the system state; $u(t) \in \mathbb{R}^m$ is the input vector; $f : \mathcal{D} \subset \mathbb{R}^n \to \mathbb{R}^n$ and $g : \mathcal{D} \subset \mathbb{R}^n \to \mathbb{R}^{n \times m}$ are rational functions of the state, Lipschitz in a region of interest $\mathcal{B}_x$ containing the origin. We assume that $f(0) = 0$ and that the equilibrium point of interest is the origin. $K \in \mathbb{R}^{m \times n}$ is a constant matrix.

As $f$ and $g$ are rational functions and $u$ is a state feedback, system 3.5 always admits a DAR in the following form:

$$\begin{cases} \dot{x} = A_1(x)x + A_2(x)\xi(x,u) + A_3(x)u \\ 0 = \Omega_1(x)x + \Omega_2(x)\xi(x,u) + \Omega_3(x)u \end{cases} \tag{3.6}$$

where $\xi(x) \in \mathbb{R}^q$ is an auxiliary vector containing the polynomial and rational terms of $f(x)$ and $g(x)$; $A_1(x) \in \mathbb{R}^{n \times n}$, $A_2(x) \in \mathbb{R}^{n \times q}$, $A_3(x) \in \mathbb{R}^{n \times m}$, $\Omega_1(x) \in \mathbb{R}^{q \times n}$, $\Omega_2(x) \in \mathbb{R}^{q \times q}$ and $\Omega_3(x) \in \mathbb{R}^{q \times m}$ are matrix functions affine with respect to $x$. $\Omega_2(x)$ is supposed to be full column rank for all $x$ of interest, i.e. $\forall x \in \mathcal{B}_x$. The representation is valid only in the region of interest $\mathcal{B}_x$. The time dependency of $x$ and $u$ was omitted to simplify notation.

## 3.3 Event-triggered control

### 3.3.1 Topology

We consider that plant and controller are in separate nodes and are connected through a general purpose network forming the closed-loop system depicted in Figure 6.1. This topology is identical to the ones depicted in figures 2.1 and 2.2 if one considers static state feedback, i.e. $y(t) = x(t)$, $u(t) = Kx(t)$. At instants $t_k$, $k = 0, 1, 2, \ldots$, determined by the event generator, a sample of the plant state is sent to the controller node. Between two trigger instants, the controller input is held constant by means of a zero-order holder. In addition, we assume $t_0 = 0$. Therefore, the closed-loop system can be represented by the equation:

$$\begin{cases} \dot{x}(t) = f(x(t)) + g(x(t))u(t) \\ u(t) = Kx(t_k) \end{cases} \qquad \forall t \in [t_k, t_{k+1}) \tag{3.7}$$

and, considering $\delta(t) = x(t_k) - x(t)$, as defined in (2.3), we can re-write (3.7) as follows:

$$\begin{cases} \dot{x}(t) = f(x(t)) + g(x(t))u(t) \\ u(t) = K(x(t) + \delta(t)) \end{cases} \qquad \forall t \in [t_k, t_{k+1}) \tag{3.8}$$

### 3.3.2 Event generator

We assume that the event generator has access to the entire state of the system and we propose the use of the weighted relative error threshold trigger condition (Algorithm 5) recalled here as a convenience for the reader:

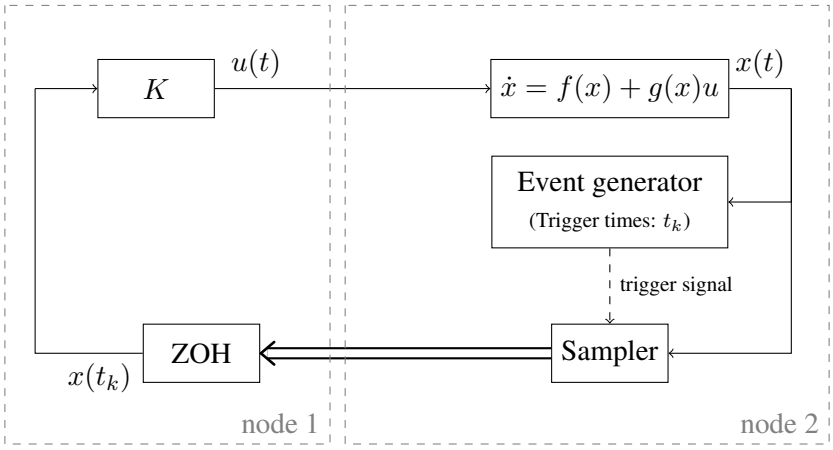


Figure 3.1: Topology being considered for rational systems.

**Algorithm 5** Weighted relative error threshold trigger

**if** $\delta'(t)Q_\delta\delta(t) - x'(t)Q_x x(t) > 0$ **then**
  Generate an event;
  $t_k = t$;
**end if**

We recall also that the symmetric positive-definite matrices $Q_\delta$ and $Q_x$ are design parameters.

### 3.3.3 Zeno behavior

The first original result presented in this thesis is the proof that the triggering strategy defined by Algorithm 5 considering the topology described in section 3.3.1 is free from Zeno behavior. The following theorem addresses this.

**Theorem 3.1.** *Assume that the origin of the closed-loop system given by* (3.7) *is asymptotically stable under the triggering strategy given by Algorithm 5, then the inter-event times are lower bounded, i.e.* $\exists\, T_{min} :\ t_{k+1} - t_k \geq T_{min},\ \forall k \in \mathbb{N}$.

*Proof.* Observe that the trigger criterion, $\delta'(t)Q_\delta\delta(t) - x'(t)Q_x x(t) > 0$, can be rewritten as follows:

$$\text{Trigger if } \frac{\delta' Q_\delta \delta}{x' Q_x x} > 1 \tag{3.9}$$

where we omitted the time dependency for clarity.

When a trigger event occurs, $\delta$ becomes $0$ and a new trigger event will occur only when the relation above is satisfied again. That is, no new event can occur while $\frac{\delta' Q_\delta \delta}{x' Q_x x} \leq 1$. Hence, noticing that $\frac{\delta' Q_\delta \delta}{x' Q_x x} \leq \lambda \frac{\|\delta\|^2}{\|x\|^2}$, with $\lambda = \frac{\lambda_{max}(Q_\delta)}{\lambda_{min}(Q_x)}$; no new trigger can occur while:

$$\lambda \left(\frac{\|\delta\|}{\|x\|}\right)^2 < 1 \iff \frac{\|\delta\|}{\|x\|} < \sqrt{\frac{1}{\lambda}}$$

From this point, the proof follows the steps presented in (TABUADA, 2007, Theorem

III.1). Consider the dynamics of $\frac{\|\delta\|}{\|x\|}$ between two sampling instants as follows:

$$\begin{aligned}
&\frac{d}{dt}\left(\frac{\|\delta\|}{\|x\|}\right) = -\frac{\delta'\dot{x}}{\|\delta\|\|x\|} - \frac{x'\dot{x}}{\|x\|^2}\frac{\|\delta\|}{\|x\|} \leq \\
&\leq \frac{\|\delta\|\|\dot{x}\|}{\|\delta\|\|x\|} + \frac{\|x\|\|\dot{x}\|}{\|x\|^2}\frac{\|\delta\|}{\|x\|} = \left(1+\frac{\|\delta\|}{\|x\|}\right)\frac{\|\dot{x}\|}{\|x\|} = \\
&= \left(1+\frac{\|\delta\|}{\|x\|}\right)\frac{\|h(x,x+\delta)\|}{\|x\|} \leq \\
&\leq \left(1+\frac{\|\delta\|}{\|x\|}\right)\frac{L\|x\|+L\|\delta\|}{\|x\|} = L\left(1+\frac{\|\delta\|}{\|x\|}\right)^2
\end{aligned} \tag{3.10}$$

where $h(x, x+\delta) \triangleq f(x) + g(x)K(x+\delta)$ and $L$ is the Lipschitz constant of $h$ in the set $\{[x'\ \delta']' \in \mathbb{R}^{2n} : x \in \mathcal{B}_x,\ \delta : \delta' Q_\delta \delta - x' Q_x x \leq 0\}$. The last inequality in (3.10) comes from the fact that since $f(x)$ and $g(x)$ are Lipschitz, so is $h(x, x+\delta)$, thus:

$$\begin{aligned}
&\|h(r_1, r_1+s_1) - h(r_2, r_2+s_2)\| \leq \\
&\leq L\|(r_1, s_1) - (r_2, s_2)\|
\end{aligned} \tag{3.11}$$

and, taking $r_1 = x$, $s_1 = \delta$, $r_2 = s_2 = 0$:

$$\begin{aligned}
&\|h(x, x+\delta) - h(0,0)\| = \\
&= \|h(x, x+\delta)\| \leq \\
&\leq L\|(x,\delta) - (0,0)\| = L\|(x,\delta)\| \leq \\
&\leq L\|x\| + L\|\delta\|
\end{aligned} \tag{3.12}$$

Defining $\varphi \triangleq \frac{\|\delta\|}{\|x\|}$, (3.10) becomes:

$$\dot{\varphi} \leq L(1+\varphi)^2 \tag{3.13}$$

Thus, $\frac{\delta' Q_\delta \delta}{x' Q_x x}$ takes more time to go from 0 to 1 than $\varphi(t)$, solution of the initial value problem $\dot{\varphi} = L(1+\varphi)^2$ with $\varphi(0) = 0$, takes to reach $\sqrt{1/\lambda}$ for the first time. The solution to this initial value problem is given by:

$$\varphi(t) = \frac{Lt}{1-Lt} \tag{3.14}$$

which is continuous at $t = 0$. Therefore, it takes a finite (as opposed to infinitesimal) amount of time to reach the value $\sqrt{1/\lambda}$. Thus, we conclude that the inter-event times are lower-bounded by this amount.

□

From Theorem 3.1, one can guarantee that the proposed triggering strategy does not lead to Zeno behavior when constant static state feedback is considered, i.e. $u(t) = Kx(t_k)$. Nevertheless, this theorem can be trivially extended for the case where the control law is a function of the sampled state, i.e. $u(t) = K(x(t_k))$, as long as $K(\cdot)$ is Lipschitz in $\mathcal{B}_x$. The proof is identical to the one presented for Theorem 3.1.

## 3.4 Problem formulation

Considering system (3.7), the main goal is to design an event-triggered strategy that reduces number of control updates while ensuring the asymptotic stability of the origin of closed-loop system. Moreover, we want to ensure that the region of attraction of the origin includes a given set of initial conditions $\mathcal{X}_0$. This set represents a region of safe operation for the system. The sections in the sequel formally define two problems aiming at these goals.

### 3.4.1 Emulation design

In the context of emulation design, one starts from a previously computed control law gains matrix $K$ and the task is to compute only the event generator parameters $Q_\delta$ and $Q_x$. With this aim, the following hypothesis are considered.

**Hypothesis 3.1.** *$K$ is such that the origin of system* (3.5) *is asymptotically stable.*

**Hypothesis 3.2.** *The set $\mathcal{X}_0$ is contained in the region of attraction of the origin of system* (3.5)*.*

It should be noted that Hypothesis 3.1 implies that a stabilizing controller was previously designed considering a continuous-time implementation of the control system, i.e. considering direct connection between the controller and plant, without sampling or event-trigger mechanisms.

Hence, assuming fulfillment of Hypothesis 3.1 and Hypothesis 3.2, the emulation design problem is defined as follows:

**Problem 3.1.** *Devise an event generator that ensures the asymptotic stability of the origin of the closed-loop* (3.7) *under the triggering strategy defined by Algorithm 5 such that $\mathcal{X}_0$ is contained in the domain of attraction of the origin, while aiming at reducing the number of triggered events.*

### 3.4.2 Co-design

In the co-design context, the goal is to compute simultaneously the parameters of the event generator and the control law. The problem at hand can be formalized as follows:

**Problem 3.2.** *Compute simultaneously a gain matrix $K$ and an event generator that ensure the asymptotic stability of the origin of system* (3.7) *under the triggering strategy defined by Algorithm 5 such that $\mathcal{X}_0$ is contained in the domain of attraction of the origin, while aiming at reducing the number of triggered events.*

## 3.5 Conclusion

In this chapter we defined the characteristics of the systems that are considered in Part I of this thesis. The subject of this part are rational systems under an event-triggered control whose triggering condition is based on a weighted relative error threshold criterion. Static state-feedback is considered and the system topology is the one depicted in Figure 3.3.1.

We stated that differential-algebraic representations (DARs) of the nonlinear system will be used to obtain tractable stability conditions (in the form of LMIs). The choice

of this representation was due to its potential for less conservatism than the other possible representations, e.g. linear-fractional representations (LFRs), quasi-linear parameter-varying (quasi-LPV) and Takagi-Sugeno (T-S).

We formulated the emulation and co-design problems to be addressed considering rational plants. For the emulation design, it is assumed, as usual in this context, that a stabilizing control law for the continuous-time implementation of the closed-loop system is known.

We also presented in this chapter the first original result of this research: the proof that the triggering strategy at hand features lower bounded inter-event times and, therefore, does not lead to Zeno behavior.

In the next sections, we will address the emulation and co-design problems formulated here.

# 4 EMULATION DESIGN

In this chapter, we address Problem 3.1. Considering a given control law parameter $K$ that asymptotically stabilizes the origin of the continuous-time system (3.5) and a set $\mathcal{X}_0$ for which we want to ensure convergence to the origin, our goal is to compute the parameters $Q_\delta$ and $Q_x$ of the event generator described in Algorithm 5 for the event-triggered control system (3.7), whose equation is recalled here for the readers convenience:

$$\begin{cases} \dot{x}(t) = f(x(t)) + g(x(t))u(t) \\ u(t) = Kx(t_k) \qquad \forall t \in [t_k, t_{k+1}) \end{cases} \tag{4.1}$$

Considering the sampling error definition from (2.3), $\delta(t) \triangleq x(t_k) - x(t)$, we can rewrite (4.1) as:

$$\begin{aligned} \dot{x}(t) &= f(x(t)) + g(x(t))K(x(t) + \delta(t)) \\ &= f(x(t)) + g(x(t))Kx(t) + g(x(t))K\delta(t) \\ &\qquad\qquad \forall t \in [t_k, t_{k+1}) \end{aligned} \tag{4.2}$$

Since $f(x)$ and $g(x)$ are, by assumption, rational functions with respect to the state, $f(x) + g(x)Kx$ and $g(x)Kx$ are also rational and it is always possible to find a DAR decomposition for (4.2) with the following form:

$$\begin{cases} \dot{x} = A_1(x)x + A_2(x)\xi(x,\delta) + A_3(x)\delta \\ 0 = \Omega_1(x)x + \Omega_2(x)\xi(x,\delta) + \Omega_3(x)\delta \end{cases} \tag{4.3}$$

with $A_1(x) \in \mathbb{R}^{n\times n}$, $A_2(x) \in \mathbb{R}^{n\times q}$, $A_3(x) \in \mathbb{R}^{n\times n}$, $\Omega_1(x) \in \mathbb{R}^{q\times n}$, $\Omega_2(x) \in \mathbb{R}^{q\times q}$ and $\Omega_3(x) \in \mathbb{R}^{q\times n}$ being affine matrix functions of $x$ and $\xi(x,\delta) \in \mathbb{R}^q$ being an auxiliary vector variable containing rational and polynomial terms of $f(x)$ and $g(x)K(x+\delta)$. It is assumed that (4.2) can be recovered from (4.3) by eliminating $\xi(x,\delta)$, which implies that $\Omega_2(x)$ is full column rank for all $x$ of interest, i.e. $\forall x \in \mathcal{B}_x$. Notice that the time dependency of $x$ and $\delta$ is omitted to simplify notation.

**Remark 4.1.** *Notice that, if $K$ is a rational matrix function of the state $K(x)$ instead of a constant matrix, $f(x) + g(x)K(x)x$ is still rational and the same form of DAR can be considered. Therefore, the results presented in this section also apply for the case of nonlinear static state feedback depending rationally on the state.*

## 4.1 Stability conditions with quadratic Lyapunov functions

In this section, we apply Lyapunov theory techniques to obtain asymptotic stability conditions for the origin of system (4.1) under the triggering strategy given by Algorithm 5. Considering a quadratic Lyapunov function candidate, we derive conditions that ensure that its time derivative is negative along the trajectories of the system between the sampling events. The event generator is designed to trigger a new control update each time the Lyapunov derivative is about to become positive, forcing the derivative to stay negative. This is accomplished by incorporating the trigger parameters to the stability conditions via S-Procedure (see, e.g. (BOYD et al., 1994, Section 2.6.3) for details on S-Procedure). We also employ Finsler Lemma (BOYD et al., 1994, Section The S-Procedure, Notes and References) and linear/affine annihilators to reduce the conservatism introduced by the DAR and to minimize the effects of its choice.

We consider a convex region of interest $\mathcal{B}_x$ given by a polytope in the state space:

$$\mathcal{B}_x = \{x \in \mathbb{R}^n : h_i' x \leq 1;\ h_i \in \mathbb{R}^n; i = 1, \ldots, n_f\} \tag{4.4}$$

where $n_f$ is its number of faces. By denoting the set of vertices of $\mathcal{B}_x$ as $\mathrm{Ver}(\mathcal{B}_x) = \{x_1, x_2, \ldots, x_{n_v}\}$, note that $\mathcal{B}_x$ can be alternatively described as the convex hull of its vertices.

The following theorem, which is an original contribution of this thesis, establishes sufficient conditions for the stability of the rational system (4.1) under the event-triggered control strategy described by Algorithm 5.

**Theorem 4.1.** *Consider a DAR* (4.3) *for the system* (4.1) *which is valid in the region of interest $\mathcal{B}_x$. If there exist constant positive-definite matrices $P, Q_x, Q_\delta \in \mathbb{R}^{n\times n}$ and a constant matrix $L \in \mathbb{R}^{(3n+q)\times(2n+q-1)}$ such that the following inequalities are satisfied $\forall x \in \mathrm{Ver}(\mathcal{B}_x)$ :*

$$Q + L\mathscr{N}_2(x) + \mathscr{N}_2'(x)L' < 0 \tag{4.5}$$

$$\begin{bmatrix} P & h_i \\ h_i' & 1 \end{bmatrix} > 0, \quad i = 1 \ldots n_f \tag{4.6}$$

*where*

$$\mathscr{N}_2(x) = \begin{bmatrix} \mathscr{N}_0(x) & 0 \\ \mathscr{N}_1(x) & \end{bmatrix} \quad \mathscr{N}_1(x) = \begin{bmatrix} A_1(x) & -I & A_2(x) & A_3(x) \\ \Omega_1(x) & 0 & \Omega_2(x) & \Omega_3(x) \end{bmatrix}$$

$$Q = \begin{bmatrix} Q_x & P & 0 & 0 \\ P & 0 & 0 & 0 \\ 0 & 0 & 0 & 0 \\ 0 & 0 & 0 & -Q_\delta \end{bmatrix}$$

*with $\mathscr{N}_0$ as defined in* (3.4)*, then the origin of system* (4.1)*, under the event-triggering strategy given by Algorithm 5, is locally asymptotically stable and $\mathcal{E}(P) = \{x \in \mathbb{R}^n : x'Px \leq 1\}$ is contained in its region of attraction, i.e. $\forall x(0) \in \mathcal{E}(P)$, $x(t) \to 0$ when $t \to \infty$.*

*Proof.* Considering a quadratic Lyapunov function $V(x) = x'Px$ and the following vector:

$$\zeta = \begin{bmatrix} x \\ \dot{x} \\ \xi \\ \delta \end{bmatrix} \tag{4.7}$$

the time derivative of $V$ can be written as follows:

$$\dot{V}(x) = \zeta' \begin{bmatrix} 0 & P & 0 & 0 \\ P & 0 & 0 & 0 \\ 0 & 0 & 0 & 0 \\ 0 & 0 & 0 & 0 \end{bmatrix} \zeta \tag{4.8}$$

Now, as $\mathscr{N}_2(x)$ is affine in $x$, (4.5) verified $\forall x \in \mathrm{Ver}(\mathcal{B}_x)$ implies, by convexity, that (4.5) is verified $\forall x \in \mathcal{B}_x$. Thus, by Finsler Lemma, it follows that

$$\zeta' Q \zeta < 0, \quad \forall \zeta : \mathscr{N}_2(x)\zeta = 0 \tag{4.9}$$

is verified $\forall x \in \mathrm{Ver}(\mathcal{B}_x)$. By construction, $\mathscr{N}_2(x)\zeta = 0$ along the trajectories of the system [1], therefore, $\zeta' Q \zeta < 0$ along the trajectories of the system.

On the other hand, $\zeta' Q \zeta < 0$ is equivalent to:

$$\dot{V}(x) - \delta' Q_\delta \delta + x' Q_x x < 0 \tag{4.10}$$

which can be re-written as:

$$\dot{V}(x) < \delta' Q_\delta \delta - x' Q_x x \leq 0 \tag{4.11}$$

where the last inequality is ensured by the triggering strategy. At the event instants, a new sample is triggered, which makes $\delta = 0$ and $\dot{V}(x) < -x' Q_x x < 0$ (recalling that $Q_x$ is positive-definite). Hence, it is proved that the satisfaction of (4.5) implies $\dot{V}(x) < 0$ along the trajectories of the system that are confined in $\mathcal{B}_x$ and that the origin is asymptotically stable as long as there is no Zeno behavior. On the other hand, Theorem 3.1 ensures that there is no Zeno behavior when the proposed trigger condition is used.

We end the proof by noting that, given the conditions above, any level set of the Lyapunov function $V$ that is inside $\mathcal{B}_x$ is contained in the region of attraction of the origin, since these level surfaces are contained in a region where $\dot{V}(x) < 0$ and thus they are positively invariant and contractive with respect to the trajectories of the closed-loop system. Satisfaction of (4.6) ensures $\mathcal{E}(P) \subset \mathcal{B}_x$ (see TARBOURIECH et al., 2011, Appendix C.8, for details), which concludes the proof. □

## 4.2 Stability conditions with rational Lyapunov functions

In this section we propose to use a similar procedure to that of Section 4.1 to obtain stability conditions considering a rational Lyapunov function which, for being more generic, will potentially allow to further reduce the number of events generated for the class of systems at hand.

The stability conditions will be based on the following class of Lyapunov candidates, as presented in (COUTINHO; GOMES DA SILVA JR., 2010):

$$V(x) = \theta'(x) P \theta(x) \tag{4.12}$$

where $\theta(x) \in \mathbb{R}^{n_\theta}$ is a given rational vector function of the state $x$, non-singular in $\mathcal{B}_x$, and $P \in \mathbb{R}^{n_\theta \times n_\theta}$ is a matrix to be determined. Notice that this formulation encompasses

[1] Note that $\mathscr{N}_2(x)\,\zeta = 0$, since, by construction, $\mathscr{N}_0(x)\,x = 0$, $\forall x$ and from (4.3), it follows that $\mathscr{N}_1(x)\,\zeta = 0$ along the trajectories of the system.

a broad class of functions, including quadratic (with $\theta(x) = x$), bi-quadratic, polynomial and rational (with $\theta(x)$ being a polynomial or non-singular rational vector function of $x$) (COUTINHO; GOMES DA SILVA JR., 2010).

The level sets associated to $V(x)$ are defined as follows:

$$\mathcal{L}_V(c) = \{x \in \mathbb{R}^n : V(x) \leq c,\, c > 0\} \tag{4.13}$$

Since $\theta(x)$ and $\dot{x}$ are rational with respect to $x$, it is clear that $\dot{\theta}$ is also rational with respect to $x$. Thus, based on the same arguments of Section 3.1.2, the following representations for $\theta$ and $\dot{\theta}$ can be obtained:

$$\begin{cases} \theta = E_1(x)x + E_2(x)\xi_\theta(x) \\ 0 = \Gamma_1(x)x + \Gamma_2(x)\xi_\theta(x) \end{cases} \tag{4.14}$$

$$\begin{cases} \dot{\theta} = F_1(x)\dot{x} + F_2(x)\xi_{\dot{\theta}}(x,\dot{x}) \\ 0 = \Phi_1(x)\dot{x} + \Phi_2(x)\xi_{\dot{\theta}}(x,\dot{x}) \end{cases} \tag{4.15}$$

with $\xi_\theta(x) \in \mathbb{R}^{q_\theta}$, $\xi_{\dot{\theta}}(x,\dot{x}) \in \mathbb{R}^{q_{d\theta}}$ being auxiliary nonlinear vector functions, $E_1(x) \in \mathbb{R}^{n_\theta \times n}$, $E_2(x) \in \mathbb{R}^{n_\theta \times q_\theta}$, $\Gamma_1(x) \in \mathbb{R}^{q_\theta \times n}$, $\Gamma_2(x) \in \mathbb{R}^{q_\theta \times q_\theta}$, $F_1(x) \in \mathbb{R}^{n_\theta \times n}$, $F_2(x) \in \mathbb{R}^{n_\theta \times q_{d\theta}}$, $\Phi_1(x) \in \mathbb{R}^{q_{d\theta} \times n}$, $\Phi_2(x) \in \mathbb{R}^{q_{d\theta} \times q_{d\theta}}$ being affine matrix functions of $x$ and $E_1(x)$, $\Gamma_2(x)$ and $\Phi_2(x)$ being full rank $\forall x \in \mathcal{B}_x$.

Now the following theorem, which constitutes an original contribution of this thesis, applies the representations (4.14) and (4.15) to establish sufficient conditions for the stability of the rational system (4.1) considering an underlying rational Lyapunov function (4.12).

**Theorem 4.2.** *Consider a DAR* (4.3) *for system* (4.1) *and a given rational vector-valued rational function $\theta(x)$ non-singular in $\mathcal{B}_x$, with corresponding representations given in* (4.14) *and* (4.15)*. If there exist constant symmetric positive definite matrices $Q_x$, $Q_\delta$, $P$ and generic constant matrices $L_1$, $L_2$, $L_{3i}$ $(i = 1, ..., n_f)$ of appropriate dimensions, such that the following LMIs are satisfied $\forall x \in \mathcal{B}_x$:*

$$\Sigma + L_1\mathscr{N}_1(x) + \mathscr{N}_1'(x)L_1' > 0 \tag{4.16}$$

$$Q + L_2\mathscr{N}_2(x) + \mathscr{N}_2'(x)L_2' < 0 \tag{4.17}$$

$$\begin{bmatrix} 1 & -h_i'N \\ * & \Sigma \end{bmatrix} + L_{3i}\mathscr{N}_3(x) + \mathscr{N}_3'(x)L_{3i}' > 0, \quad i = 1 \ldots n_f \tag{4.18}$$

*with $\mathscr{N}_0$ as defined in* (3.4) *and:*

$$\Sigma = \begin{bmatrix} 0 & 0 & 0 \\ 0 & P & 0 \\ 0 & 0 & 0 \end{bmatrix} \quad \mathscr{N}_1(x) = \begin{bmatrix} \mathscr{N}_0(x) & 0 & 0 \\ E_1(x) & -I & E_2(x) \\ \Gamma_1(x) & 0 & \Gamma_2(x) \end{bmatrix}$$

$$Q = \begin{bmatrix} Q_x & 0 & 0 & 0 & 0 & 0 & 0 & 0 \\ 0 & 0 & 0 & 0 & 0 & 0 & 0 & 0 \\ 0 & 0 & 0 & 0 & 0 & 0 & 0 & 0 \\ 0 & 0 & 0 & -Q_\delta & 0 & 0 & 0 & 0 \\ 0 & 0 & 0 & 0 & 0 & P & 0 & 0 \\ 0 & 0 & 0 & 0 & P & 0 & 0 & 0 \\ 0 & 0 & 0 & 0 & 0 & 0 & 0 & 0 \\ 0 & 0 & 0 & 0 & 0 & 0 & 0 & 0 \end{bmatrix}$$

$$\mathscr{N}_2(x) = \begin{bmatrix} \mathscr{N}_0(x) & 0 & 0 & 0 & 0 & 0 & 0 & 0 \\ A_1(x) & -I & A_2(x) & A_3(x) & 0 & 0 & 0 & 0 \\ \Omega_1(x) & 0 & \Omega_2(x) & \Omega_3(x) & 0 & 0 & 0 & 0 \\ E_1(x) & 0 & 0 & 0 & -I & 0 & E_2(x) & 0 \\ \Gamma_1(x) & 0 & 0 & 0 & 0 & 0 & \Gamma_2(x) & 0 \\ 0 & F_1(x) & 0 & 0 & 0 & -I & 0 & F_2(x) \\ 0 & \Phi_1(x) & 0 & 0 & 0 & 0 & 0 & \Phi_2(x) \end{bmatrix}$$

$$\mathscr{N}_3(x) = \begin{bmatrix} 0 & \mathscr{N}_1(x) \\ -x & N \end{bmatrix} \quad N = \begin{bmatrix} I & 0 & 0 \end{bmatrix}$$

*Then, the origin of system* (4.1)*, under the event-triggering strategy given by Algorithm 5, is locally asymptotically stable and* $\mathcal{L}_V(1) = \{x \in \mathbb{R}^n : V(x) \leq 1\}$ *is contained in its region of attraction, i.e.* $\forall x(0) \in \mathcal{L}_V(1)$*,* $x(t) \to 0$ *when* $t \to \infty$*.*

*Proof.* We show first that condition (4.16) guarantees that $V(x) = \theta'(x)P\theta(x) > 0,\ \forall x \in \mathcal{B}_x, x \neq 0$. For this, consider the augmented state vector

$$\zeta_1 = \begin{bmatrix} x \\ \theta \\ \xi_\theta \end{bmatrix}$$

which from representation (4.14) leads to:

$$V(x) = \zeta_1' \Sigma \zeta_1$$

Now, pre- and post-multiplying (4.16) by $\zeta_1'$ and $\zeta_1$ respectively and applying the Finsler's Lemma, we have that satisfaction of (4.16) is equivalent to satisfaction of the following inequality:

$$\zeta_1' \Sigma \zeta_1 > 0, \qquad \forall \zeta_1 : \mathscr{N}_1(x)\zeta_1 = 0 \tag{4.19}$$

Since $\mathscr{N}_1(x)$ is affine in $x$ and (4.16) is verified $\forall x \in \mathrm{Ver}(\mathcal{B}_x)$, by convexity, it implies that (4.19) holds for all $x \in \mathcal{B}_x$. From (3.4) and (4.14), we have $\mathscr{N}_1(x)\zeta_1 = 0$; hence, in fact, (4.16) implies $V(x) > 0,\ \forall x \in \mathcal{B}_x$.

Next we show that condition (4.17) guarantees $\dot{V}(x) < 0$ along the trajectories of the system, as long as they remain confined in $\mathcal{B}_x$. In this case, consider the following vector:

$$\zeta_2 = \begin{bmatrix} x \\ \dot{x} \\ \xi \\ \delta \\ \theta \\ \dot{\theta} \\ \xi_\theta \\ \xi_{\dot{\theta}} \end{bmatrix}$$

which leads to:

$$\dot{V}(x) = \theta' P \dot{\theta} + \dot{\theta}' P \theta = \zeta_2' \begin{bmatrix} 0 & 0 & 0 & 0 & 0 & 0 & 0 & 0 \\ 0 & 0 & 0 & 0 & 0 & 0 & 0 & 0 \\ 0 & 0 & 0 & 0 & 0 & 0 & 0 & 0 \\ 0 & 0 & 0 & 0 & 0 & 0 & 0 & 0 \\ 0 & 0 & 0 & 0 & 0 & P & 0 & 0 \\ 0 & 0 & 0 & 0 & P & 0 & 0 & 0 \\ 0 & 0 & 0 & 0 & 0 & 0 & 0 & 0 \\ 0 & 0 & 0 & 0 & 0 & 0 & 0 & 0 \end{bmatrix} \zeta_2$$

By the same arguments used earlier, one can conclude that satisfaction of (4.17) at the vertices of $\mathcal{B}_x$ implies that $\zeta_2' Q \zeta_2 < 0$ along the trajectories of the system (notice that $\mathscr{N}_2(x)\zeta_2 = 0$), as long as the trajectories remain confined in $\mathcal{B}_x$.

Now, observe that $\zeta_2' Q \zeta_2 < 0$ is equivalent to:

$$\dot{V}(x) - \delta' Q_\delta \delta + x' Q_x x < 0 \tag{4.20}$$

which implies that

$$\dot{V}(x) < \delta' Q_\delta \delta - x' Q_x x \leq 0 \tag{4.21}$$

where the last inequality is guaranteed by the event-trigger criterion, since at the instants when $\delta' Q_\delta \delta - x' Q_x x$ is about to become positive, an event is generated, causing a new sampling, which makes $\delta = 0$ again and guarantees the negativity of $\dot{V}$, since $-x' Q_x x$ is negative for $x \neq 0$, provided that $Q_x > 0$.

Given the above, any level set of the Lyapunov function $V$ belonging to $\mathcal{B}_x$ is contained in the region of attraction of the origin, since those level sets are contained in a region where $\dot{V}(x) < 0$ and thus they are positively invariant and contractive with respect to the trajectories of the closed-loop system.

Satisfaction of (4.18) guarantees $\mathcal{L}_V(1) \subset \mathcal{B}_x$, as shown in the sequel.

Observe now that

$$x \in \mathcal{B}_x \iff 2h_i' x = h_i' x + x' h_i \leq 2 \iff 2 - h_i' x - x' h_i \geq 0 \tag{4.22}$$

and

$$x \in \mathcal{L}_V(1) \iff V(x) = \zeta_1' \Sigma \zeta_1 \leq 1 \iff \zeta_1' \Sigma \zeta_1 - 1 \leq 0 \tag{4.23}$$

Moreover,

$$\mathcal{L}_V(1) \subset \mathcal{B}_x \iff (\forall x \in \mathcal{L}_V(1) \implies x \in \mathcal{B}_x)$$

which, from (4.22) and (4.23) is equivalent to:

$$2 - h_i' x - x' h_i \geq 0, \quad \forall x : 1 - \zeta_1' \Sigma \zeta_1 \geq 0 \tag{4.24}$$

Hence, using the S-Procedure, satisfaction of the following condition guarantees that (4.24) holds:

$$1 - h_i' x - x' h_i + \zeta_1' \Sigma \zeta_1 \geq 0 \tag{4.25}$$

By noting that $N\zeta_1 = x$, with $N = \begin{bmatrix} I & 0 & 0 \end{bmatrix}$, condition (4.25) can be written in matrix form as:

$$\begin{bmatrix} 1 \\ \zeta_1 \end{bmatrix}' \begin{bmatrix} 1 & -h_i' N \\ * & \Sigma \end{bmatrix} \begin{bmatrix} 1 \\ \zeta_1 \end{bmatrix} \geq 0 \tag{4.26}$$

Now, noticing that $\mathscr{N}_3(x) \begin{bmatrix} 1 \\ \zeta_1 \end{bmatrix} = 0$ and applying the Finsler's Lemma, it follows that if (4.18) is satisfied. Then (4.26) holds and, in fact, $\mathcal{L}_V(1) \subset \mathcal{B}_x$, which concludes the proof.

□

## 4.3 Optimization problems

From the definition of Problem 3.1, we aim to design the trigger criterion, i.e. the matrices $Q_\delta$ and $Q_x$ in order to ensure the asymptotic stability of the origin for all initial conditions in a given set $\mathcal{X}_0$ while minimizing the events occurrence. Theorem 4.1 and Theorem 4.2 can be used with the additional condition $\mathcal{X}_0 \subset \mathcal{E}(P)$ to ensure stability for this set of initial conditions. Recalling that to reduce the number of events one aims at finding $Q_\delta$ as "small" as possible and $Q_x$ as "large" as possible, the minimization of an objective function like $\mathrm{tr}(Q_\delta - Q_x)$ could be used. Unfortunately, it leads to poor results due to the use of the trace of the difference of the decision variables which is not a good approximation to the actual objective that needs to be minimized, which is related to the ratio between eigenvalues of matrices $Q_x$ and $Q_\delta$. Moreover, when the objective function is defined as the minimization of the difference between two variables, if both are increased by the same amount, the objective value will remain the same, which is not interesting in our case. An alternative is to apply the Schur's complement to the first element of matrices $Q$ in (4.5) and (4.17), as follows.

a) For quadratic Lyapunov functions:

$$\bar{Q} + \bar{L}\bar{\mathscr{N}_2}(x) + \bar{\mathscr{N}_2}'(x)\bar{L}' < 0 \tag{4.27}$$

with

$$\bar{Q} = \begin{bmatrix} 0 & P & 0 & 0 & I \\ P & 0 & 0 & 0 & 0 \\ 0 & 0 & 0 & 0 & 0 \\ 0 & 0 & 0 & -Q_\delta & 0 \\ I & 0 & 0 & 0 & -\bar{Q}_x \end{bmatrix}$$

$$\bar{\mathscr{N}_2} = [\mathscr{N}_2\ 0], \quad \bar{Q}_x = Q_x^{-1}, \quad \bar{L} = \begin{bmatrix} L \\ 0 \end{bmatrix}$$

b) For rational Lyapunov functions:

$$\bar{Q} + \bar{L}_2\bar{\mathscr{N}_2}(x) + \bar{\mathscr{N}_2}'(x)\bar{L}_2' < 0 \tag{4.28}$$

with

$$\bar{Q} = \begin{bmatrix} 0 & 0 & 0 & 0 & 0 & 0 & 0 & 0 & I \\ 0 & 0 & 0 & 0 & 0 & 0 & 0 & 0 & 0 \\ 0 & 0 & 0 & 0 & 0 & 0 & 0 & 0 & 0 \\ 0 & 0 & 0 & -Q_\delta & 0 & 0 & 0 & 0 & 0 \\ 0 & 0 & 0 & 0 & 0 & P & 0 & 0 & 0 \\ 0 & 0 & 0 & 0 & P & 0 & 0 & 0 & 0 \\ 0 & 0 & 0 & 0 & 0 & 0 & 0 & 0 & 0 \\ 0 & 0 & 0 & 0 & 0 & 0 & 0 & 0 & 0 \\ I & 0 & 0 & 0 & 0 & 0 & 0 & 0 & -\bar{Q}_x \end{bmatrix},$$

$$\bar{\mathscr{N}_2} = [\mathscr{N}_2\ 0], \quad \bar{Q}_x = Q_x^{-1}, \quad \bar{L}_2 = \begin{bmatrix} L_2 \\ 0 \end{bmatrix}$$

Formulations (4.27) and (4.28) of (4.5) and (4.17), respectively, allows us to maximize the trace of $Q_x$ implicitly by minimizing the trace of $\bar{Q}_x = Q_x^{-1}$ and use the objective function $\mathrm{tr}(Q_\delta + \bar{Q}_x)$, which leads to better results in terms of the number of events.

Considering $\mathcal{X}_0 = \{x \in \mathbb{R}^n : x'P_0x \leq 1\}$, with a symmetric positive-definite $P_0 \in \mathbb{R}^{n\times n}$, condition $\mathcal{X}_0 \subset \mathcal{E}(P)$ can be expressed as:

$$P < P_0 \tag{4.29}$$

Summarizing, these considerations lead to the following convex optimization problems proposed as means to compute the parameters of the event generator, i.e. $Q_x = \bar{Q}_x^{-1}$ and $Q_\delta$.

a) For the quadratic Lyapunov function case:

$$\begin{aligned} &\min(\mathrm{tr}(Q_\delta + \bar{Q}_x)) \\ &\quad \text{subject to:} \\ &\qquad (4.6),\ (4.27),\ (4.29) \end{aligned} \tag{4.30}$$

b) For the case of rational Lyapunov functions:

$$\begin{aligned} &\min(\mathrm{tr}(Q_\delta + \bar{Q}_x)) \\ &\quad \text{subject to:} \\ &\qquad (4.16),\ (4.18),\ (4.28), \\ &\qquad \begin{bmatrix} P_0 & 0 \\ 0 & 0 \end{bmatrix} - \Sigma + L\mathscr{N}_1(x) + \mathscr{N}_1(x)'L \geq 0 \end{aligned} \tag{4.31}$$

where $L$ is a generic matrix of appropriate dimension. Note that the last constraint in (4.31) ensures that $\mathcal{X}_0 \subset \mathcal{L}_V(1)$.

It should be noticed that the choice of $\mathcal{B}_x$ impacts the results obtained from these optimization problems. To overcome such problem, we parametrize $\mathcal{B}_x = \{x \in \mathbb{R}^n : h_i'x \leq \rho,\ h_i \in \mathbb{R}^n,\ i = 1, \ldots, n_f;\ \rho > 0\}$, where the vectors $h_i$ determine the shape and the parameter $\rho$ determines the size of $\mathcal{B}_x$. Then we solve the optimization problems performing a search over $\rho$.

**Remark 4.2.** *Since only stabilization of the closed-loop system with no further performance criteria was employed to derive the constraints of optimization problems* (4.30) *and* (4.31)*, these problems are not well-posed to open-loop stable systems, in the sense that they will lead to a very large $Q_x$ and a very small $Q_\delta$. Under these circumstances, the event-trigger will not generate any events and the system will operate in open-loop. To avoid this, additional LMIs can be added to require some performance index of the closed-loop system. For instance, one can add LMIs to require a minimum exponential decay rate of the Lyapunov function. This reasoning is also valid for all optimization problems discussed in the sequel of this thesis.*

## 4.4 Numerical examples

In this section, we illustrate the application of the proposed emulation design method by means of numerical examples. Three examples of systems are considered: a polynomial planar, a rational planar and a third-order polynomial one. We also compare the results obtained with the use of quadratic and bi-quadratic Lyapunov functions to illustrate the impact of the use of more complex Lyapunov functions.

### 4.4.1 Example 1 – Unstable polynomial system

Consider the following plant:

$$\begin{cases} \dot{x}_{(1)}(t) = x_{(2)}(t) \\ \dot{x}_{(2)}(t) = \left(1 + x_{(1)}^2(t)\right) x_{(1)}(t) + x_{(2)}(t) + u(t) \end{cases} \tag{4.32}$$

where $x = [x_{(1)}\ x_{(2)}]' \in \mathbb{R}^2$ is the plant state. The open-loop systems features only one equilibrium point, the origin, which is a saddle point.

Considering the linearization of the system around the origin, we designed a gain matrix $K = \begin{bmatrix} -2 & -2 \end{bmatrix}$ that ensures the asymptotic stability of the origin of the continuous-time closed-loop system [2]. Then we chose the following DAR for the event-triggered closed-loop system:

$$\begin{cases} \dot{x} = \begin{bmatrix} 0 & 1 \\ -1 & -1 \end{bmatrix} x + \begin{bmatrix} 0 \\ x_{(1)} \end{bmatrix} x_{(1)}^2 + \begin{bmatrix} 0 & 0 \\ -2 & -2 \end{bmatrix} \delta \\ 0 = \begin{bmatrix} x_{(1)} & 0 \end{bmatrix} x + \begin{bmatrix} -1 \end{bmatrix} x_{(1)}^2 + \begin{bmatrix} 0 & 0 \end{bmatrix} \delta \end{cases} \tag{4.33}$$

Let $\mathcal{B}_x = \{x \in \mathbb{R}^2 : |x_{(i)}| < \rho;\ \rho \in \mathbb{R}^+\}$, with $\rho$ being a parameter defining the side length of $\mathcal{B}_x$ and $\mathcal{X}_0 = \{x \in \mathbb{R}^2 : x' P_0 x \leq 1\}$, with $P_0 = 50I$.

We will solve the emulation problem considering a quadratic and a bi-quadratic Lyapunov function. For the bi-quadratic one, we consider the vectors

$$\theta = \begin{bmatrix} x_{(1)}^2 \\ x_{(1)}x_{(2)} \\ x_{(2)}^2 \\ x_{(1)} \\ x_{(2)} \end{bmatrix} \qquad \dot{\theta} = \begin{bmatrix} 2x_{(1)}\dot{x}_{(1)} \\ x_{(1)}\dot{x}_{(2)} + x_{(2)}\dot{x}_{(1)} \\ 2x_{(2)}\dot{x}_{(2)} \\ \dot{x}_{(1)} \\ \dot{x}_{(2)} \end{bmatrix} \tag{4.34}$$

and the following parameters for representations (4.14) and (4.15):

$$\begin{gathered} \xi_\theta = \begin{bmatrix} x_{(1)}^2 \\ x_{(1)}x_{(2)} \\ x_{(2)}^2 \end{bmatrix} \qquad E_1 = \begin{bmatrix} 0 & 0 \\ 0 & 0 \\ 0 & 0 \\ 1 & 0 \\ 0 & 1 \end{bmatrix} \qquad E_2 = \begin{bmatrix} 1 & 0 & 0 \\ 0 & 1 & 0 \\ 0 & 0 & 1 \\ 0 & 0 & 0 \\ 0 & 0 & 0 \end{bmatrix} \\ \Gamma_1 = \begin{bmatrix} x_{(1)} & 0 \\ 0 & x_{(1)} \\ 0 & x_{(2)} \end{bmatrix} \qquad \Gamma_2 = \begin{bmatrix} -1 & 0 & 0 \\ 0 & -1 & 0 \\ 0 & 0 & -1 \end{bmatrix} \\ \xi_{\dot{\theta}} = \begin{bmatrix} x_{(1)}\dot{x}_{(1)} \\ x_{(1)}\dot{x}_{(2)} \\ x_{(2)}\dot{x}_{(1)} \\ x_{(2)}\dot{x}_{(2)} \end{bmatrix} \qquad F_1 = \begin{bmatrix} 0 & 0 \\ 0 & 0 \\ 0 & 0 \\ 1 & 0 \\ 0 & 1 \end{bmatrix} \qquad F_2 = \begin{bmatrix} 2 & 0 & 0 & 0 \\ 0 & 1 & 1 & 0 \\ 0 & 0 & 0 & 2 \\ 0 & 0 & 0 & 0 \\ 0 & 0 & 0 & 0 \end{bmatrix} \\ \Phi_1 = \begin{bmatrix} x_{(1)} & 0 \\ 0 & x_{(1)} \\ x_{(2)} & 0 \\ 0 & x_{(2)} \end{bmatrix} \qquad \Phi_2 = \begin{bmatrix} -1 & 0 & 0 & 0 \\ 0 & -1 & 0 & 0 \\ 0 & 0 & -1 & 0 \\ 0 & 0 & 0 & -1 \end{bmatrix} \end{gathered} \tag{4.35}$$

[2] With this control law, the continuous-time closed-loop has additional equilibria at $x_{e1} = \begin{bmatrix} 1 & 0 \end{bmatrix}'$ and $x_{e2} = \begin{bmatrix} -1 & 0 \end{bmatrix}'$.

We computed the trigger parameters using optimization problems (4.30) for the quadratic Lyapunov function and (4.31) for the bi-quadratic one. These problems were solved for various values of $\rho$ (i.e., various sizes of $\mathcal{B}_x$), with the additional restriction of $Q_\delta < 0.0001I$ to prevent $Q_\delta$ from becoming ill-conditioned. The obtained results are shown in Table 4.1. One can observe that the best value of the objective function is obtained with the use of a bi-quadratic Lyapunov function. This is the first indication that the use of more complex Lyapunov functions can lead to better results. In the sequel we confirm this expectation by means of simulations.

Table 4.1: Example 1 – Linear search over $\mathcal{B}_x$ size for different Lyapunov functions.

| $\rho$ | Objective function value | |
|---|---|---|
| | Quadratic, OP (4.30) | Bi-quadratic, OP (4.31) |
| 0.15 | 189 | 186 |
| 0.20 | 112 | 109 |
| 0.30 | 56.7 | 53.7 |
| 0.40 | 38.3 | 35.0 |
| 0.50 | 30.8 | 26.9 |
| 0.55 | 29.1 | 24.8 |
| 0.60 | **28.4** | 23.3 |
| 0.65 | 28.5 | 22.5 |
| 0.70 | 29.6 | **22.2** |
| 0.75 | 31.9 | 22.6 |
| 0.80 | 36.0 | 24.1 |
| 0.85 | 43.8 | 27.5 |
| 0.95 | 111 | 62.1 |
| 1.0 | unfeasible | unfeasible |

Now we consider the event generator parameters with the values of $Q_x$ and $Q_\delta$ corresponding to the best objective values obtained in each case, that is, $\rho = 0.60$ for the quadratic case and $\rho = 0.70$ for the bi-quadratic one. The values of these matrices and of the corresponding $P$ for each case are depicted in Table 4.2.

Table 4.2: Example 1 – Matrices obtained from the optimization problems with different Lyapunov functions.

| | Quadratic, OP (4.30) | Bi-quadratic, OP (4.31) |
|---|---|---|
| $Q_x$ | $\begin{bmatrix} 0.332 & -0.118 \\ -0.118 & 0.593 \end{bmatrix}$ | $\begin{bmatrix} 0.299 & -0.059 \\ -0.059 & 0.638 \end{bmatrix}$ |
| $Q_\delta$ | $\begin{bmatrix} 11.6514 & 11.6486 \\ 11.6486 & 11.6514 \end{bmatrix}$ | $\begin{bmatrix} 8.5812 & 8.5799 \\ 8.5799 & 8.58012 \end{bmatrix}$ |
| $P$ | $\begin{bmatrix} 2.86 & 0.553 \\ 0.553 & 3.71 \end{bmatrix}$ | $\begin{bmatrix} -1.81 & 0.00732 & -0.00697 & 1.78 \cdot 10^{-5} & 0.437 \\ 0.00732 & 0.0113 & 0.00106 & -0.437 & -0.501 \\ -0.00697 & 0.00106 & -0.00133 & 0.501 & -4.16 \cdot 10^{-5} \\ 1.78 \cdot 10^{-5} & -0.437 & 0.501 & 3.38 & 0.345 \\ 0.437 & -0.501 & -4.16 \cdot 10^{-5} & 0.345 & 3.45 \end{bmatrix}$ |

Simulations of the closed-loop systems using these values for the parameters give the results shown in figures 4.1 and 4.2. In Figure 4.1, the top plots show the evolution of the state for an initial condition $x(0) = [0.1\ 0.1]'$. The dashed lines represent the state

of a continuous-time implementation of the control system, i.e. without an event-trigger policy. One can see that the event-triggered implementation rendered the closed-loop slightly faster and slightly more oscillatory, but the overall dynamics are very similar to the one obtained with a continuous-time implementation. The plots in the middle show the control signal, with the dashed lines representing again the corresponding continuous-time implementation. Note that in the event-triggered implementation, the control signal is held constant between two events (as expected) and that the control signals are very similar to the continuous-time implementation. In particular, the event-trigger has not led into much larger control efforts. The bottom plots depict the event instants, with the sizes of the bars representing the inter-event times, i.e. the difference between the time of that event and of the previous one. It should however be noticed that the important information about the events is not the maximum inter-event time (which is clearly visible in these plots), but the minimum inter-event time and the number of events. To quantify this information we need to consider various initial conditions, taking the minimum inter-event time and the average number of events among them.

For this, we computed the average number of events and the minimum inter-event time for 200 initial conditions inside $\mathcal{X}_0$, 50 of them equally spaced along the border of $\mathcal{X}_0$. The time interval simulated in each case was $t \in [0, 15]$. The results are summarized in Table 4.3. These results confirm the predictions from the analysis of the objective function values: the use of a bi-quadratic Lyapunov function indeed reduced the average number of events and increased the minimum inter-event time.

Table 4.3: Example 1 – Comparison of event-trigger effectiveness for $P_0 = 50I$.

| | Quadratic, OP (4.30) | Bi-quadratic, OP (4.31) |
|---|---|---|
| Average number of events | 60.98 | 56.01 |
| Minimum inter-event time | 144 | 160 |

Figure 4.2 depicts the borders of the set $\mathcal{X}_0$ (in red) and of the Lyapunov level sets $\mathcal{E}(P)$ and $\mathcal{L}_V(1)$ (in black) along with some convergent (in blue) and divergent (in magenta) trajectories of the event-triggered implementation. As one can see, the set $\mathcal{X}_0$ is contained in $\mathcal{E}(P)$ and $\mathcal{L}_V(1)$, respectively, and in the regions of attraction of the origin, as expected. Note also that, although there are subtle differences in the trajectories for each optimization case, the overall domains of attraction are very similar for all the considered cases and that the set $\mathcal{L}_V(1)$ is indeed not an ellipsoid in the bi-quadratic case. It is important to highlight that the optimization problems at hand do not aim at maximizing the size of $\mathcal{E}(P)$ and $\mathcal{L}_V(1)$ in any sense, so it is not expected that they lead to good estimates of the region of attraction. Actually, it is only ensured that $\mathcal{X}_0$ is contained in these level sets to guarantee that all trajectories starting inside $\mathcal{X}_0$ converge to the origin, as desired.

#### *4.4.1.1 Influence of $\mathcal{X}_0$ size*

Now we consider larger sets $\mathcal{X}_0$, by choosing $P_0 = 4I$ and $P_0 = 2.8I$. Figures 4.3 and 4.4 show phase portraits of the closed-loop system with the borders of the sets $\mathcal{X}_0$ (in red) and of the Lyapunov level sets $\mathcal{E}(P)$ and $\mathcal{L}_V(1)$ (in black) obtained for each of these values of $P_0$, respectively.

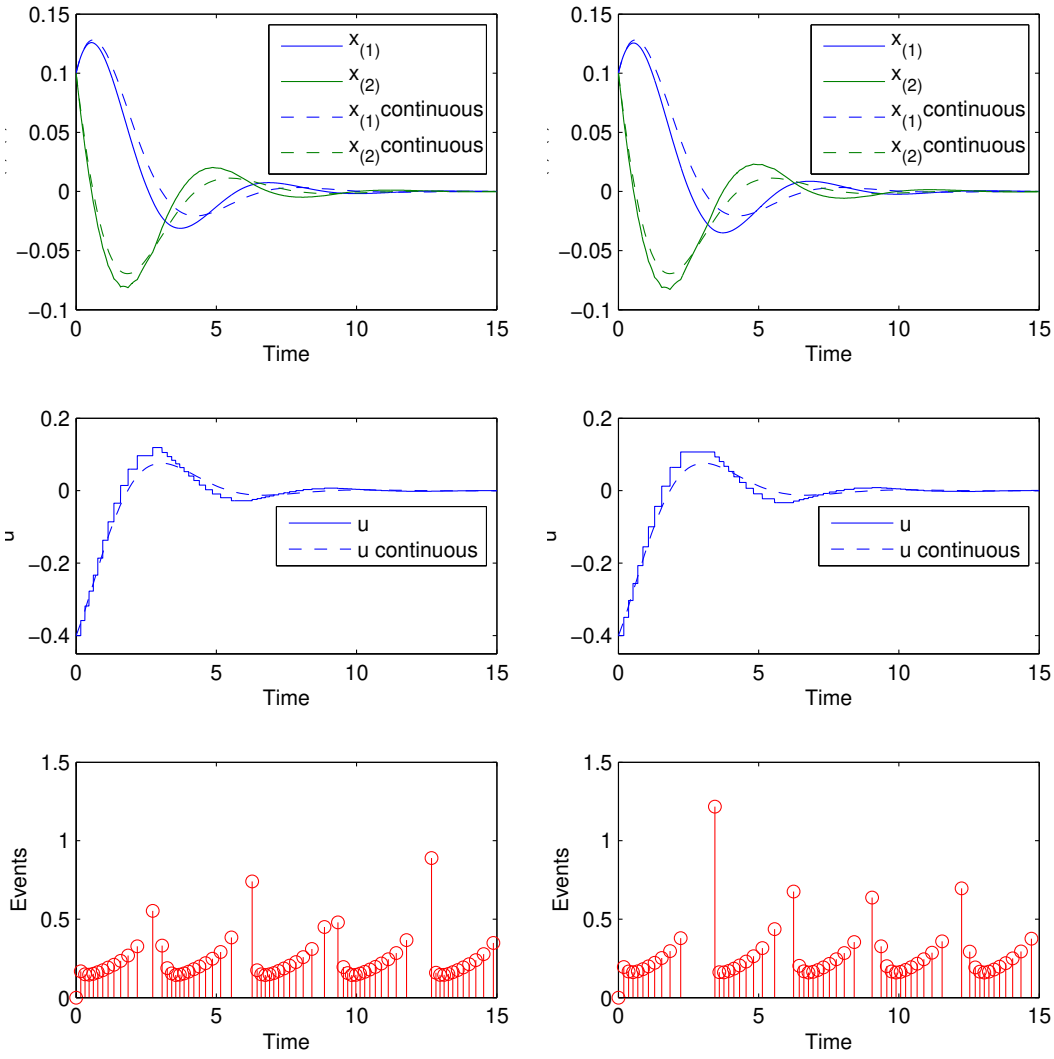


a) Quadratic, OP (4.30)

b) Bi-quadratic, OP (4.31)

Figure 4.1: Example 1 – Simulations for $x(0) = [0.1\ 0.1]'$ – emulation.

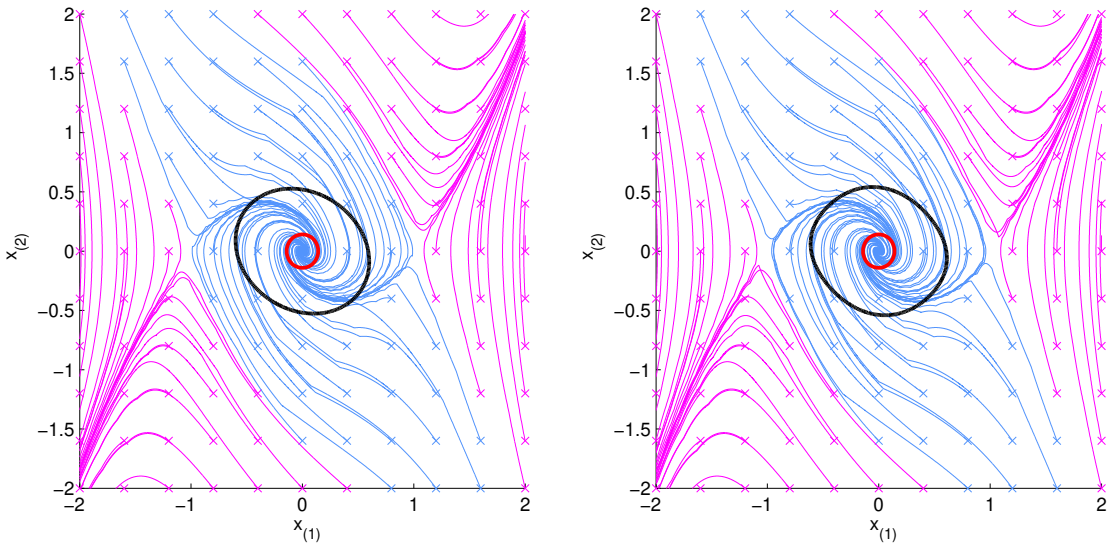


a) Quadratic, OP (4.30) b) Bi-quadratic, OP (4.31)

Figure 4.2: Example 1 – Phase portraits with $P_0 = 50I$ – emulation.

Tables 4.4 and 4.5 present the average number of events and the minimum inter-event times for 200 initial conditions inside $\mathcal{X}_0$. It can be seen that there are no sensible changes for $P_0 = 4I$ when compared to the results obtained for $P_0 = 50I$ shown previously. In this case, the increment in $\mathcal{X}_0$ size has not represented an additional constraint for this particular system and the optimization problem yields essentially the same results as for $P_0 = 50I$. On the other hand, when we consider $P_0 = 2.8I$, we are effectively asking more from the system and, in this case, the average number of events increases and the minimum inter-event times decreases. This illustrates a trade-off between the size of the region of certified asymptotic stability and the performance of the event-triggered control in terms of the number of events. If larger regions are considered, more events and smaller minimum inter-event times are expected.

It can be seem also that, in this case, the quadratic Lyapunov function gave better results than the bi-quadratic for $P_0 = 2.8I$. Note that the conditions for the quadratic Lyapunov function cannot be obtained as a particular case of those for the bi-quadratic. This explains why sometimes the quadratic can outperform the bi-quadratic.

Table 4.4: Example 1 – Events information for $P_0 = 4I$.

| | Quadratic, OP (4.30) | Bi-quadratic, OP (4.31) |
|---|---|---|
| Average number of events | 61.05 | 55.66 |
| Minimum inter-event time | 144 | 160 |

Table 4.5: Example 1 – Events information for $P_0 = 2.8I$.

| | Quadratic, OP (4.30) | Bi-quadratic, OP (4.31) |
|---|---|---|
| Average number of events | 70.89 | 84.12 |
| Minimum inter-event time | 99 | 70 |

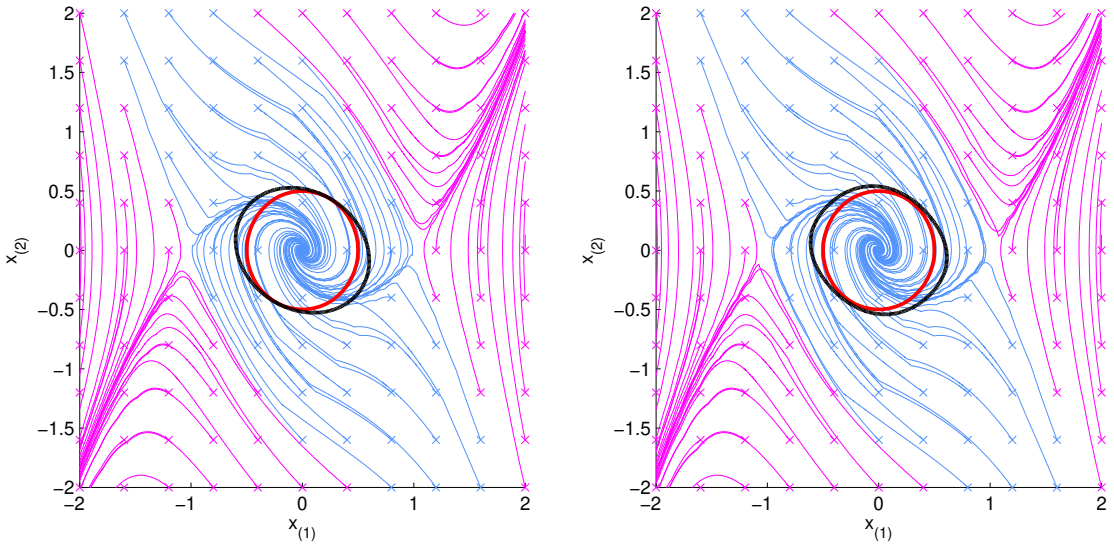


a) Quadratic, OP (4.30) b) Bi-quadratic, OP (4.31)

Figure 4.3: Example 1 – Phase portraits with $P_0 = 4I$ – emulation.

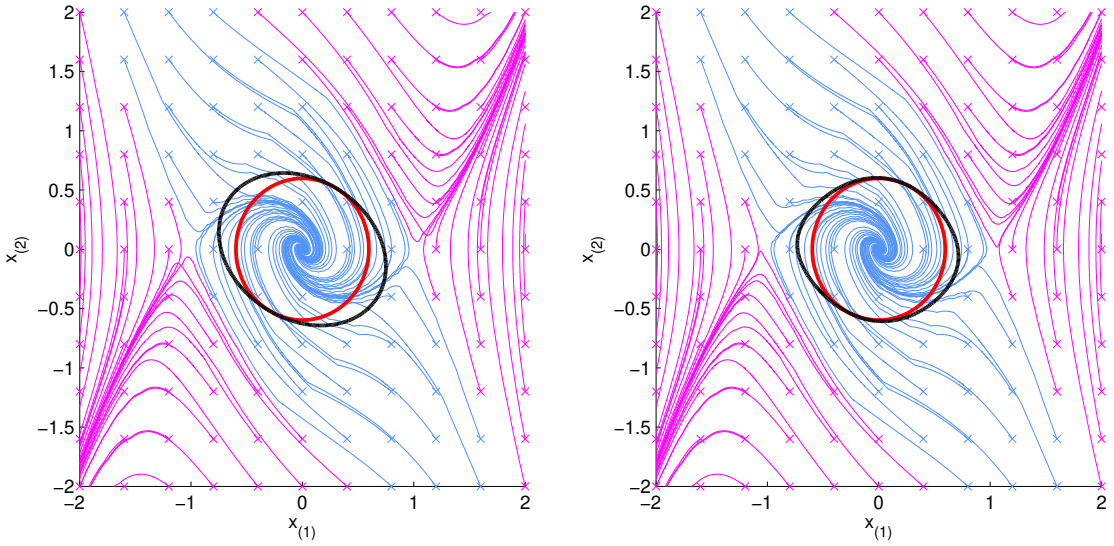


a) Quadratic, OP (4.30) b) Bi-quadratic, OP (4.31)

Figure 4.4: Example 1 – Phase portraits with $P_0 = 2.8I$ – emulation.

### 4.4.2 Example 2 – Rational system

In this example we consider the following plant:

$$\begin{cases} \dot{x}_{(1)}(t) = \dfrac{1 + x_{(1)}^2(t)}{2} x_{(2)}(t) \\ \dot{x}_{(2)}(t) = \dfrac{2}{1 + x_{(1)}^2(t)} x_{(1)}(t) - x_{(2)}(t) - \dfrac{1 - x_{(1)}^2(t)}{1 + x_{(1)}^2(t)} u(t) \end{cases} \tag{4.36}$$

where $x = [x_{(1)}\ x_{(2)}]' \in \mathbb{R}^2$ is the state of the plant. This system models the rotational motion of a cart with an inverted pendulum after some variable changes to convert the system from transcendental into rational (see (COUTINHO; GOMES DA SILVA JR., 2010) for the details).

Considering a linearization of the system around the origin, we designed the controller gain matrix $K = \begin{bmatrix} 20 & 13 \end{bmatrix}$, which stabilizes the origin asymptotically. Then we considered the following matrices for the DAR (4.3):

$$\xi(x, \delta) = \begin{bmatrix} x_{(1)}x_{(2)} & \frac{x_{(1)}}{1+x_{(1)}^2} & \frac{x_{(1)}^2}{1+x_{(1)}^2} & \frac{K(x+\delta)}{1+x_{(1)}^2} & \frac{x_{(1)}K(x+\delta)}{1+x_{(1)}^2} \end{bmatrix}'$$

and

$$A_1 = \begin{bmatrix} 0 & 0.5 \\ -20 & -14 \end{bmatrix} \qquad A_2 = \begin{bmatrix} 0.5x_{(1)} & 0 & 0 & 0 & 0 \\ 0 & 2 & 0 & 0 & 2x_{(1)} \end{bmatrix} \qquad A_3 = \begin{bmatrix} 0 & 0 \\ -20 & -13 \end{bmatrix}$$

$$\Omega_1 = \begin{bmatrix} -x_{(2)} & 0 \\ -1 & 0 \\ 0 & 0 \\ -20 & -13 \\ 0 & 0 \end{bmatrix} \qquad \Omega_2 = \begin{bmatrix} 1 & 0 & 0 & 0 & 0 \\ 0 & 1 & x_{(1)} & 0 & 0 \\ 0 & -x_{(1)} & 1 & 0 & 0 \\ 0 & 0 & 0 & 1 & x_{(1)} \\ 0 & 0 & 0 & -x_{(1)} & 1 \end{bmatrix} \qquad \Omega_3 = \begin{bmatrix} 0 & 0 \\ 0 & 0 \\ 0 & 0 \\ -20 & -13 \\ 0 & 0 \end{bmatrix}$$

Considering $\mathcal{B}_x = \{x \in \mathbb{R}^2 : |x_{(i)}| < \rho;\ \rho \in \mathbb{R}^+\}$ and $\mathcal{X}_0 = \{x \in \mathbb{R}^2 : x'P_0x \leq 1\}$, with $P_0 = 50I$, optimization problems (4.30) and (4.31) are solved for various values of $\rho$. For problem (4.31), we consider a bi-quadratic Lyapunov function with $\theta$ and representations (4.14) and (4.15) as defined in the previous example. To prevent $Q_\delta$ from becoming ill-conditioned, the additional restriction of $Q_\delta < 0.0001I$ is considered. The results are shown in Table 4.6. One can see that, in terms of the value of the objective function, once again, the use of bi-quadratic Lyapunov functions yields the best results.

Considering the event generator with the parameter values corresponding to the best objective in each case (i.e. $\rho = 0.86$ for the quadratic case and $\rho = 0.89$ for the bi-quadratic case, which leads to the matrices depicted in Table 4.7) and simulating the closed-loop systems with these settings, one obtains the results shown in figures 4.5 and 4.6.

In Figure 4.5, the top plots show the evolution of the state for an initial condition $x(0) = [0.1\ 0.1]'$. The dashed lines represent the state of the corresponding continuous-time system, i.e. considering the direct connection between plant and controller, without the event-triggering mechanism. The performance of the event-triggered system is very similar to the performance of the continuous-time system in all cases considered. The control signals, depicted in the middle plots, are also very similar between the continuous-time and the event-triggered implementations, without no substantial increase in the control effort in the event-triggered cases. The bottom plots show the instants when the events

Table 4.6: Example 2 – Linear search on $\mathcal{B}_x$ size for different Lyapunov functions.

| $\rho$ | Objective function value | |
|---|---|---|
| | Quadratic, OP (4.30) | Bi-quadratic, OP (4.31) |
| 0.75 | 41.2070 | 41.7787 |
| 0.80 | 37.7597 | 37.9668 |
| 0.81 | 37.2467 | 37.3400 |
| 0.82 | 36.7917 | 36.7611 |
| 0.83 | 36.4265 | 36.2325 |
| 0.84 | 36.1265 | 35.7585 |
| 0.85 | 35.9383 | 35.3454 |
| 0.86 | **35.8686** | 35.0018 |
| 0.87 | 35.9433 | 34.7395 |
| 0.88 | 36.2024 | 34.5780 |
| 0.89 | 36.7390 | **34.5533** |
| 0.90 | 37.6713 | 34.7214 |
| 0.91 | 39.2032 | 35.1807 |
| 0.95 | unfeasible | unfeasible |

Table 4.7: Example 2 – Matrices obtained from the optimization problems with different Lyapunov functions.

| | Quadratic, OP (4.30) | Bi-quadratic, OP (4.31) |
|---|---|---|
| $Q_x$ | $\begin{bmatrix} 1.46 & -0.0740 \\ -0.0740 & 0.802 \end{bmatrix}$ | $\begin{bmatrix} 1.69 & -0.0425 \\ -0.0425 & 0.902 \end{bmatrix}$ |
| $Q_\delta$ | $\begin{bmatrix} 23.9 & 15.5 \\ 15.5 & 10.1 \end{bmatrix}$ | $\begin{bmatrix} 23.1 & 15.0 \\ 15.0 & 9.76 \end{bmatrix}$ |
| $P$ | $\begin{bmatrix} 12.3 & 1.59 \\ 1.59 & 1.56 \end{bmatrix}$ | $\begin{bmatrix} -2.76 & 0.822 & -0.0527 & 0.0187 & 0.0691 \\ 0.822 & 3.26 & -0.0558 & -0.0215 & -0.450 \\ -0.0527 & -0.0558 & -0.00137 & 0.450 & 0.00141 \\ 0.0187 & -0.0215 & 0.450 & 17.0 & 1.41 \\ 0.0691 & -0.450 & 0.00141 & 1.41 & 1.51 \end{bmatrix}$ |

occurred. The size of the bars reflect the time elapsed since the last event. There are more events during the transient in all cases and the inter-event times become more spaced in steady-state.

Figure 4.6 depicts the set $\mathcal{X}_0$ (in red) along with some convergent (in blue) and divergent (in magenta) trajectories of the event-triggered implementation. Figure 4.7 shows zoomed views around the origin. As in the previous example, the sets $\mathcal{X}_0$ are contained in $\mathcal{L}_V(1)$ and in the domains of attraction, as expected.

Computing the average number of events and the minimum inter-event time for 200 initial conditions inside $\mathcal{X}_0$ and considering $t \in [0, 10]$, we obtain the results summarized in Table 4.8. These results show again that the use of a bi-quadratic Lyapunov function slightly reduced the average number of events and increased the minimum inter-event time.

Table 4.8: Example 2 – Comparison of event-trigger effectiveness.

| | Quadratic, OP (4.30) | Bi-quadratic, OP (4.31) |
|---|---|---|
| Average number of events | 9.84 | 9.31 |
| Minimum inter-event time | 14 | 15 |

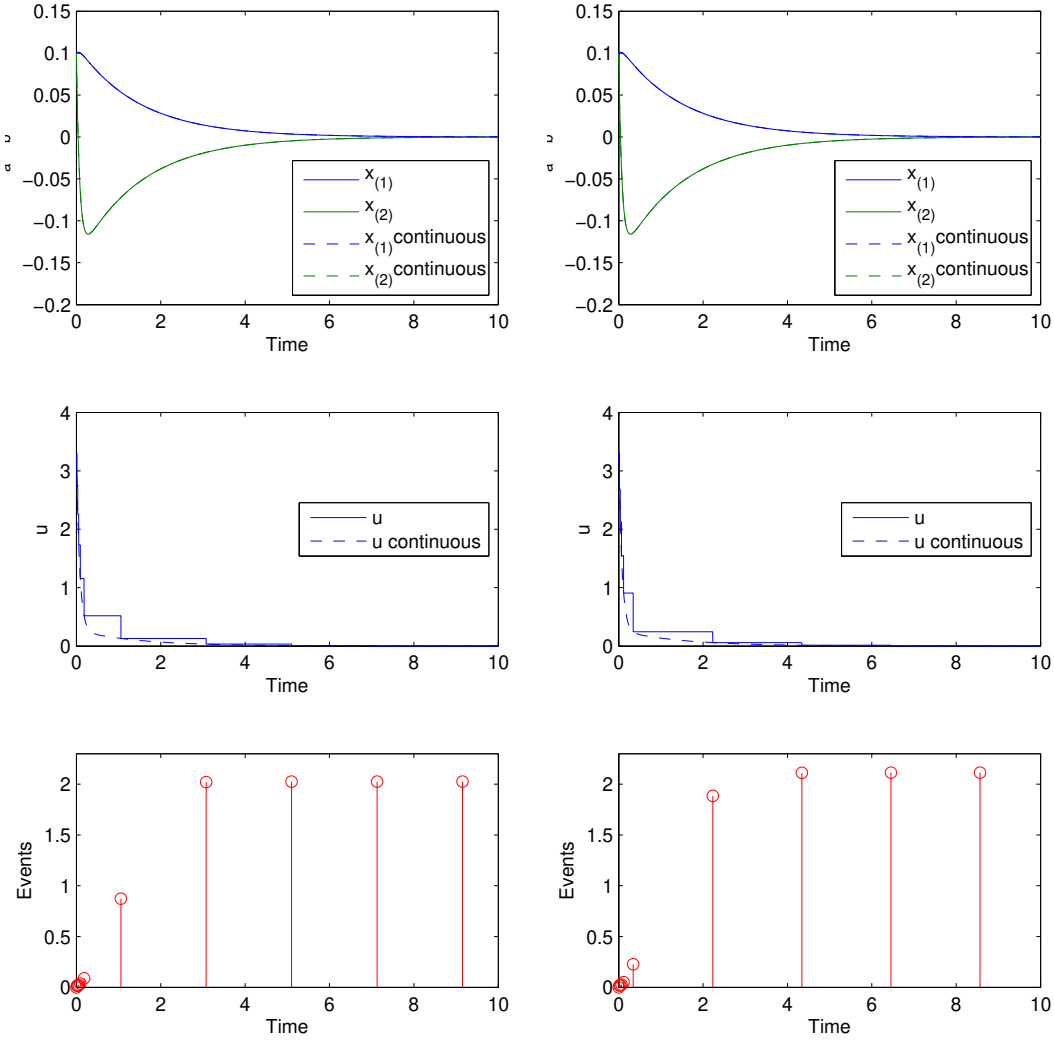


a) Quadratic, OP (4.30)

b) Bi-quadratic, OP (4.31)

Figure 4.5: Example 2 – Simulations for $x(0) = [0.1\ 0.1]'$ – emulation.

#### *4.4.2.1 Influence of $\mathcal{X}_0$ size*

In this section, we assess the influence of $\mathcal{X}_0$ size. We set $P_0 = \alpha I$ for various values of the positive scalar $\alpha$, solve the optimization problems (4.30) and (4.31), for quadratic and bi-quadratic Lyapunov functions, respectively, and evaluate the average and minimum inter-event times from simulations considering 200 initial conditions inside $\mathcal{X}_0$. The results are shown in tables 4.9 and 4.10. One can observe again that the average number of events tends to increase and the minimum inter-event time decreases as the size of $\mathcal{X}_0$ increases.

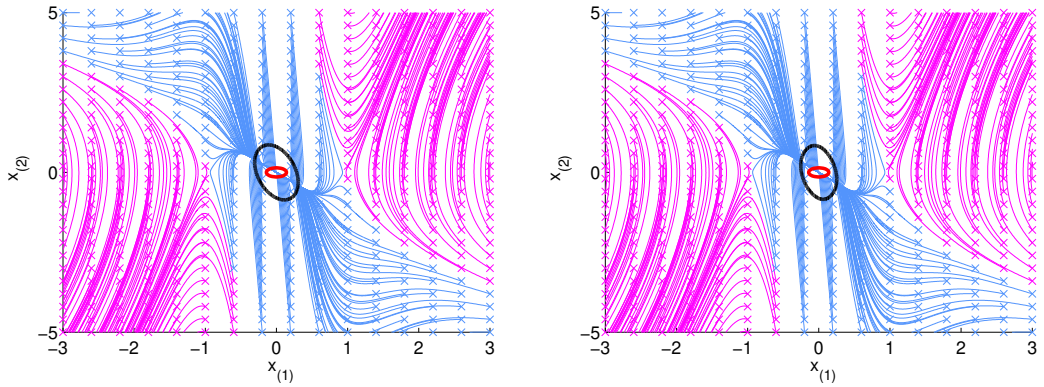


a) Quadratic, OP (4.30) b) Bi-quadratic, OP (4.31)

Figure 4.6: Example 2 – Phase portraits – emulation.

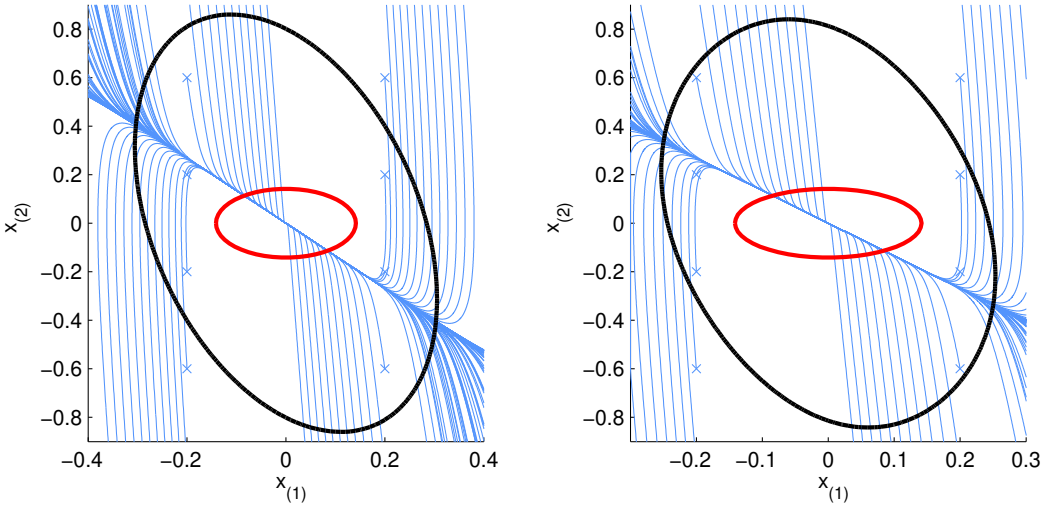


a) Quadratic, OP (4.30) b) Bi-quadratic, OP (4.31)

Figure 4.7: Example 2 – Phase portraits (Zoom)– emulation.

Table 4.9: Example 2 – Influence of $\mathcal{X}_0$ size – Quadratic Lyapunov function.

| $\alpha$ | Average number of events | Minimum inter-event time |
|---|---|---|
| 25 | 9.84 | 14 |
| 12 | 10.00 | 14 |
| 8 | 12.31 | 14 |
| 6 | 17.95 | 11 |

Table 4.10: Example 2 – Influence of $\mathcal{X}_0$ size – Bi-quadratic Lyapunov function.

| $\alpha$ | Average number of events | Minimum inter-event time |
|---|---|---|
| 25 | 9.33 | 15 |
| 12 | 10.29 | 14 |
| 8 | 13.87 | 11 |
| 6 | 25.93 | 7 |

### 4.4.3 Example 3 – Lorenz system

The Lorenz system (LORENZ, 1963) is a classical dynamical system that features chaotic behavior. It is a third-order polynomial system, represented by the following equation:

$$\begin{cases} \dot{x}_{(1)} = \sigma(x_{(2)} - x_{(1)}) \\ \dot{x}_{(2)} = x_{(1)}(\nu - x_{(3)}) - x_{(2)} + u \\ \dot{x}_{(3)} = x_{(1)}x_{(2)} - \beta x_{(3)} \end{cases} \tag{4.37}$$

where $x = [x_{(1)}\ x_{(2)}\ x_{(3)}]' \in \mathbb{R}^3$ is the state and $u \in \mathbb{R}$ is the control input. $\sigma$, $\nu$ and $\beta$ are positive scalar parameters. In this text we will consider $\sigma = 10$, $\nu = 28$ and $\beta = 8/3$, which leads to chaotic behavior when $u = 0$.

We consider the stabilizing gain $K = \begin{bmatrix} -29 & 0 & 0 \end{bmatrix}$, $\xi(x, \delta) = x_{(1)}$ and the following matrices for DAR (4.3):

$$A_1 = \begin{bmatrix} -10 & 10 & 0 \\ -1 & -1 & 0 \\ 0 & 0 & -2.67 \end{bmatrix} \qquad A_2 = \begin{bmatrix} 0 \\ -x_{(3)} \\ x_{(2)} \end{bmatrix} \qquad A_3 = \begin{bmatrix} 0 & 0 & 0 \\ -29 & 0 & 0 \\ 0 & 0 & 0 \end{bmatrix}$$

$$\Omega_1 = \begin{bmatrix} 1 & 0 & 0 \end{bmatrix} \qquad \Omega_2 = \begin{bmatrix} -1 \end{bmatrix} \qquad \Omega_3 = \begin{bmatrix} 0 & 0 & 0 \end{bmatrix}$$

As in the previous examples, we assume $\mathcal{B}_x = \{x \in \mathbb{R}^3 : |x_{(i)}| < \rho;\ \rho \in \mathbb{R}^+\}$ and $\mathcal{X}_0 = \{x \in \mathbb{R}^3 : x'P_0x \leq 1\}$, with $P_0 = 50I$.

To consider a bi-quadratic Lyapunov function, since we are dealing with a third-order system, we choose the following structure for $\theta$ and the representations (4.14) and (4.15):

$$\theta = \begin{bmatrix} x_{(1)} \\ x_{(2)} \\ x_{(3)} \\ x_{(1)}^2 \\ x_{(2)}^2 \\ x_{(3)}^2 \\ x_{(1)}x_{(2)} \\ x_{(2)}x_{(3)} \\ x_{(1)}x_{(3)} \end{bmatrix} \qquad \dot{\theta} = \begin{bmatrix} \dot{x}_{(1)} \\ \dot{x}_{(2)} \\ \dot{x}_{(3)} \\ 2x_{(1)}\dot{x}_{(1)} \\ 2x_{(2)}\dot{x}_{(2)} \\ 2x_{(3)}\dot{x}_{(3)} \\ x_{(1)}\dot{x}_{(2)} + x_{(2)}\dot{x}_{(1)} \\ x_{(2)}\dot{x}_{(3)} + x_{(3)}\dot{x}_{(2)} \\ x_{(1)}\dot{x}_{(3)} + x_{(3)}\dot{x}_{(1)} \end{bmatrix} \qquad \xi_\theta = \begin{bmatrix} x_{(1)}^2 \\ x_{(2)}^2 \\ x_{(3)}^2 \\ x_{(1)}x_{(2)} \\ x_{(2)}x_{(3)} \\ x_{(1)}x_{(3)} \end{bmatrix} \qquad \xi_{\dot{\theta}} = \begin{bmatrix} x_{(1)}\dot{x}_{(1)} \\ x_{(2)}\dot{x}_{(2)} \\ x_{(3)}\dot{x}_{(3)} \\ x_{(1)}\dot{x}_{(2)} \\ x_{(2)}\dot{x}_{(1)} \\ x_{(2)}\dot{x}_{(3)} \\ x_{(3)}\dot{x}_{(2)} \\ x_{(1)}\dot{x}_{(3)} \\ x_{(3)}\dot{x}_{(1)} \end{bmatrix}$$

$$E_1 = \begin{bmatrix} 1 & 0 & 0 \\ 0 & 1 & 0 \\ 0 & 0 & 1 \\ 0 & 0 & 0 \\ 0 & 0 & 0 \\ 0 & 0 & 0 \\ 0 & 0 & 0 \\ 0 & 0 & 0 \\ 0 & 0 & 0 \end{bmatrix} \qquad E_2 = \begin{bmatrix} 0 & 0 & 0 & 0 & 0 & 0 \\ 0 & 0 & 0 & 0 & 0 & 0 \\ 0 & 0 & 0 & 0 & 0 & 0 \\ 1 & 0 & 0 & 0 & 0 & 0 \\ 0 & 1 & 0 & 0 & 0 & 0 \\ 0 & 0 & 1 & 0 & 0 & 0 \\ 0 & 0 & 0 & 1 & 0 & 0 \\ 0 & 0 & 0 & 0 & 1 & 0 \\ 0 & 0 & 0 & 0 & 0 & 1 \end{bmatrix}$$

$$\Gamma_1 = \begin{bmatrix} x_{(1)} & 0 & 0 \\ 0 & x_{(2)} & 0 \\ 0 & 0 & x_{(3)} \\ 0 & x_{(1)} & 0 \\ 0 & 0 & x_{(2)} \\ 0 & 0 & x_{(1)} \end{bmatrix} \qquad \Gamma_2 = \begin{bmatrix} -1 & 0 & 0 & 0 & 0 & 0 \\ 0 & -1 & 0 & 0 & 0 & 0 \\ 0 & 0 & -1 & 0 & 0 & 0 \\ 0 & 0 & 0 & -1 & 0 & 0 \\ 0 & 0 & 0 & 0 & -1 & 0 \\ 0 & 0 & 0 & 0 & 0 & -1 \end{bmatrix}$$

$$F_1 = \begin{bmatrix} 1 & 0 & 0 \\ 0 & 1 & 0 \\ 0 & 0 & 1 \\ 0 & 0 & 0 \\ 0 & 0 & 0 \\ 0 & 0 & 0 \\ 0 & 0 & 0 \\ 0 & 0 & 0 \\ 0 & 0 & 0 \end{bmatrix} \qquad F_2 = \begin{bmatrix} 0 & 0 & 0 & 0 & 0 & 0 & 0 & 0 & 0 \\ 0 & 0 & 0 & 0 & 0 & 0 & 0 & 0 & 0 \\ 0 & 0 & 0 & 0 & 0 & 0 & 0 & 0 & 0 \\ 2 & 0 & 0 & 0 & 0 & 0 & 0 & 0 & 0 \\ 0 & 2 & 0 & 0 & 0 & 0 & 0 & 0 & 0 \\ 0 & 0 & 2 & 0 & 0 & 0 & 0 & 0 & 0 \\ 0 & 0 & 0 & 1 & 1 & 0 & 0 & 0 & 0 \\ 0 & 0 & 0 & 0 & 0 & 1 & 1 & 0 & 0 \\ 0 & 0 & 0 & 0 & 0 & 0 & 0 & 1 & 1 \end{bmatrix}$$

$$\Phi_1 = \begin{bmatrix} x_{(1)} & 0 & 0 \\ 0 & x_{(2)} & 0 \\ 0 & 0 & x_{(3)} \\ 0 & x_{(1)} & 0 \\ x_{(2)} & 0 & 0 \\ 0 & 0 & x_{(2)} \\ 0 & x_{(3)} & 0 \\ 0 & 0 & x_{(1)} \\ x_{(3)} & 0 & 0 \end{bmatrix} \qquad \Phi_2 = \begin{bmatrix} -1 & 0 & 0 & 0 & 0 & 0 & 0 & 0 & 0 \\ 0 & -1 & 0 & 0 & 0 & 0 & 0 & 0 & 0 \\ 0 & 0 & -1 & 0 & 0 & 0 & 0 & 0 & 0 \\ 0 & 0 & 0 & -1 & 0 & 0 & 0 & 0 & 0 \\ 0 & 0 & 0 & 0 & -1 & 0 & 0 & 0 & 0 \\ 0 & 0 & 0 & 0 & 0 & -1 & 0 & 0 & 0 \\ 0 & 0 & 0 & 0 & 0 & 0 & -1 & 0 & 0 \\ 0 & 0 & 0 & 0 & 0 & 0 & 0 & -1 & 0 \\ 0 & 0 & 0 & 0 & 0 & 0 & 0 & 0 & -1 \end{bmatrix}$$

As one can see, the dimensions of the optimization problem increase quickly with the order of the system when rational Lyapunov functions are considered. In this case, we increased the order of the system from two (in the previous examples) to three and, even using a relatively simple bi-quadratic Lyapunov function, the number of lines of the matrices matrices in the DARs ($E_1$, $E_2$, $F_1$, $F_2$, etc.) increased from 5 to 9, complexifying the optimization problem that needs to be solved. The additional complexity comes from the fact that the number of optimization variables increases from 951 (for the second-order systems) to 2463 (for the third-order system) and that the number of constraints also increases due to the larger number of vertices and faces. This constitutes the main drawback of the use of more complex underlying Lyapunov functions. In the example at hand, attempts to solve optimization problem (4.31) with the formulation above did not complete within 96 hours [3] for the first value of $\rho$. Since we need to execute a line search over $\rho$, the use of bi-quadratic Lyapunov functions for this example was considered too computationally demanding to be worth. Moreover, comparing the optimization problems with quadratic and bi-quadratic Lyapunov functions for the system at hand, the former features 96 decision variables while the later features 2463, showing how more computationally demanding the problem based on bi-quadratic can be. Hence, we will consider here only quadratic Lyapunov functions and optimization problem (4.30). Solving it with different values of $\rho$ and the additional condition $Q_\delta < 0.0001I$ to prevent $Q_\delta$ from becoming ill-conditioned, we obtain the results depicted in Table 4.11. The line

[3] Using a personal computer with Intel Core i7-4770 8-Core 3.4 GHz CPU, 8 MB cache, 8 GB of memory.

in boldface corresponds to the best value found for the objective function, obtained with $\rho = 4.80$.

Table 4.11: Example 3 – Linear search over $\mathcal{B}_x$ size.

| $\rho$ | Objective function $\mathrm{tr}(Q_\delta + \bar{Q}_x)$ |
|---|---|
| 0.14 | unfeasible |
| 0.20 | $1.149 \cdot 10^4$ |
| 1.00 | 249.3 |
| 4.50 | 51.32 |
| 4.60 | 51.29 |
| 4.70 | 51.27 |
| **4.80** | **51.26** |
| 4.90 | 51.28 |
| 5.00 | 51.31 |
| 10.0 | 57.81 |
| 100 | 72.78 |

With $\rho = 4.80$, the optimization problem yields:

$$Q_x = \begin{bmatrix} 0.292 & -0.219 & -1.44 \cdot 10^{-8} \\ -0.219 & 0.263 & 7.33 \cdot 10^{-9} \\ -1.44 \cdot 10^{-8} & 7.33 \cdot 10^{-9} & 0.248 \end{bmatrix}$$

$$Q_\delta = \begin{bmatrix} 28 & 0 & 0 \\ 0 & 0.000104 & 0 \\ 0 & 0 & 0.000104 \end{bmatrix}$$

$$P = \begin{bmatrix} 0.071 & -0.0598 & 4.38 \cdot 10^{-9} \\ -0.0598 & 0.129 & -3.54 \cdot 10^{-9} \\ 4.38 \cdot 10^{-9} & -3.54 \cdot 10^{-9} & 0.0747 \end{bmatrix}$$

Figure 4.8 depicts simulations of the closed-loop system considering $x(0) = \begin{bmatrix} 0.08 & 0.08 & 0.08 \end{bmatrix}'$. The top plot shows, in solid lines, the state of the event-triggered implementation and, in dashed lines, the state of an equivalent (in the sense that it has the same control law) continuous-time implementation of the system. One can see that the event-triggered control in this case leads to more sensible differences with respect to the continuous-time implementation. The middle plot depicts the control signals for the event-triggered implementation, again in solid line, and the equivalent continuous-time implementation in dashed line. The plot at the bottom shows the event instants. During the time interval $[0, 4]$, 98 events were generated and the minimum inter-events time was of 24 ms. Simulating the event-triggered implementation for 400 initial conditions on the border of $\mathcal{X}_0$, the average number of events is 115.8 and the minimum inter-events time observed is 9 ms.

Figure 4.9 depicts the set $\mathcal{X}_0$ in green and the ellipsoid $\mathcal{E}(P)$ in red. One can observe that $\mathcal{X}_0 \subset \mathcal{E}(P)$ as imposed by the conditions in the optimization problem. Indeed, $\mathcal{E}(P)$ is much bigger than $\mathcal{X}_0$.

#### *4.4.3.1 Influence of $\mathcal{X}_0$ size*

Now we consider larger sets $\mathcal{X}_0$, by choosing $P_0 = \alpha I$ for various values of the positive scalar $\alpha$. Table 4.12 presents the average number of events and the minimum

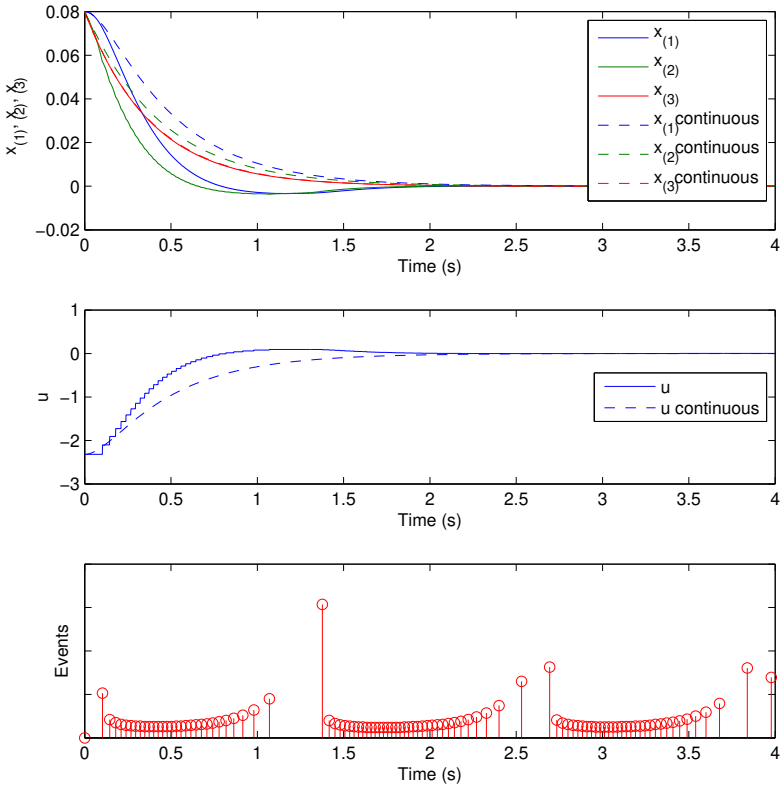


Figure 4.8: Example 3 – Simulation for $x(0) = [0.08\ 0.08\ 0.08]'$ – emulation.

inter-event times obtained from simulations considering 400 initial conditions on the border of $\mathcal{X}_0$. One can observe again that the average number of events tends to increase and the minimum inter-event time decreases as the size of $\mathcal{X}_0$ increases.

Table 4.12: Example 3 – Influence of $\mathcal{X}_0$ size.

| $\alpha$ | Average number of events | Minimum inter-event time |
|---|---|---|
| 4.00 | 114.5 | 10 |
| 0.10 | 111.2 | 7 |
| 0.01 | 131.2 | 3 |
| 0.001 | 202.0 | 1 |

## 4.5 Conclusion

In this chapter we addressed the emulation problem for the class of rational systems. We established asymptotic stability conditions in the form of LMIs that allow to compute the parameters of the triggering condition considering a given state-feedback control law that stabilizes the origin of the continuous-time nonlinear system. These conditions were cast into convex optimization problems proposed as means of computing the event generator parameters $Q_\delta$ and $Q_x$.

We considered quadratic and rational underlying Lyapunov functions and we illustrated, by means of numerical experiments, that with the use of more complex Lyapunov functions (bi-quadratic, in the experiments) trigger functions leading to less events gener-

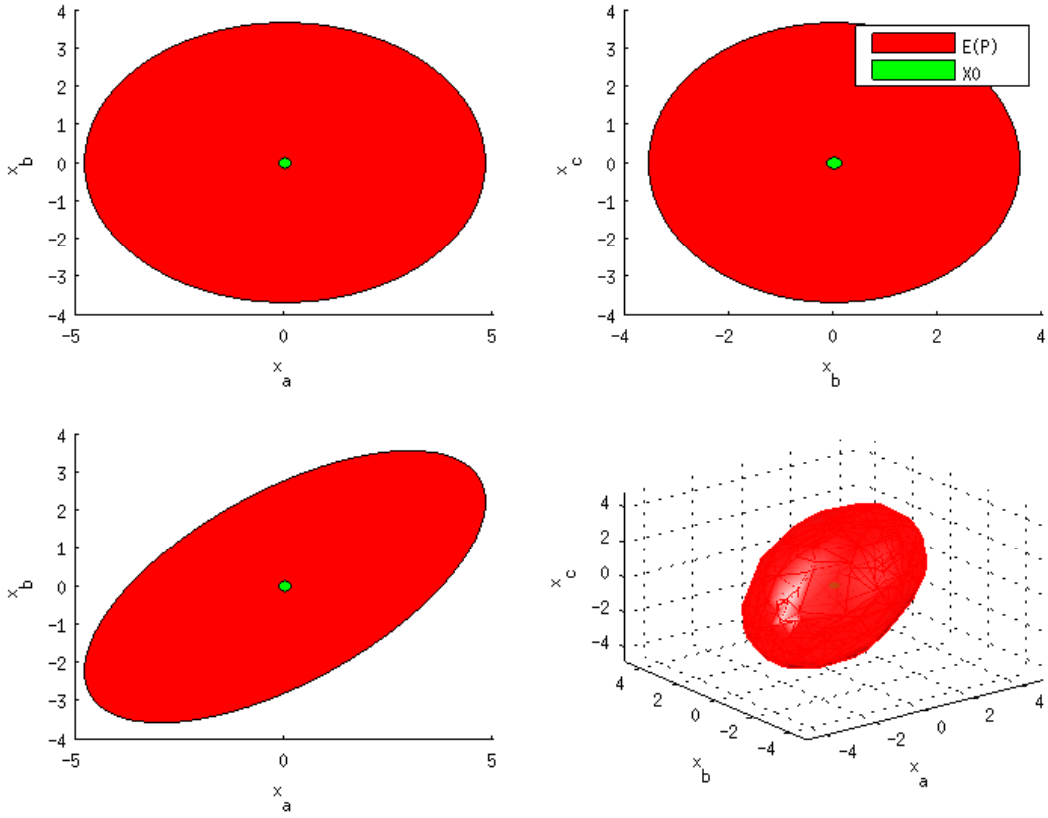


Figure 4.9: Example 3 – $\mathcal{E}(P)$ and $\mathcal{X}_0$.

ation can be obtained. The more complex Lyapunov functions do not impose additional online computation burden (i.e. computational complexity in the event generator) but highly increase the off-line computational burden, i.e. the complexity of the optimization problem that one needs to solve to compute the event generator parameters. It was shown that even considering a third-order polynomial system and a bi-quadratic Lyapunov function, the optimization problems can scale to a complexity that renders difficult to solve them using ordinary equipment. Thus, from this point, we will consider only quadratic Lyapunov functions.

Compared to other approaches in the event-triggered control for nonlinear systems literature, the proposed approach has the following advantages: It provides a systematic method for designing of the event-triggering condition parameters and, in the co-design case, also the control law. The underlying Lyapunov function does not need to be designed *a priori*, since it is implicitly computed as part of the method. The method certifies a set of initial conditions where convergence to the origin is ensured, ensuring that this set represents a region of safe operation of the system. It was shown that there is a trade-off between the size of this region and the expected number of events and the minimum inter-event time. As larger sets are considered, initial conditions farther away from the origin are included and these ones will typically require a more effective control action. This translates into smaller inter-event times and, consequently, more events.

The results presented in this chapter considering quadratic Lyapunov functions were published in (MOREIRA; GROFF; GOMES DA SILVA JR., 2016b) and (MOREIRA et al., 2017a).

# 5 CO-DESIGN

In this chapter, we address Problem 3.2, i.e. the simultaneous design of the control law gain $K$ and the event generator parameters $Q_x$ and $Q_\delta$. We consider again the trigger condition described by Algorithm 5 and the system (3.7), whose representation is recalled here for the reader's convenience:

$$\begin{cases} \dot{x}(t) = f(x(t)) + g(x(t))u(t) \\ u(t) = Kx(t_k) \qquad \forall t \in [t_k, t_{k+1}) \end{cases} \tag{5.1}$$

We assume again that the set of initial conditions where we want to ensure asymptotic stability is given by $\mathcal{X}_0 = \{x \in \mathbb{R}^n : x'P_0x \leq 1\}$, with $P_0$ being a symmetric positive-definite matrix.

Recalling that $\delta(t) = x(t_k) - x(t)$, here we slightly change the DAR so that we have $K$ explicitly in the representation as follows:

$$\begin{cases} \dot{x} = (A_1(x) + A_3(x)K)\, x + A_2(x)\xi(x,\delta) + A_3(x)K\delta \\ 0 = (\Omega_1(x) + \Omega_3(x)K)\, x + \Omega_2(x)\xi(x,\delta) + \Omega_3(x)K\delta \end{cases} \tag{5.2}$$

with $\xi(x,\delta) \in \mathbb{R}^q$ being an auxiliary variable vector containing the polynomial and rational terms of $f(x)$ and of $g(x)K(x+\delta)$; $A_1(x) \in \mathbb{R}^{n\times n}$, $A_2(x) \in \mathbb{R}^{n\times q}$, $A_3(x) \in \mathbb{R}^{n\times m}$, $\Omega_1(x) \in \mathbb{R}^{q\times n}$, $\Omega_2(x) \in \mathbb{R}^{q\times q}$ and $\Omega_3(x) \in \mathbb{R}^{q\times m}$ being affine matrix functions of $x$. We assume again that $\Omega_2(x)$ is full column rank $\forall x \in \mathcal{B}_x$.

## 5.1 Stability conditions

Here we consider a Lyapunov function candidate and design simultaneously the event generator parameters (i.e. $Q_\delta$ and $Q_x$) and the gain matrix $K$ so that the time derivative of the Lyapunov function is negative along the trajectories of the system.

Differently from the emulation design, here we will consider only the quadratic Lyapunov functions. The extension to rational Lyapunov functions using the same ideas applied for the emulation design is not difficult from a theoretical perspective, but the computational complexity of the resulting conditions does not seem to justify the possible gains in performance, as discussed in the previous chapter.

Also differently from the emulation, here we do not use annihilators. If one uses them in a context where $K$ is variable, like in the co-design, it is not possible to obtain stability conditions that are affine with respect to the decision variables due to the terms $L\mathscr{N}_2(x)$ and $\mathscr{N}_2'(x)L'$ [1]. As an alternative to reduce conservatism, we are going to use particular

[1] When $K$ is a decision variable, $\mathscr{N}_1(x)$ depends on $K$, and, as a consequence, $\mathscr{N}_2(x)$ also depends on $K$. Therefore, the terms $L\mathscr{N}_2(x)$ and $\mathscr{N}_2'(x)L'$ become bilinear.

multipliers similar to those in (OLIVEIRA; GOMES DA SILVA JR.; COUTINHO, 2012; OLIVEIRA, 2012).

The following theorem was developed as original research for this thesis and provides sufficient stability conditions in the co-design context.

**Theorem 5.1.** *Consider a DAR* (5.2) *for system* (5.1)*, valid in the region of interest $\mathcal{B}_x$, defined as in* (4.4)*. If there exist constant positive-definite matrices $\bar{Q}_x, \bar{Q}_\delta, N_2 \in \mathbb{R}^{n\times n}$ and constant matrices $N_1 \in \mathbb{R}^{n\times n}$, $N_3 \in \mathbb{R}^{q\times q}$ and $Y \in \mathbb{R}^{n\times m}$ such that the following inequalities are satisfied $\forall x \in \mathrm{Ver}(\mathcal{B}_x)$:*

$$\begin{bmatrix} \psi_a & \psi_b & \psi_c & A_3(x)Y' & N_2 \\ * & -\mathrm{He}\{N_1\} & A_2(x)N_3' & A_3(x)Y' & 0 \\ * & * & \mathrm{He}\{\Omega_2(x)N_3'\} & \Omega_3(x)Y' & 0 \\ * & * & * & -\bar{Q}_\delta & 0 \\ * & * & * & * & -\bar{Q}_x \end{bmatrix} < 0 \tag{5.3}$$

$$\begin{bmatrix} N_2 & N_2 h_i \\ h_i' N_2 & \rho_i^2 \end{bmatrix} > 0, \quad i = 1 \dots n_f \tag{5.4}$$

*with*

$$\begin{aligned} \psi_a &= \mathrm{He}\{A_1(x)N_2' + A_3(x)Y'\} \\ \psi_b &= N_2 A_1'(x) + Y A_3'(x) \\ \psi_c &= A_2(x)N_3' + N_2\Omega_1'(x) + Y\Omega_3'(x) \end{aligned}$$

*then the origin of system* (5.1) *with $K = YN_2^{-1}$, under the event triggering strategy given by Algorithm 5 with $Q_x = \bar{Q}_x^{-1}$ and $Q_\delta = N_2^{-1}\bar{Q}_\delta N_2^{-1}$, is asymptotically stable and $\mathcal{E}(N_2^{-1}) = \{x \in \mathbb{R}^n : x'N_2^{-1}x \leq 1\}$ is contained in its region of attraction, i.e. $\forall x(0) \in \mathcal{E}(N_2^{-1})$, $x(t) \to 0$ when $t \to \infty$.*

*Proof.* Observe that the terms of (5.2) can be re-arranged as follows:

$$\begin{cases} -\dot{x} + (A_1 + A_3K)x + A_2\xi + A_3K\delta = 0 \\ (\Omega_1 + \Omega_3K)x + \Omega_2\xi + \Omega_3K\delta = 0 \end{cases} \tag{5.5}$$

For simplicity, the dependence on $x$ in the matrix functions was omitted. Then, from (5.5), one can derive the following relations:

$$\begin{aligned} \beta_1 &= \dot{x}'M_1(-\dot{x} + (A_1 + A_3K)x + A_2\xi + A_3K\delta) = 0, \quad \forall M_1 \in \mathbb{R}^{n\times n} \\ \beta_2 &= x'M_2(-\dot{x} + (A_1 + A_3K)x + A_2\xi + A_3K\delta) = 0, \quad \forall M_2 \in \mathbb{R}^{n\times n} \\ \beta_3 &= \xi'M_3((\Omega_1 + \Omega_3K)x + \Omega_2\xi + \Omega_3K\delta) = 0, \qquad \forall M_3 \in \mathbb{R}^{q\times q} \end{aligned} \tag{5.6}$$

Consider now a quadratic Lyapunov function $V(x) = x'Px$, with symmetric positive-definite $P$. Defining $\zeta = \begin{bmatrix} x' & \dot{x}' & \xi' & \delta' \end{bmatrix}'$ and considering $\beta_1$, $\beta_2$ and $\beta_3$ as above, one can write $\dot{V}(x)$ as:

$$\begin{aligned} \dot{V}(x) &= \dot{V}(x) + 2\beta_1 + 2\beta_2 + 2\beta_3 = \\ &= \zeta' \begin{bmatrix} \psi_1 & \psi_2 & \psi_3 & M_2A_3K \\ * & -\mathrm{He}\{M_1\} & M_1A_2 & M_1A_3K \\ * & * & \mathrm{He}\{M_3\Omega_2\} & M_3\Omega_3K \\ * & * & * & 0 \end{bmatrix} \zeta \end{aligned} \tag{5.7}$$

with

$$\begin{aligned}\psi_1 &= \mathrm{He}\{M_2(A_1 + A_3K)\}\\ \psi_2 &= P + (A_1 + A_3K)'M_1' - M_2\\ \psi_3 &= M_2A_2 + (\Omega_1 + \Omega_3K)'M_3'\end{aligned}$$

From Algorithm 5, it follows that, along the trajectories of the system, $\delta' Q_\delta \delta - x' Q_x x \leq 0$. Thus, if the following matrix inequality is verified:

$$\begin{bmatrix} \psi_1 + Q_x & \psi_2 & \psi_3 & M_2A_3K \\ * & -\mathrm{He}\{M_1\} & M_1A_2 & M_1A_3K \\ * & * & \mathrm{He}\{M_3\Omega_2\} & M_3\Omega_3K \\ * & * & * & -Q_\delta \end{bmatrix} < 0 \tag{5.8}$$

one ensures $\dot{V}(x) < \delta' Q_\delta \delta - x' Q_x x \leq 0$.

Assuming now that $M_1, M_2, M_3$ are non-singular matrices, define $N_1 = M_1^{-1}$, $N_2 = M_2^{-1}$, $N_3 = M_3^{-1}$. Hence, pre- and post-multiplying (5.8) by $\mathrm{diag}\, N_2, N_1, N_3, N_2$ and $\mathrm{diag}\, N_2', N_1', N_3', N_2'$ respectively, leads to:

$$\begin{bmatrix} \psi_4 & \psi_5 & \psi_6 & A_3KN_2' \\ * & -\mathrm{He}\{N_1\} & A_2N_3' & A_3KN_2' \\ * & * & \mathrm{He}\{\Omega_2N_3'\} & \Omega_3KN_2' \\ * & * & * & -N_2Q_\delta N_2' \end{bmatrix} < 0 \tag{5.9}$$

with

$$\begin{aligned}\psi_4 &= \mathrm{He}\{(A_1 + A_3K)N_2'\} + N_2Q_xN_2'\\ \psi_5 &= N_2PN_1' + N_2(A_1 + A_3K)' - N_1'\\ \psi_6 &= A_2N_3' + N_2(\Omega_1 + \Omega_3K)'\end{aligned}$$

Applying the Schur's complement to the term $\psi_4$, restricting $P = M_2$ (which implies $N_2PN_1' = N_1'$ and $M_2 = M_2' > 0$) and applying the changes of variables $Y = N_2K'$, $\bar{Q}_\delta = N_2Q_\delta N_2'$ one obtains the relation (5.3). Note that, from (5.3) and (5.4), it follows that $\mathrm{He}\{\Omega_2N_3'\} < 0$, $\mathrm{He}(N_1) > 0$ and $N_2 > 0$, which indeed ensure that $M_1$, $M_2$ and $M_3$ are non-singular. Hence, since (5.3) is affine with respect to $x$, by convexity arguments, if it is verified at the vertices of $\mathcal{B}_x$, we can conclude that $\dot{V}(x) < 0, \forall x \in \mathcal{B}_x$ and that the origin is asymptotically stable.

Satisfaction of (5.4) guarantees that $\mathcal{E}(N_2^{-1}) \subset \mathcal{B}_x$, making $\mathcal{E}(N_2^{-1})$ an estimate of the domain of attraction of the origin.

□

**Remark 5.1.** *Since conditions of Theorem 5.1 imply $\dot{V}(x) < 0$ for the particular case where $\delta(t) = 0$, any gain $K$ satisfying these conditions stabilizes a continuous-time implementation of the closed-loop system.*

**Remark 5.2.** *The multipliers used in this section can be seen as a particular form of the multipliers $L$ used in the emulation context, in Chapter 4. Actually, considering the equalities given in* (5.6)*, satisfaction of* (5.3) *implies satisfaction of* (4.5) *with:*

$$L = \begin{bmatrix} \begin{bmatrix} 0 & M_2 \\ 0 & M_1 \\ 0 & 0 \\ 0 & 0 \end{bmatrix} & M_3 \end{bmatrix} \tag{5.10}$$

*The first column of zeros that appear in the relation is due to the absence of the annihilator $\mathscr{N}_0(x)$ and the zeros in the second column are due to the absence of the cross-product of terms.*

**Remark 5.3.** *Notice that $\Psi_a = \mathrm{He}\{A_1(x)N_2' + A_3(x)Y'\} < 0$ is a necessary condition to verify* (5.3)*. This condition is feasible only if the pair $(A_1(x), A_3(x))$ is stabilizable for all $x \in \mathcal{B}_x$.*

## 5.2 Optimization problem

From the definition of Problem 3.2, we aim at designing $K$, $Q_\delta$ and $Q_x$ to ensure the asymptotic stability of the origin in a given set $\mathcal{X}_0$ of initial conditions while reducing the number of events. Once again, we look for $Q_\delta$ as small as possible and $Q_x$ as "large" as possible, but in the current context, considering the stability conditions of Theorem 5.1 and $\mathcal{X}_0 \subset \mathcal{E}(N_2^{-1})$. Assuming that $\mathcal{X}_0 = \{x \in \mathbb{R}^n : x'P_0x \leq 1\}$, with symmetric positive-definite $P_0 \in \mathbb{R}^{n\times n}$, $\mathcal{X}_0 \subset \mathcal{E}(N_2^{-1})$ can be ensured if the condition $N_2 > P_0^{-1}$ is satisfied.

Note however that the event generator parameters $Q_x$ and $Q_\delta$ do not appear explicitly in the stability conditions. Therefore, we need to employ approximations or algebraic manipulations to obtain an appropriate optimization problem. Since $\bar{Q}_x = Q_x^{-1}$ appears in (5.3), we can use the same procedure applied in the emulation design, minimizing $\mathrm{tr}(\bar{Q}_x)$ to obtain a "large" $Q_x$. To obtain a "small" $Q_\delta$, we can minimize the trace of $\bar{Q}_\delta = N_2Q_\delta N_2'$. Since $\mathrm{tr}(N_2Q_\delta N_2')$ can be reduced either by reducing $\mathrm{tr}(Q_\delta)$ or by reducing $\mathrm{tr}(N_2)$, this has the drawback that $N_2$ will be minimized together with $Q_\delta$, potentially reducing the size of the estimate of the domain of attraction until it reaches the limit imposed by the definition of $\mathcal{X}_0$. This does not impact the problem at hand since our objective is to compute the trigger function and the controller parameters instead of estimating the domain of attraction. Therefore, we propose the following optimization problem as means to address the co-design case:

$$\begin{aligned} &\min(\mathrm{tr}(\bar{Q}_\delta + \bar{Q}_x)) \\ &\quad \text{subject to:} \\ &\qquad (5.3),\ (5.4),\ N_2 > P_0^{-1} \end{aligned} \tag{5.11}$$

Similarly to the emulation design case, the set $\mathcal{B}_x$ impacts the results obtained from this optimization problem. Hence, we will adopt the same approach as for that case, parameterizing $\mathcal{B}_x = \{x \in \mathbb{R}^n : h_i'x \leq \rho,\ h_i \in \mathbb{R}^n,\ i = 1, \ldots, n_f;\ \rho > 0\}$, where the vectors $h_i$ determine the shape and the parameter $\rho$ determines the size of $\mathcal{B}_x$. Then we solve the optimization problem performing a search over $\rho$.

## 5.3 Numerical example

In the current section we illustrate the proposed co-design methodology by means of numerical simulations. We consider the same examples presented in the emulation design, in Section 4.4.

### 5.3.1 Example 1 – Unstable polynomial system

Here we consider the plant defined by equation (4.32), recalled here for the reader's convenience:

$$\begin{cases} \dot{x}_{(1)}(t) = x_{(2)}(t) \\ \dot{x}_{(2)}(t) = \left(1 + x_{(1)}^2(t)\right) x_{(1)}(t) + x_{(2)}(t) + u(t) \end{cases} \tag{5.12}$$

We choose $\xi(x) = x_{(1)}^2$ and the following matrices for the DAR (5.2):

$$A_1 = \begin{bmatrix} 0 & 1 \\ 1 & 1 \end{bmatrix} \quad A_2 = \begin{bmatrix} 0 \\ x_{(1)} \end{bmatrix} \quad A_3 = \begin{bmatrix} 0 \\ 1 \end{bmatrix}$$
$$\Omega_1 = \begin{bmatrix} x_{(1)} & 0 \end{bmatrix} \quad \Omega_2 = \begin{bmatrix} -1 \end{bmatrix} \quad \Omega_3 = \begin{bmatrix} 0 \end{bmatrix}$$

Considering once again $\mathcal{B}_x = \{x \in \mathbb{R}^2 : |x_{(i)}| < \rho\}$ and $\mathcal{X}_0 = \{x \in \mathbb{R}^2 : x' P_0 x \leq 1\}$, with $P_0 = 50I$, and solving the optimization problem (5.11) with different values of $\rho$ and the additional condition $\bar{Q}_\delta < 0.0001I$ to prevent $Q_\delta$ from becoming ill-conditioned, we obtain the results depicted in Table 5.1. The line in boldface corresponds to the best value found for the objective function, $0.1653$, obtained with $\rho = 0.18$.

Table 5.1: Example 1 – Linear search over $\mathcal{B}_x$ size.

| $\rho$ | Objective function $\mathrm{tr}(N_2 Q_\delta N_2' + Q_x^{-1})$ |
|---|---|
| 0.15 | 0.2097 |
| 0.16 | 0.1719 |
| 0.17 | 0.1655 |
| **0.18** | **0.1653** |
| 0.19 | 0.1655 |
| 0.20 | 0.1657 |
| 0.21 | 0.1659 |
| 0.50 | 0.1756 |
| 1 | 0.2126 |
| 10 | 7.486 |
| 50 | 208.2 |
| 100 | 847.7 |
| 120 | 1224 |
| 124 | 1308 |
| 125 | unfeasible |

With $\rho = 0.18$, the optimization problem yields:

$$Q_x = \begin{bmatrix} 22.8 & 8.18 \\ 8.18 & 40.2 \end{bmatrix} \qquad Q_\delta = \begin{bmatrix} 63.5 & 94.9 \\ 94.9 & 141 \end{bmatrix}$$
$$P = N_2^{-1} = \begin{bmatrix} 37.2 & 12.6 \\ 12.6 & 37.6 \end{bmatrix} \qquad K = \begin{bmatrix} -2.62 & -3.92 \end{bmatrix}$$

The results of simulations of the closed-loop system considering these parameter values for the event generator and for the control law are depicted in figures 5.1 and 5.2. Figure 5.1 depicts the set $\mathcal{X}_0$ in red, some trajectories that converge to the origin in blue and some divergent trajectories in magenta. The ellipsoid $\mathcal{E}(P)$ is shown in black. One can observe that $\mathcal{X}_0$ is contained in the region of attraction as expected and that $\mathcal{X}_0 \subset \mathcal{E}(P)$ as imposed by the conditions in the optimization problem.

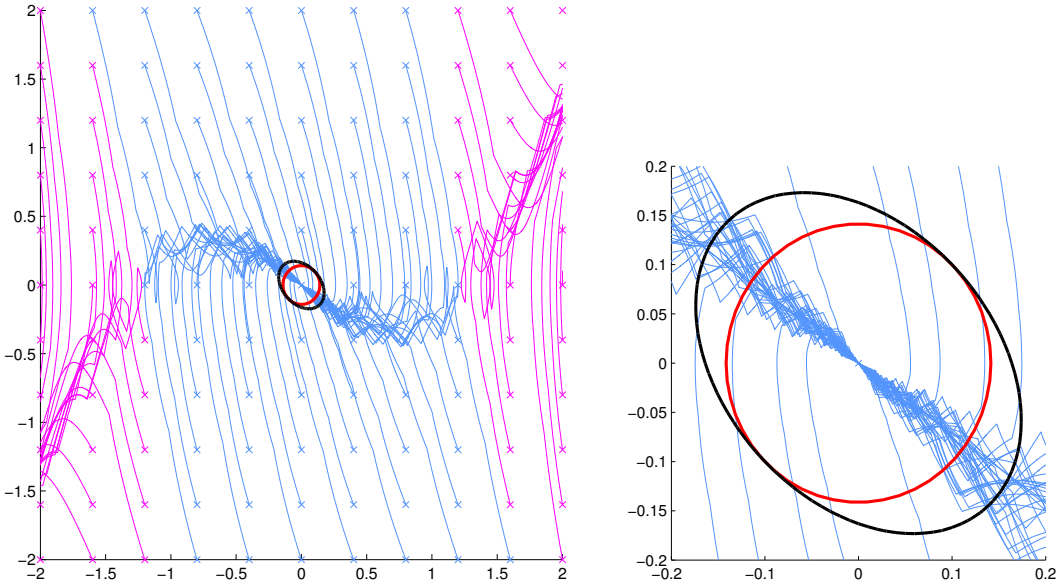


a) Big picture b) Zoom

Figure 5.1: Example 1 – Phase portrait (big picture and zoom) – co-design.

Figure 5.2 depicts simulations considering $x(0) = [0.1\ 0.1]'$. The top plot shows, in solid lines, the state of the event-triggered implementation and, in dashed lines, the state of an equivalent (in the sense that it has the same control law) continuous-time implementation of the system. One can see that the event-triggered system, in this case, featured better performance than the equivalent continuous-time one in terms of settling time. Nevertheless, this characteristic cannot be generalized. Usually, the event-trigger mechanism degrades the performance of the system. The middle plot depicts the control signals for the event-triggered implementation, again in solid line, and the equivalent continuous-time implementation, in dashed line. The plot in the bottom shows the event instants. During the time interval $[0, 15]$ seconds, 31 events were generated and the minimum inter-events time was of 126 ms.

The average number of events for 200 initial conditions inside $\mathcal{X}_0$, 50 of them equally spaced along the border of $\mathcal{X}_0$, is 29.2 and the minimum inter-events time observed is 122 ms. Comparing this average number of events to that obtained in an emulation design context for the same example in Chapter 4 (60.98 events when considering the quadratic Lyapunov function), one can see that the co-design led to a closed-loop system that demanded less events.

#### *5.3.1.1 Influence of $\mathcal{X}_0$ size*

To illustrate the influence of $\mathcal{X}_0$ size, we consider $P_0 = \alpha I$ for various values of the positive scalar $\alpha$. Table 5.2 presents the average number of events and the minimum inter-event times obtained from simulations considering the same 200 initial conditions inside $\mathcal{X}_0$ as before. One can observe that, as in the emulation case, the average number of events increases and the minimum inter-event time decreases as the size of $\mathcal{X}_0$ increases.

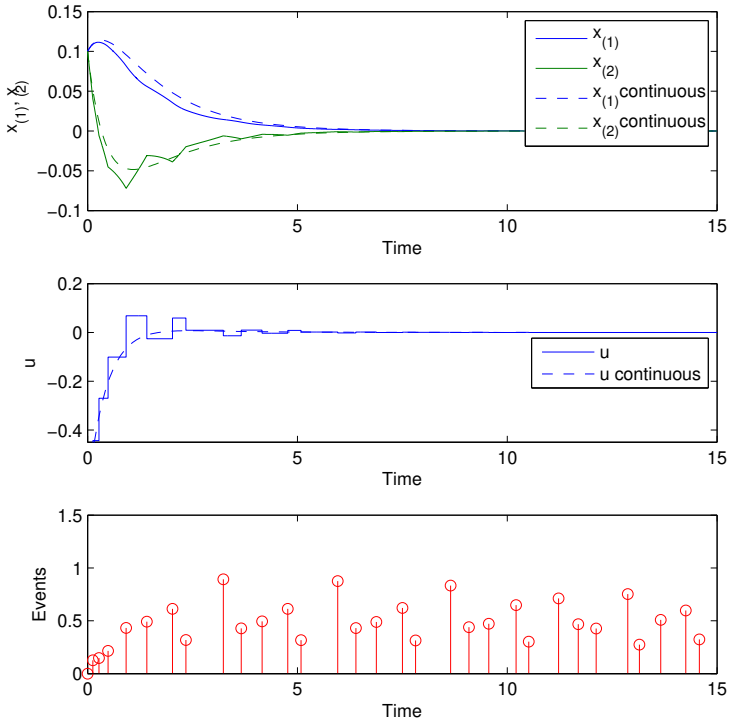


Figure 5.2: Example 1 – Simulation for $x(0) = [0.1\ 0.1]'$ – co-design.

Table 5.2: Example 1 – Influence of $\mathcal{X}_0$ size – co-design.

| $\alpha$ | Average number of events | Minimum inter-event time |
|---|---|---|
| 4.0 | 31.33 | 99 |
| 2.8 | 33.44 | 88 |
| 1.0 | 42.31 | 52 |

### 5.3.2 Example 2 – Rational system

Here we consider again the plant defined by (4.36), recalled below for the reader's convenience:

$$\begin{cases} \dot{x}_{(1)}(t) = \dfrac{1 + x_{(1)}^2(t)}{2} x_{(2)}(t) \\ \dot{x}_{(2)}(t) = \dfrac{2}{1 + x_{(1)}^2(t)} x_{(1)}(t) - x_{(2)}(t) - \dfrac{1 - x_{(1)}^2(t)}{1 + x_{(1)}^2(t)} u(t) \end{cases} \tag{5.13}$$

We choose

$$\xi(x, \delta) = \left[ x_{(1)} x_{(2)} \quad \frac{x_{(1)}}{1+x_{(1)}^2} \quad \frac{x_{(1)}^2}{1+x_{(1)}^2} \quad \frac{K(x+\delta)}{1+x_{(1)}^2} \quad \frac{x_{(1)} K(x+\delta)}{1+x_{(1)}^2} \right]'$$

and the following matrices for the DAR (5.2):

$$A_1 = \begin{bmatrix} 0 & 0.5 \\ 0 & -1 \end{bmatrix} \quad A_2 = \begin{bmatrix} 0.5x_{(1)} & 0 & 0 & 0 & 0 \\ 0 & 2 & 0 & 0 & 2x_{(1)} \end{bmatrix} \quad A_3 = \begin{bmatrix} 0 \\ -1 \end{bmatrix}$$

$$\Omega_1 = \begin{bmatrix} -x_{(2)} & 0 \\ -1 & 0 \\ 0 & 0 \\ 0 & 0 \\ 0 & 0 \end{bmatrix} \quad \Omega_2 = \begin{bmatrix} 1 & 0 & 0 & 0 & 0 \\ 0 & 1 & x_{(1)} & 0 & 0 \\ 0 & -x_{(1)} & 1 & 0 & 0 \\ 0 & 0 & 0 & 1 & x_{(1)} \\ 0 & 0 & 0 & -x_{(1)} & 1 \end{bmatrix} \quad \Omega_3 = \begin{bmatrix} 0 \\ 0 \\ 0 \\ -1 \\ 0 \end{bmatrix}$$

Considering once again $\mathcal{B}_x = \{x \in \mathbb{R}^2 : |x_{(i)}| < \rho\}$ and $\mathcal{X}_0 = \{x \in \mathbb{R}^2 : x'P_0x \leq 1\}$, with $P_0 = 50I$, and solving the optimization problem (5.11) with different values of $\rho$ and the additional condition $\bar{Q}_\delta < 0.0001I$ to prevent $Q_\delta$ from becoming ill-conditioned, we obtain the results depicted in Table 5.3. The line in boldface corresponds to the best value found for the objective function, $0.2181$, obtained with $\rho = 0.31$.

Table 5.3: Example 2 – Linear search over $\mathcal{B}_x$ size.

| $\rho$ | Objective function $\mathrm{tr}(N_2Q_\delta N_2' + Q_x^{-1})$ |
|---|---|
| 0.14 | unfeasible |
| 0.15 | 1.0329 |
| 0.20 | 0.2965 |
| 0.30 | 0.2182 |
| **0.31** | **0.2181** |
| 0.32 | 0.2189 |
| 0.35 | 0.2246 |
| 0.60 | 0.3740 |
| 1 | unfeasible |

With $\rho = 0.31$, the optimization problem yields:

$$Q_x = \begin{bmatrix} 18.0 & 7.63 \\ 7.63 & 16.3 \end{bmatrix} \qquad Q_\delta = \begin{bmatrix} 112 & 51.5 \\ 51.5 & 23.6 \end{bmatrix}$$

$$P = N_2^{-1} = \begin{bmatrix} 46.1 & 12.0 \\ 12.0 & 13.5 \end{bmatrix} \qquad K = \begin{bmatrix} 4.17 & 1.90 \end{bmatrix}$$

The results of simulations of the closed-loop system considering these parameter values for the event generator and for the control law are depicted in figures 5.3 and 5.4. Figure 5.3 depicts the set $\mathcal{X}_0$ in red, some trajectories that converge to the origin in blue and some divergent trajectories in magenta. The ellipsoid $\mathcal{E}(P)$ is shown in black. One can observe that $\mathcal{X}_0$ is contained in the region of attraction and that $\mathcal{E}(P)$ includes $\mathcal{X}_0$, as expected.

Figure 5.4 depicts simulations considering $x(0) = [0.1\ 0.1]'$. The top plot shows, in solid lines, the state of the event-triggered implementation and, in dashed lines, the state of an equivalent (in the sense that it has the same control law) continuous-time implementation of the system. One can see that both implementations have almost identical performance. The middle plot depicts the control signals for the event-triggered implementation, again in solid line, and the equivalent continuous-time implementation, in dashed line. The plot in the bottom shows the event instants. During the time interval

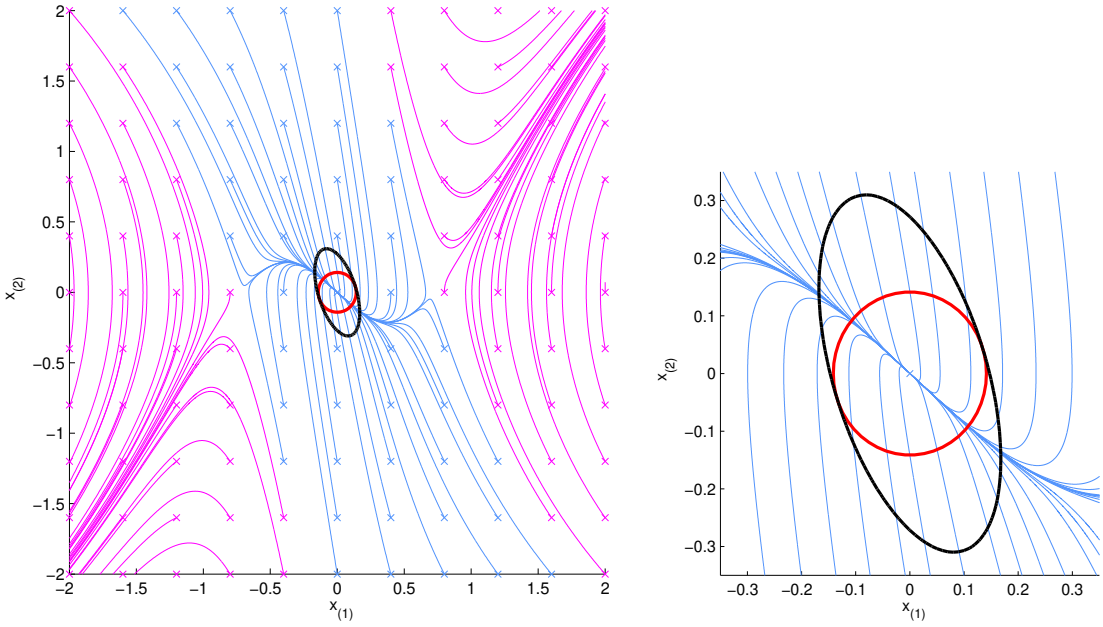


a) Big picture b) Zoom

Figure 5.3: Example 2 – Phase portrait (big picture and zoom) – co-design.

$[0, 15]$ seconds, 11 events were generated and the minimum inter-events time was of 314 ms.

The average number of events for 200 initial conditions inside $\mathcal{X}_0$ is 10.52 and the minimum inter-events time observed is 270 ms. In this case, the closed-loop system obtained with the co-design demanded slightly more events than emulation. It is important to keep in mind that the comparison to the emulation design is misleading in this example because the feedback gain matrices are very different ($\begin{bmatrix}20 & 13\end{bmatrix}$ in the emulation case, $\begin{bmatrix}4.17 & 1.90\end{bmatrix}$ in the co-design).

#### *5.3.2.1 Influence of $\mathcal{X}_0$ size*

Here we consider again sets $\mathcal{X}_0$ of various sizes by setting $P_0 = \alpha I$ for various values of the positive scalar $\alpha$. Table 5.4 presents the average number of events and the minimum inter-event times obtained from simulations considering 200 initial conditions inside $\mathcal{X}_0$. One can observe again that the average number of events increases and the minimum inter-event time decreases as the size of $\mathcal{X}_0$ increases. For $\alpha \leq 4.1$ the problem becomes unfeasible.

Table 5.4: Example 2 – Influence of $\mathcal{X}_0$ size – co-design.

| $\alpha$ | Average number of events | Minimum inter-event time |
|---|---|---|
| 25 | 10.68 | 162 |
| 12 | 11.53 | 56 |
| 6 | 16.23 | 7 |
| 4.2 | 20.73 | 1 |

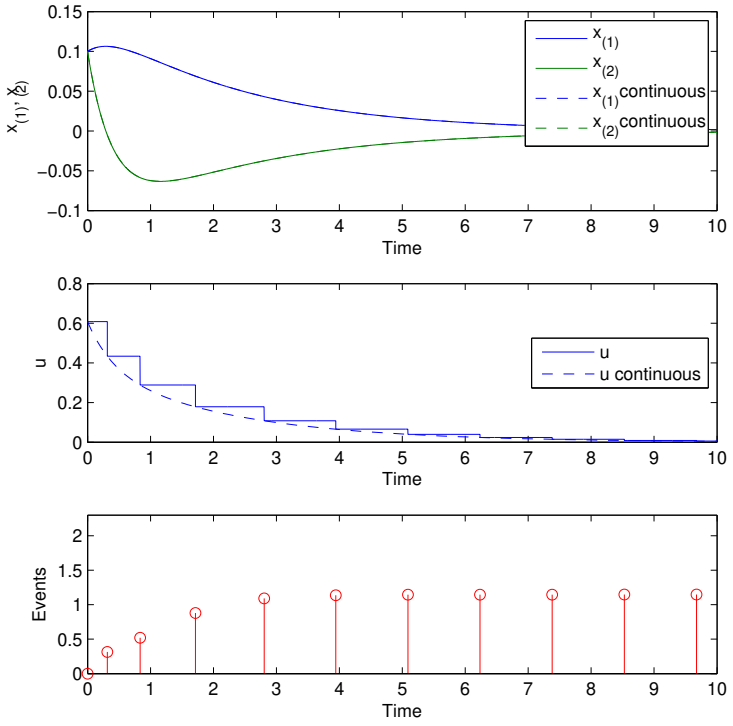


Figure 5.4: Example 2 – Simulation for $x(0) = [0.1\ 0.1]'$ – co-design.

### 5.3.3 Example 3 – Lorenz system

Here we address again the Lorenz system (LORENZ, 1963), whose equation is recalled here for the reader's convenience:

$$\begin{cases} \dot{x}_{(1)} = \sigma(x_{(2)} - x_{(1)}) \\ \dot{x}_{(2)} = x_{(1)}(\nu - x_{(3)}) - x_{(2)} + u \\ \dot{x}_{(3)} = x_{(1)}x_{(2)} - \beta x_{(3)} \end{cases} \tag{5.14}$$

with $\sigma = 10$, $\nu = 28$ and $\beta = 8/3$.

As in the emulation context, we consider $\mathcal{B}_x = \{x \in \mathbb{R}^3 : |x_{(i)}| < \rho;\ \rho \in \mathbb{R}^+\}$; $\mathcal{X}_0 = \{x \in \mathbb{R}^3 : x'P_0x \leq 1\}$, with $P_0 = 50I$.

We choose $\xi(x, \delta) = x_{(1)}$ and the following matrices for DAR (5.2):

$$A_1 = \begin{bmatrix} -10 & 10 & 0 \\ -28 & -1 & 0 \\ 0 & 0 & -2.67 \end{bmatrix} \qquad A_2 = \begin{bmatrix} 0 \\ -x_{(3)} \\ x_{(2)} \end{bmatrix} \qquad A_3 = \begin{bmatrix} 0 \\ 1 \\ 0 \end{bmatrix}$$

$$\Omega_1 = \begin{bmatrix} 1 & 0 & 0 \end{bmatrix} \qquad \Omega_2 = \begin{bmatrix} -1 \end{bmatrix} \qquad \Omega_3 = \begin{bmatrix} 0 \end{bmatrix}$$

Solving optimization problem (5.11) for various values of $\rho$ with the additional condition $\bar{Q}_\delta < 0.01I$ to prevent $Q_\delta$ from becoming ill-conditioned, we obtain the results depicted in Table 5.5. The line in boldface corresponds to the best value found for the objective function, 0.5435, obtained with $\rho = 0.41$.

Table 5.5: Example 3 – Linear search over $\mathcal{B}_x$ size.

| $\rho$ | Objective function $\mathrm{tr}(N_2 Q_\delta N_2' + Q_x^{-1})$ |
|---|---|
| 0.14 | unfeasible |
| 0.20 | 0.5888 |
| 0.30 | 0.5678 |
| 0.40 | 0.5636 |
| **0.41** | **0.5635** |
| 0.42 | 0.5636 |
| 0.50 | 0.5648 |
| 0.60 | 0.5667 |
| 0.80 | 0.5707 |
| 1.00 | 0.5747 |

With $\rho = 0.41$, the optimization problem yields:

$$Q_x = \begin{bmatrix} 157 & -53.1 & 3.28 \cdot 10^{-12} \\ -53.1 & 69.9 & -8.33 \cdot 10^{-13} \\ 3.28 \cdot 10^{-12} & -8.33 \cdot 10^{-13} & 219 \end{bmatrix}$$

$$Q_\delta = \begin{bmatrix} 797 & 618 & 2.79 \cdot 10^{-13} \\ 618 & 479 & -1.34 \cdot 10^{-13} \\ 2.79 \cdot 10^{-13} & -1.34 \cdot 10^{-13} & 25 \end{bmatrix}$$

$$P = N_2^{-1} = \begin{bmatrix} 32.8 & 22.3 & 2.99 \cdot 10^{-13} \\ 22.3 & 21.1 & -4.18 \cdot 10^{-13} \\ 2.99 \cdot 10^{-13} & -4.18 \cdot 10^{-13} & 50 \end{bmatrix}$$

$$K = \begin{bmatrix} 31.5 & -24.5 & 1.73 \cdot 10^{-14} \end{bmatrix}$$

As in previous examples, Figure 5.5 depicts simulations of the closed-loop system considering $x(0) = [0.08\ 0.08\ 0.08]'$. The top plot shows, in solid lines, the state of the event-triggered implementation and, in dashed lines, the state of an equivalent (in the sense that it has the same control law) continuous-time implementation of the system. One can see that the event-triggered control in this case also leads to sensible differences with respect to the continuous-time implementation. The middle plot depicts the control signals for the event-triggered implementation, again in solid line, and the equivalent continuous-time implementation, in dashed line. Control signals are very similar with slightly larger amplitude in the event-triggered implementation. The plot in the bottom shows the event instants. During the time interval $[0, 4]$ seconds, 34 events were generated and the minimum inter-events time was of 25 ms. Simulating the event-triggered implementation for 400 initial conditions on the border of $\mathcal{X}_0$, the average number of events is 31.1 and the minimum inter-events time observed is 13 ms. In this example we observe, again, less events with co-design than with emulation (average of 31.1 events with co-design and of 115.8 with emulation). Nevertheless, one should keep in mind that the closed-loop system dynamics are very different due to large differences in the feedback gain matrices for each case.

Figure 5.6 depicts the set $\mathcal{X}_0$ in green and the ellipsoid $\mathcal{E}(P)$ in red. One can observe that $\mathcal{X}_0 \subset \mathcal{E}(P)$ as imposed by the conditions in the optimization problem and that, in this

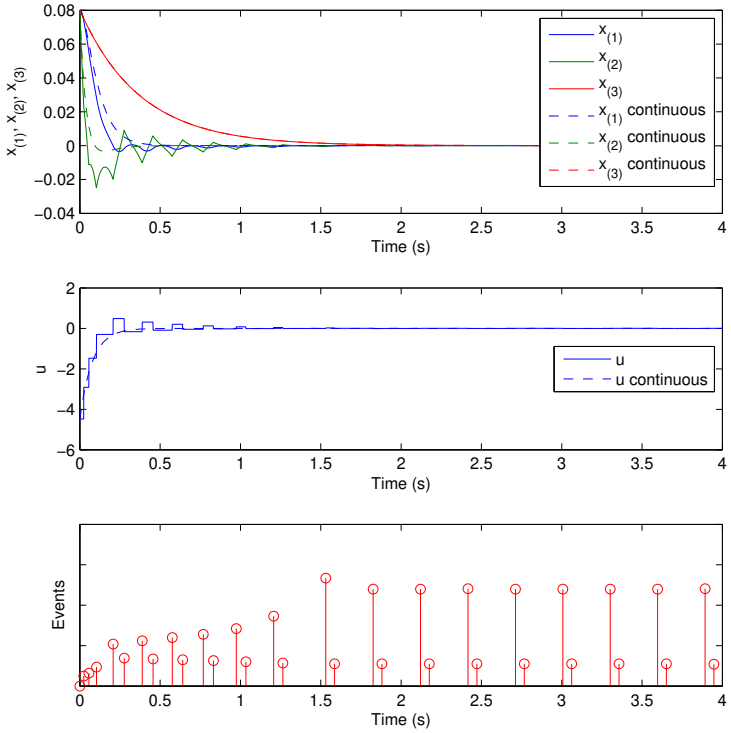


Figure 5.5: Example 3 – Simulation for $x(0) = [0.08\ 0.08\ 0.08]'$ – co-design.

case, the borders of the sets actually touch each other. This can be seen as an indication that the optimization problem was very effective, what is also confirmed by the small number of events.

#### *5.3.3.1 Influence of $\mathcal{X}_0$ size*

To illustrate the influence of $\mathcal{X}_0$ size we consider $P_0 = \alpha I$ for various values of the positive scalar $\alpha$. Table 5.6 presents the average number of events and the minimum inter-event times obtained from simulations considering 729 initial conditions over a grid equally spaced inside a cube of side 20 centered at the origin. Once again, the average number of events tends to increase and the minimum inter-event time decreases as the size of $\mathcal{X}_0$ increases.

Table 5.6: Example 3 – Influence of $\mathcal{X}_0$ size – co-design.

| $\alpha$ | Average number of events | Minimum inter-event time |
|---|---|---|
| 1.00 | 33.56 | 12 |
| 0.10 | 35.62 | 10 |
| 0.01 | 55.38 | 3 |
| 0.006 | 100.39 | 2 |

## 5.4 Conclusion

In this chapter we established sufficient stability conditions considering a co-design context. We proposed a convex optimization problem based on these conditions as means to compute the event generator parameters and the control law aiming at a reduced number

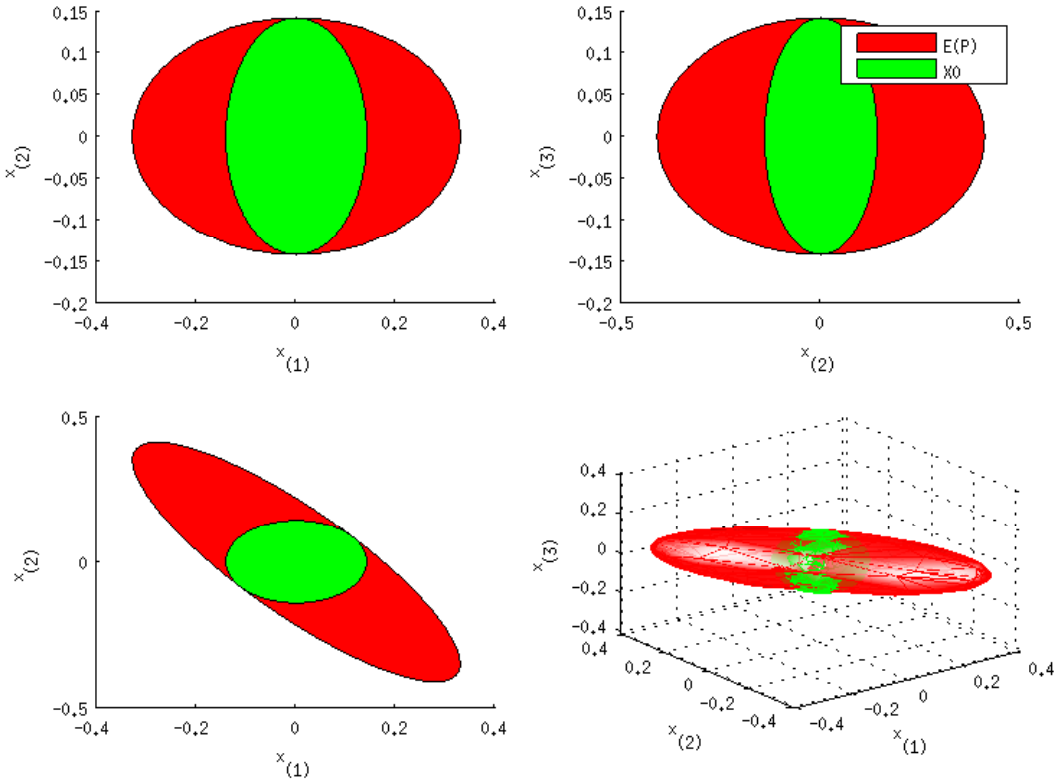


Figure 5.6: Example 3 – $\mathcal{E}(P)$ and $\mathcal{X}_0$.

of events. We illustrated the method by means of numerical experiments, showcasing its efficacy and giving evidences that the co-design, besides simplifying the task for the designer, can lead to better results in terms of the number of events.

# Part II

# Lur’e systems

# 6 LUR'E SYSTEMS WITH INPUT NONLINEARITIES

In this chapter we address the emulation and co-design problems considering Lur'e systems where the nonlinearity depends only on the plant input. We assume that the event generator and the controller do not have access to the entire state of the system and we use a nonlinear state observer to recover the missing information. The event-generator and the controller are designed to use only the available information, i.e. the system inputs, outputs and the observed state. This configures an output-based event-trigger scenario and we use a dwell-time to avoid Zeno behavior (MAZO; ANTA; TABUADA, 2010). The dwell-time imposes an explicit minimum inter-event time. Following the ideas introduced in (TARBOURIECH et al., 2017) to ensure the asymptotic stability of the origin in the presence of the dwell-time, an additional condition, similar to the one for ensuring the stability of discrete-time linear systems is included. Taking into account that the system input (and thus, the nonlinearity value) is kept constant during the interval between an event and the end of the dwell-time, this condition is derived from the computation of the solutions of the system in this interval. The stability analysis is therefore split in two intervals. The first one just described, i.e. $t \in [t_k, t_k + T]$, and the second one, from the end of the dwell-time up to the next event, i.e. $t \in (t_k + T, t_{k+1})$, where the triggering condition is designed to ensure the negativity of the time derivative of the underlying Lyapunov function along the trajectories of the closed-loop system.

## 6.1 Addressed system

We consider a continuous-time plant, represented by the following equation:

$$\begin{cases} \dot{x}_p(t) = A_p x_p(t) + B_p u(t) + B_{pf} f(u(t)) \\ y_p(t) = C_p x_p(t) + D_{pf} f(u(t)) \end{cases} \tag{6.1}$$

where $x_p(t) \in \mathbb{R}^n$, $u(t) \in \mathbb{R}^m$, $y_p(t) \in \mathbb{R}^p$ are the state, the input and the output of the plant, respectively. The matrices $A_p$, $B_p$, $B_{pf}$, $C_p$ and $D_{pf}$ are constant and of appropriate dimensions. Pairs $(A_p,B_p)$ and $(C_p,A_p)$ are supposed to be stabilizabile and detectable, respectively. Function $f : \mathbb{R}^m \to \mathbb{R}^m$ is a continuous, decentralized cone-bounded nonlinearity (see, e.g. (KHALIL, 1996), for details) affecting the input $u$. Hence, it satisfies the following property:

$$f(u)'S(f(u) + Ru) \leq 0 \tag{6.2}$$

where $S \in \mathbb{R}^{m\times m}$ is any diagonal positive definite matrix. Matrix $R \in \mathbb{R}^{m\times m}$ is supposed to be a diagonal positive matrix that is fixed by the designer and depends on the

nonlinearity characteristics. Property (6.2) can be satisfied either globally (i.e. it is valid $\forall u \in \mathbb{R}^m$) or regionally (i.e. it is valid for all $u$ in a given set $\mathcal{S}_u \subset \mathbb{R}^m$ containing the origin). In the present work, for the regional stabilization cases, we consider that $\mathcal{S}_u$ is a polyhedral set, symmetric around the origin, generically defined as follows:

$$\mathcal{S}_u = \{u \in \mathbb{R}^m : |h_i' u| \leq 1;\ h_i \in \mathbb{R}^m, i = 1, ..., n_f\} \tag{6.3}$$

where $n_f$ is half the number of faces.

We consider the following observer-based state feedback controller to asymptotically stabilize system (6.1):

$$\begin{cases} \dot{\hat{x}}(t) = A_p\hat{x}(t) + B_p u(t) + B_{pf} f(u(t)) - L e_y(t) \\ \hat{y}(t) = C_p\hat{x}(t) + D_{pf} f(u(t)) \\ e_y(t) = y_p(t) - \hat{y}(t) \\ u(t) = K\hat{x}(t) \end{cases} \tag{6.4}$$

where $\hat{x}(t) \in \mathbb{R}^n$ and $\hat{y}(t) \in \mathbb{R}^p$ are the state and the output of the observer, respectively, and $e_y(t) = y_p(t) - \hat{y}(t)$ is the output error. $L \in \mathbb{R}^{n\times p}$ and $K \in \mathbb{R}^{m\times n}$ are the observer and controller gains, respectively.

In the event-triggered implementation, the control action applied to the plant input is updated only at the instants $t_k$ and kept constant between these instants by means of a zero-order hold. Hence, $\forall t \in [t_k\ ,\ t_{k+1})$, the closed-loop system can be represented by the following equations:

$$\begin{cases} \dot{x}_p(t) = A_p x_p(t) + B_p u(t_k) + B_{pf} f(u(t_k)) \\ \dot{\hat{x}}(t) = A_p\hat{x}(t) + B_p u(t_k) + B_{pf} f(u(t_k)) - L e_y(t) \\ u(t_k) = K\hat{x}(t_k) \\ y_p(t) = C_p x_p(t) + D_{pf} f(u(t_k)) \\ \hat{y}(t) = C_p\hat{x}(t) + D_{pf} f(u(t_k)) \\ e_y(t) = y_p(t) - \hat{y}(t) \end{cases} \tag{6.5}$$

The topology is depicted in Figure 6.1. The observer, plant and event generator are in one node of a generic data communication network while the controller and, possibly, the actuator are in another one. This generic data communication network is represented by the double line in the figure.

At this point, it is convenient to re-write system (6.5) in terms of the observer state $\hat{x}(t)$ and the observer error $e(t) = x_p(t) - \hat{x}(t)$, obtaining:

$$\begin{cases} \dot{\hat{x}}(t) = (A_p + B_p K)\hat{x}(t) + B_p K\delta(t) + B_{pf} f(u(t_k)) - L C_p e(t) \\ \dot{e}(t) = (A_p + L C_p)e(t) \end{cases} \tag{6.6}$$

It is also convenient to define the augmented state vector $x = \begin{bmatrix}\hat{x}' & e'\end{bmatrix}'$. This definition and the representation (6.6) will be used in the stability theorems that follow.

## 6.2 Event generator

Since we are now considering an output-based event-trigger, we need to introduce a new trigger condition which relies solely on available information. Therefore, we re-define $\delta(t)$ as the error between the value of the observed state at the last trigger instant

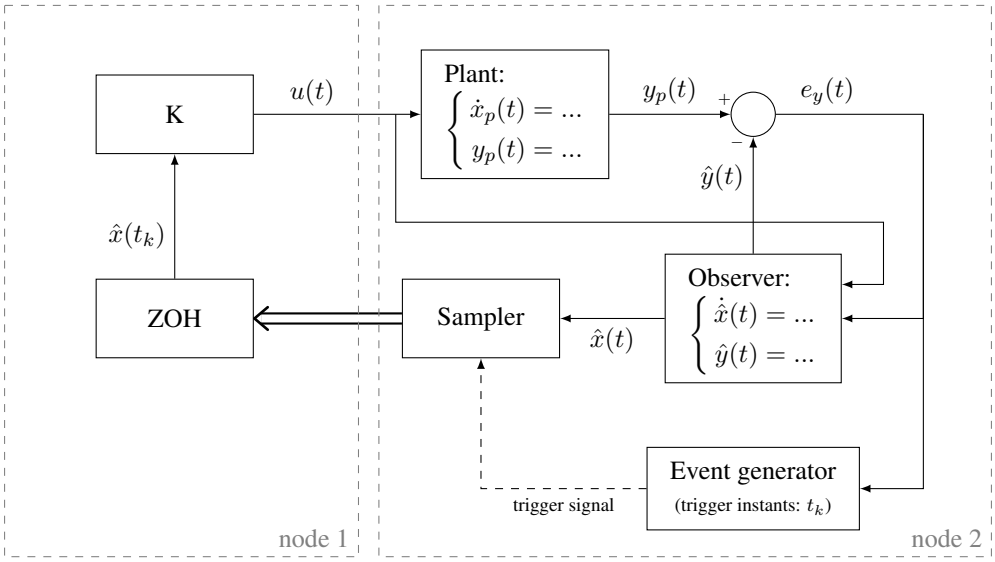


Figure 6.1: Topology for Lur'e systems with input nonlinearities.

and the current one, i.e.:

$$\delta(t) = \hat{x}(t_k) - \hat{x}(t) \tag{6.7}$$

and we define the following triggering strategy, which is a modified version of the weighted relative error threshold one:

$$t_{k+1} = \min\{t \geq t_k + T, \quad s.t. \quad \delta(t)'Q_\delta\delta(t) - \begin{bmatrix}\hat{x}(t)\\ e_y(t)\end{bmatrix}' Q_\epsilon^{-1} \begin{bmatrix}\hat{x}(t)\\ e_y(t)\end{bmatrix} \geq 0\} \tag{6.8}$$

$Q_\delta$ and $Q_\epsilon$ are constant symmetric positive-definite matrices of appropriate dimensions and the dwell-time $T$ is a positive scalar. The dwell-time ensures a minimum inter-event time, which prevents Zeno behavior. The condition uses only available information since $\delta(t)$ only depends on the observed state $\hat{x}(t)$ and its sampled value at the instant $t_k$.

## 6.3 Emulation case

In this section we use techniques from the Lyapunov theory to derive sufficient conditions for the asymptotic stability of the origin of system (6.5) under the triggering strategy (6.8) in an emulation design context, considering both the global and the regional stabilization cases. The global stabilization for the same class of systems with a slightly different trigger condition has been addressed previously in (TARBOURIECH et al., 2017), while the regional stabilization is an original result developed for this thesis.

### 6.3.1 Stability conditions

The following theorem establishes sufficient conditions for the regional asymptotic stability of the origin when the class of systems at hand is considered.

**Theorem 6.1.** *Consider system* (6.6) *with* $f$ *satisfying* (6.2) *and* $K$ *and* $L$ *given. If there exist symmetric positive definite matrices* $\bar{Q}_\delta$, $Q_\epsilon$, $W = \left[\begin{smallmatrix} W_1 & W_2 \\ * & W_3 \end{smallmatrix}\right]$, *diagonal positive definite matrices* $U_1$ *and* $U_2$ *of appropriate dimensions and a positive scalar* $T$ *such that the*

*conditions:*

$$\Phi_1 = \begin{bmatrix} Q_1 & \begin{bmatrix} WC_a' \\ 0 \\ 0 \end{bmatrix} \\ * & -Q_\epsilon \end{bmatrix} < 0 \tag{6.9}$$

$$\Phi_2 = \begin{bmatrix} -W & -W\begin{bmatrix} K' \\ 0 \end{bmatrix} R & W\left(A_{ad}(T)' + \begin{bmatrix} K' \\ 0 \end{bmatrix} B_a' B_{ad}(T)'\right) \\ * & -2U_2 & U_2 B_{af}' B_{ad}(T)' \\ * & * & -W \end{bmatrix} < 0 \tag{6.10}$$

$$\Phi_3 = \begin{bmatrix} W & W\begin{bmatrix} K' \\ 0 \end{bmatrix} h_i \\ * & 1 \end{bmatrix} > 0 \tag{6.11}$$

*are verified with*

$$Q_1 = \mathrm{He}\left\{ \begin{bmatrix} I \\ 0 \\ 0 \end{bmatrix} \begin{bmatrix} (A_a + B_a \begin{bmatrix} K & 0 \end{bmatrix})W & B_a K W_1 & B_{af} U_1 \end{bmatrix} \right\} - \begin{bmatrix} 0 \\ I \\ 0 \end{bmatrix} \bar{Q}_\delta \begin{bmatrix} 0 & I & 0 \end{bmatrix}$$
$$- \mathrm{He}\left\{ \begin{bmatrix} 0 \\ 0 \\ I \end{bmatrix} \begin{bmatrix} R \begin{bmatrix} K & 0 \end{bmatrix} W & RKW_1 & U_1 \end{bmatrix} \right\}$$

$$A_a = \begin{bmatrix} A_p & -LC_p \\ 0 & A_p + LC_p \end{bmatrix} \qquad B_a = \begin{bmatrix} B_p \\ 0 \end{bmatrix} \qquad B_{af} = \begin{bmatrix} B_{pf} \\ 0 \end{bmatrix} \qquad C_a = \begin{bmatrix} I & 0 \\ 0 & C_p \end{bmatrix}$$

$$A_{ad} = e^{A_a T} \qquad B_{ad} = \int_0^T e^{A_a s} ds \tag{6.12}$$

*Then, the event-triggered sampling rule* (6.8) *with* $Q_\delta = W_1^{-1} \bar{Q}_\delta W_1^{-1}$ *is such that the origin of system* (6.5) *is regionally asymptotically stable and the set* $\mathcal{L}_V(1) = \{x \in \mathbb{R}^{2n} : x' W^{-1} x \leq 1\}$*, with* $x = \begin{bmatrix} \hat{x}' & e' \end{bmatrix}'$*, is included in its region of attraction. Furthermore, the inter-sampling times are lower bounded by* $T$*.*

*Proof.* Consider the quadratic Lyapunov candidate function for system (6.6) given by:

$$V(x) = x' W^{-1} x, \tag{6.13}$$

where the matrix $W^{-1}$ is positive definite thanks to the satisfaction of (6.10) and (6.11), implying that there exist scalars $\epsilon_1 > 0$ and $\epsilon_2 > 0$ such that the following relation is satisfied:

$$\epsilon_1 ||x||^2 \leq V(x) \leq \epsilon_2 ||x||^2, \forall x \in \mathbb{R}^{2n} \tag{6.14}$$

Observe also that system (6.6) can be rewritten as:

$$\dot{x}(t) = \left(A_a + B_a \begin{bmatrix} K & 0 \end{bmatrix}\right) x(t) + B_a K \delta(t) + B_{af} f(u(t_k))$$

The remaining of the proof is carried considering the time intervals $[t_k\ ,\ t_k + T]$ and $(t_k + T,\ t_{k+1})$.

Solving the linear differential equation (6.6) over the interval $[t_k, t_k + T]$ yields

$$x(t_k + T) = \Lambda_1(T)x(t_k) + \Lambda_2(T)f(u(t_k)) \tag{6.15}$$

where

$$\Lambda_1(T) \triangleq A_{ad} + B_{ad}B_a \begin{bmatrix} K & 0 \end{bmatrix}, \quad \Lambda_2(T) \triangleq B_{ad}B_{af}$$

with $A_{ad}$, $B_{ad}$, $B_a$ and $B_{af}$ defined as in (6.12).

Hence, considering the definition of $V$ in (6.13), one obtains the following expression:

$$\begin{aligned}
\Psi_T &\triangleq V(x(t_k + T)) - V(x(t_k)) - 2f(u(t_k))'S_2(f(u(t_k)) + Ru(t_k)) \\
&= \Big(x(t_k)'\Lambda_1(T)' + f(u(t_k))'\Lambda_2(T)'\Big) W^{-1} \Big(\Lambda_1(T)x(t_k) + \Lambda_2(T)f(u(t_k))\Big) \\
&\quad - x(t_k)'W^{-1}x(t_k) - 2f(u(t_k))'S_2 \Big(f(u(t_k)) + Ru(t_k)\Big) \\
&= \xi(t_k)'M_1\xi(t_k)
\end{aligned}$$

with $\xi(t_k) = \begin{bmatrix} x'(t_k) & f'(u(t_k)) \end{bmatrix}'$ and:

$$M_1 = \begin{bmatrix} \Lambda_1(T)'W^{-1}\Lambda_1(T) - W^{-1} & \Lambda_1(T)'W^{-1}\Lambda_2(T) - \begin{bmatrix} K' \\ 0 \end{bmatrix} RS_2 \\ * & \Lambda_2(T)'W^{-1}\Lambda_2(T) - 2S_2 \end{bmatrix}$$

Satisfying $M_1 < 0$, ensures $\Psi_T < 0$ and, consequently, $V(x(t_k + T)) - V(x(t_k)) < -2f(u(t_k))'S_2\big(f(u(t_k)) + Ru(t_k)\big)$. Applying Schur's complement and a congruence transformation with $\mathrm{diag}(W, U_2, W)$, where $U_2 = S_2^{-1}$, it can be seen that condition $\Phi_2 < 0$ in (6.10) is equivalent to $M_1 < 0$. Therefore, considering the sector condition (6.2), satisfaction of (6.10) effectively ensures that $V(x(t_k + T)) - V(x(t_x)) < 0,\ \forall k \in \mathbb{N}$, as long as $u(t_k) \in \mathcal{S}_u,\ \forall k \in \mathbb{N}$.

Now, considering the time-derivative of $V$ along the trajectories of system (6.6) for any $t \in (t_k + T, t_{k+1})$, the following expression is obtained:

$$\begin{aligned}
\Psi_c &\triangleq \dot{V}(x(t)) - \delta(t)'Q_\delta\delta(t) + \begin{bmatrix} \hat{x}(t) \\ e_y(t) \end{bmatrix}' Q_\epsilon^{-1} \begin{bmatrix} \hat{x}(t) \\ e_y(t) \end{bmatrix} - 2f(u(t_k))'S_1(f(u(t_k)) + Ru(t_k)) \\
&= \begin{bmatrix} x(t) \\ \delta(t) \\ f(u(t_k)) \end{bmatrix}' \Gamma \begin{bmatrix} x(t) \\ \delta(t) \\ f(u(t_k)) \end{bmatrix}
\end{aligned}$$

with

$$\begin{aligned}
\Gamma = \mathrm{He}\left\{ \begin{bmatrix} I \\ 0 \\ 0 \end{bmatrix} W^{-1} \begin{bmatrix} \big(A_a + B_a \begin{bmatrix} K & 0 \end{bmatrix}\big) & B_aK & B_{af} \end{bmatrix} \right\} - \begin{bmatrix} 0 \\ I \\ 0 \end{bmatrix} Q_\delta \begin{bmatrix} 0 & I & 0 \end{bmatrix} \\
+ \begin{bmatrix} C_a' \\ 0 \\ 0 \end{bmatrix} Q_\epsilon^{-1} \begin{bmatrix} C_a & 0 & 0 \end{bmatrix} - \mathrm{He}\left\{ \begin{bmatrix} 0 \\ 0 \\ I \end{bmatrix} \begin{bmatrix} S_1R \begin{bmatrix} K & 0 \end{bmatrix} & S_1RK & S_1 \end{bmatrix} \right\}
\end{aligned}$$

where we used the facts that $u(t_k) = K\hat{x}(t_k) = K\hat{x}(t) + K\delta(t)$ and $e_y(t) = C_p e(t)$ for the last equality.

Pre- and post-multiplying $\Gamma$ by $\mathrm{diag}(W, W_1, U_1)$ with $U_1 = S_1^{-1}$, making the change of variables $\bar{Q}_\delta = W_1Q_\delta W_1$ and considering the Schur's complement, it follows that

inequality $\Phi_1 < 0$ in (6.9) implies $\Gamma < 0$. Considering that satisfaction of $\Gamma < 0$, guarantees that $\Psi_c < 0$, it follows from (6.2) and (6.8) that $\dot{V}(x(t)) < 0$ in the interval $[t_k + T,\ t_{k+1})$ as long as $u(t_k) \in \mathcal{S}_u$ and therefore

$$V(x(t)) < V(x(t_k + T)), \quad \forall t \in [t_k + T,\ t_{k+1}), \forall k \in \mathbb{N} \tag{6.16}$$

From the arguments above, we conclude that satisfaction of (6.9) and (6.10) ensure $V(x(t_{k+1}) < V(x(t_k))$, provided that $u(t_k) \in \mathcal{S}_u$, $\forall k \in \mathbb{N}$.

Moreover, system (6.6) is composed by a linear part and a bounded nonlinearity since from relation (6.2), one gets, $\|f(v)\| \leq \gamma\|v\|$ for any vector $v \in \mathcal{S}_u$, where $\gamma$ is a positive constant depending on the norm of $R$. Then, since $V(x)$ satisfies (6.14), there exists a positive scalar $\beta$ such that $\max_{t\in[t_k,\ t_k+T]} V(x(t)) \leq \beta V(x(t_k))$, for all $k \in \mathbb{N}$, provided that $u(t_k) \in \mathcal{S}_u$. Hence, associating this property to relation (6.8) and to the fact that $\dot{V}(x) < 0$ on the interval $[t_k + T\ ,\ t_{k+1})$, the trajectories of the system are bounded between every two successive events. As a consequence, asymptotic stability is ensured, provided that $u(t_k) \in \mathcal{S}_u$, $\forall k \in \mathbb{N}$.

Now pre- and post-multiplying (6.11) by $\mathrm{diag}(W^{-1}, 1)$ and applying the Schur complement, one obtains:

$$W^{-1} - \begin{bmatrix} K'h_i \\ 0 \end{bmatrix} \begin{bmatrix} h_i'K & 0 \end{bmatrix} > 0. \tag{6.17}$$

Pre- and post-multiplying (6.17) by $x(t_k)'$ and $x(t_k)$, respectively, the satisfaction of (6.11) implies that the following condition is fulfilled:

$$x(t_k)'W^{-1}x(t_k) - \hat{x}(t_k)'K'h_ih_i'K\hat{x}(t_k) > 0. \tag{6.18}$$

Thus, recalling the definition of $V(x)$ in (6.13) and that $u(t_k) = K\hat{x}(t_k)$, the satisfaction of (6.18) (or, equivalently, of (6.11)) implies that $u(t_k) \in \mathcal{S}_u$ as long as $x(t_k) \in \mathcal{L}_V(1)$. This, in conjunction with the fact that satisfaction of conditions (6.9) and (6.10) ensures $V(x(t_{k+1}) < V(x(t_k))$, implies that $x(t_k) \in \mathcal{L}_V(1)$ and therefore $u(t_k) \in \mathcal{S}_u$, $\forall k \in \mathbb{N}$, provided that $x(t_0) = x(0) \in \mathcal{L}_V(1)$.

Hence, we can conclude that the solutions of system (6.6) converge asymptotically to the origin if they start in $\mathcal{L}_V(1)$. Furthermore, the event-triggered strategy defined by (6.8) implicitly ensures that the inter-event times are lower bounded by $T$.

□

Figure 6.2 illustrates the idea behind Theorem 6.1. The underlying Lyapunov function $V(x(t))$ can increase during the interval $[t_k, t_k + T)$ but its total variation in the interval is negative, that is, $V(x(t_k + T)) < V(x(t_k))$. On the other hand, $\dot{V}(x(t))$ is guaranteed to be negative in the time interval $[t_k + T, t_{k+1})$, hence the total variation of $V$ in the interval $[t_k, t_{k+1})$ is negative. This means that the level sets $\mathcal{L}_V$ are not positively invariant in the sense that the trajectories can exit them during the dwell time. Nevertheless, the trajectories are guaranteed to return to a smaller level set at the end of the dwell time and the existence of the uniform bound $\beta$ for the Lyapunov function ensures that the trajectories are also uniformly bounded and decreasing with the time, i.e. their excursions outside each level set decreases as $k$ increases.

The following corollary addresses the global case (i.e. when relation (6.2) is satisfied $\forall u \in \mathbb{R}^m$).

**Corollary 6.1.** *Consider system* (6.6) *with $f$ satisfying* (6.2) *and $K$ and $L$ given. If there exist symmetric positive definite matrices $\bar{Q}_\delta$, $Q_\epsilon$ and $W = \left[\begin{smallmatrix} W_1 & W_2 \\ * & W_3 \end{smallmatrix}\right]$, diagonal*

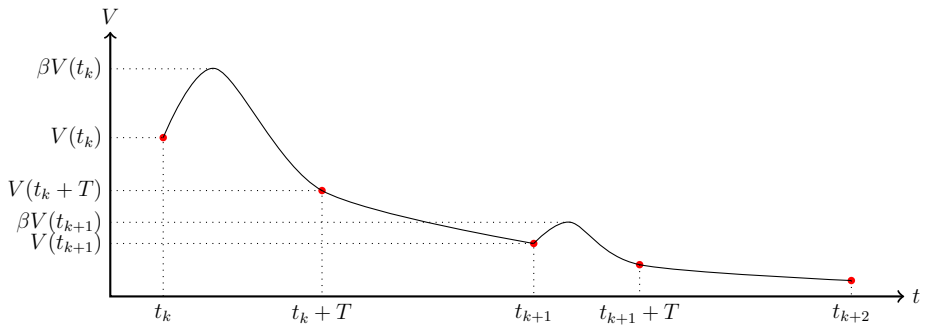


Figure 6.2: Lyapunov function bounding illustration.

*positive definite matrices $U_1$ and $U_2$ of appropriate dimensions and a positive scalar $T$ such that LMIs* (6.9) *and* (6.10) *are verified, then the event-triggered sampling rule* (6.8) *with $Q_\delta = W_1^{-1}\bar{Q}_\delta W_1^{-1}$ is such that the origin of system* (6.6) *is globally asymptotically stable. Furthermore, the inter-sampling times are lower bounded by $T$.*

*Proof.* The proof mimics that of Theorem 6.1 without the need to use constraint (6.11) since property (6.2) is globally satisfied. □

Observe that, if $T$ is fixed, conditions of Theorem 6.1 and of Corollary 6.1 are LMIs.

### 6.3.2 Optimization problems

The goal is again to choose the trigger condition parameters aiming at a reduction of the number of events while ensuring convergence to the origin for all initial conditions in a given set $\mathcal{X}_0$. We assume now that the set $\mathcal{X}_0$ is given by:

$$\mathcal{X}_0 = \left\{ x = \begin{bmatrix} \hat{x}' & e' \end{bmatrix}' \in \mathbb{R}^{2n} : x' P_0 x \leq 1 \right\} \tag{6.19}$$

with symmetric positive-definite $P_0 \in \mathbb{R}^{2n\times 2n}$ and that $T$ is given. Then we propose the following convex optimization problem as means of computing the trigger condition parameters in the regional stabilization context:

$$\begin{aligned} &\min \operatorname{tr}(\bar{Q}_\delta) + \operatorname{tr}(Q_\epsilon) \\ &\quad \text{subject to:} \\ &\quad\quad (6.9), (6.10), (6.11), W > P_0^{-1} \end{aligned} \tag{6.20}$$

The motivation behind the optimization problem (6.20) is analogous to what was presented in sections 4.3 and 5.2.

One should note that the dwell-time $T$ is also a design parameter and can be chosen according to the processing and network communication constraints. The designer can choose, for instance, the smallest dwell-time that is suitable given the infrastructure at hand or he can solve the optimization problems for various values of $T$ and choose the largest one that renders the optimization problem feasible.

For the global stabilization case, one uses the conditions of Corollary 6.1 and there is no need to ensure $\mathcal{X}_0 \subset \mathcal{L}_V(1)$. Hence, optimization problem (6.20) without conditions (6.11) and $W > P_0^{-1}$ can be considered.

## 6.4 Co-design

In this section, we address a partial co-design problem. Since the control system at hand employs a state observer, the term co-design can mean, as mentioned in Section 2.5, that the trigger condition and any other of the parameters of the system, like the control law and/or the observer gains, are designed concomitantly.

The idea here is the traditional co-design in the event-triggered control context, that is, to jointly design the matrix $K$ and the event-trigger function parameters, i.e. matrices $Q_\epsilon$ and $Q_\delta$ for a given observer gain $L$. It is worth noticing that, if $K$, $Q_\epsilon$ and $\bar{Q}_\delta$ are free variables, the conditions in Theorem 6.1 are no longer LMIs. To obtain tractable LMI stabilization conditions, the solution proposed is to impose some additional constraints on the structure of matrix $W$. The results that follow, addressing both regional and global stabilization, constitute original work developed as part of this thesis.

### 6.4.1 Stability conditions

The following theorem and corollary establish sufficient conditions for the regional and global asymptotic stabilization of the origin of the system (6.6).

**Theorem 6.2.** *Consider system* (6.6) *with $f$ satisfying* (6.2) *and $L$ given. Assume there exist symmetric positive definite matrices $\bar{Q}_\delta$, $Q_\epsilon$, $W = \left[\begin{smallmatrix} W_1 & 0 \\ 0 & W_3 \end{smallmatrix}\right]$, diagonal positive definite matrices $U_1$ and $U_2$, a matrix $Y_1$ of appropriate dimensions and a positive scalar $T$ such that the following LMIs are satisfied:*

$$\Omega_1 = \begin{bmatrix} M_2 & \begin{bmatrix} WC_a' \\ 0 \\ 0 \end{bmatrix} \\ * & -Q_\epsilon \end{bmatrix} < 0 \tag{6.21}$$

$$\Omega_2 = \begin{bmatrix} -W & -\begin{bmatrix} Y_1' \\ 0 \end{bmatrix} R & WA_{ad}(T)' + \begin{bmatrix} Y_1' \\ 0 \end{bmatrix} B_a' B_{ad}(T)' \\ * & -2U_2 & U_2 B_{af}' B_{ad}(T)' \\ * & * & -W \end{bmatrix} < 0 \tag{6.22}$$

$$\Omega_3 = \begin{bmatrix} W & \begin{bmatrix} Y_1' \\ 0 \end{bmatrix} h_i \\ * & 1 \end{bmatrix} > 0 \tag{6.23}$$

*with*

$$M_2 = \mathrm{He}\left\{ \begin{bmatrix} I \\ 0 \\ 0 \end{bmatrix} \begin{bmatrix} A_a W + B_a \begin{bmatrix} Y_1 & 0 \end{bmatrix} & B_a Y_1 & B_{af} U_1 \end{bmatrix} \right\} - \begin{bmatrix} 0 \\ I \\ 0 \end{bmatrix} \bar{Q}_\delta \begin{bmatrix} 0 & I & 0 \end{bmatrix}$$
$$- \mathrm{He}\left\{ \begin{bmatrix} 0 \\ 0 \\ I \end{bmatrix} \begin{bmatrix} R \begin{bmatrix} Y_1 & 0 \end{bmatrix} & RY_1 & U_1 \end{bmatrix} \right\}$$

*and the definitions of the auxiliary matrices $A_a$, $B_a$, $B_{af}$, $C_a$, $A_{ad}$, $B_{ad}$ as in* (6.12).

*Then, the event-triggered sampling rule defined by* (6.8) *with $Q_\delta = W_1^{-1} \bar{Q}_\delta W_1^{-1}$ is such that the origin of system* (6.6) *with $K = Y_1 W_1^{-1}$ is asymptotically stable and the set $\mathcal{L}_V(1) = \{x \in \mathbb{R}^{2n} : x' W^{-1} x \leq 1\}$ is included in its region of attraction. Furthermore, the inter-sampling times are lower bounded by $T$.*

*Proof.* The proof follows the same steps as the proof of Theorem 6.1 except that we impose the following structure to matrix $W = \left[\begin{smallmatrix} W_1 & 0 \\ 0 & W_3 \end{smallmatrix}\right]$, implying that $\begin{bmatrix} K & 0 \end{bmatrix} W = \begin{bmatrix} KW_1 & 0 \end{bmatrix}$ and then the change of variables $Y_1 = KW_1$ is done to linearize the conditions. □

The following corollary addresses the global case in the co-design context.

**Corollary 6.2.** *Given an observer gain matrix $L$ and a scalar $T > 0$, assume there exist symmetric positive definite matrices $\bar{Q}_\delta$, $Q_\epsilon$, $W = \left[\begin{smallmatrix} W_1 & 0 \\ 0 & W_3 \end{smallmatrix}\right]$, diagonal positive definite matrices $U_1$ and $U_2$ and a matrix $Y_1$ of appropriate dimensions such that the LMIs* (6.21) *and* (6.22) *are satisfied. Then, the event-triggered sampling rule defined by* (6.8) *with $Q_\delta = W_1^{-1}\bar{Q}_\delta W_1^{-1}$ is such that the origin of system* (6.6) *with $K = Y_1 W_1^{-1}$ is globally asymptotically stable. Furthermore, the inter-sampling times are lower bounded by $T$.*

*Proof.* It mimics the proof of Theorem 6.2 without the need of constraint (6.23) because property (6.2) is globally satisfied. □

### 6.4.2 Optimization problem

Conditions in Theorem 6.2 are LMIs provided $L$ and $T$ are fixed. Thus, the parameters of the trigger function $Q_\delta$ and $Q_\epsilon$ and the controller gains matrix $K$ can be simultaneously computed by solving the following convex optimization problem:

$$\begin{aligned} &\min \operatorname{tr}(\bar{Q}_\delta) + \operatorname{tr}(Q_\epsilon) \\ &\quad \text{subject to:} \\ &\qquad (6.21), (6.22), (6.23), W > P_0^{-1}. \end{aligned} \tag{6.24}$$

The reasoning behind the optimization problem (6.24) is the same as the one behind (6.20).

In the global stabilization case, i.e. when the relation (6.2) is satisfied $\forall u \in \mathbb{R}^m$, the conditions from Corollary 6.2 should be used. In this case, the optimization problem (6.24) without conditions (6.23) and $W > P_0^{-1}$ can be considered.

**Remark 6.1.** *The emulation design employs conditions that are less conservative than the co-design, as it uses an unconstrained matrix $W$. Thus, after solving co-design optimization problem* (6.24) *to obtain a suitable gain $K$, one can use this value of $K$ as an input to the emulation optimization problem* (6.20)*, aiming to a further reduction in the number of events. This process, referred as co-design refinement, is illustrated in Section 6.5, presenting the numerical examples.*

**Remark 6.2.** *The simultaneous design of $Q_\delta$, $Q_\epsilon$, $K$, $L$ and $T$ is a challenging co-design problem. Unfortunately, if one considers $L$ as a decision variable, it is not possible to linearize the conditions of Theorem 6.2. Moreover, $L$ and $T$ appear as part of exponential terms in the method used to integrate the trajectories of the system in the interval $[t_k, t_k + T]$, representing an additional difficulty.*

**Remark 6.3.** *Generic dynamic output event-triggered controllers with reduced information, i.e. controllers and event-generators with access only to the outputs and that do not use state observers, can also be addressed by the techniques presented here. For details, see (MOREIRA et al., 2017b, Section 6), which discusses generic dynamic controllers for linear plants subject to input saturation under event-triggered strategies with access only to the outputs.*

## 6.5 Numerical examples

In this section we present two numerical examples, one addressing the regional stabilization and one illustrating the global stabilization.

### 6.5.1 Example 1 – Regional stabilization

Let us consider the following plant:

$$\begin{cases} \dot{x}_p(t) = \begin{bmatrix} 0 & 1 \\ 4 & 0 \end{bmatrix} x_p(t) + \begin{bmatrix} 0 \\ 1 \end{bmatrix} q(u(t)) \\ y_p(t) = \begin{bmatrix} 1 & 0 \end{bmatrix} x_p(t) \end{cases} \tag{6.25}$$

where $q(u)$ is a logarithmic quantization function defined as follows (FU; XIE, 2005):

$$q(u) = \begin{cases} \rho_q^j \mu_q & \text{if} \quad \frac{\rho_q^j \mu_q}{1+\delta_q} \leq u < \frac{\rho_q^j \mu_q}{1-\delta_q},\ j \in \{0, 1, 2, ...\} \\ 0 & \text{if} \quad u = 0 \\ -q(-u) & \text{if} \quad u < 0 \end{cases}$$

with the quantization parameters:

$$0 < \rho_q < 1 \qquad \delta_q = \frac{1-\rho_q}{1+\rho_q} \qquad \mu_q > 0$$

where $\rho_q$ specifies the density of quantization and $\mu_q$ defines the maximum absolute level of quantization. Figure 6.3 shows a graphical representation of the positive branch of this logarithmic quantization function.

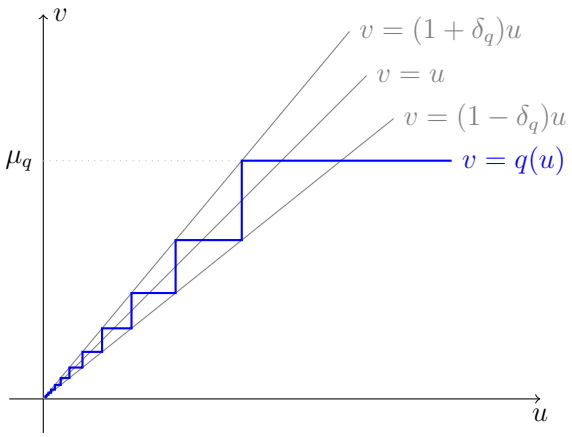


Figure 6.3: Logarithmic quantization function (positive branch).

It should be noticed that the quantization error $\tilde{q}(u) = q(u) - u$ is regionally restricted to the cone defined by $\pm\delta_q u$ (i.e. it satisfies the relation $(\tilde{q}(u) - \delta_q u)(\tilde{q}(u) + \delta_q u) < 0$) for all values of $u$ satisfying $|u| < \frac{\mu_q}{1-\delta_q}$ (see (DE SOUZA; COUTINHO; FU, 2010)). In order to cast the system in the form (6.1), with a function $f(u)$ satisfying (6.2), it suffices to consider:

$$f(u) = \tilde{q}(u) - \delta_q u \qquad A_p = \begin{bmatrix} 0 & 1 \\ 4 & 0 \end{bmatrix} \qquad B_{pf} = \begin{bmatrix} 0 \\ 1 \end{bmatrix}$$

$$B_p = (1+\delta_q)B_{pf} \qquad C_p = \begin{bmatrix} 1 & 0 \end{bmatrix} \qquad D_{pf} = 0$$

Note that in this case the relation $(\tilde{q}(u)+\delta_q u)(\tilde{q}(u)-\delta_q u)<0$ becomes $f(u)(f(u)+2\delta_q u)<0$, i.e. (6.2) is verified with $R=2\delta_q$. Moreover, this relation is satisfied as long as $|u|<\frac{\mu_q}{1-\delta_q}$, that is, $\frac{1-\delta_q}{\mu_q}|u|\leq 1$.

We consider the quantization with $\rho_q=0.9$, which leads to $R=2\delta_q=0.1053$ and $\mu_q=35$.

#### *6.5.1.1 Optimization results*

Considering the state feedback gain matrix $K=\begin{bmatrix}-4.8 & -1.9\end{bmatrix}$, the observer gain matrix $L=\begin{bmatrix}-3.5 & -7\end{bmatrix}'$, $\mathcal{X}_0$ defined as in (6.19) with $P_0=\mathrm{diag}(10^6,10^6,0.1,0.1)$ and the dwell-time $T=0.02$, we solve the emulation design optimization problem (6.20) with additional conditions $\lambda_{min}(Q_\delta)>10^{-4}$ and $\lambda_{max}(Q_\epsilon)<10^3\lambda_{min}(Q_\epsilon)$ to prevent $Q_\delta$ and $Q_\epsilon$ from becoming ill-conditioned, obtaining the following results:

$$Q_\epsilon=\begin{bmatrix}848.8 & 188.2 & 98.71\\ 188.2 & 101.4 & 18.31\\ 98.71 & 18.31 & 27.89\end{bmatrix} \qquad Q_\delta=\begin{bmatrix}1.162 & 0.4599\\ 0.4599 & 0.1822\end{bmatrix}$$

Using the same values $L=\begin{bmatrix}-3.5 & -7\end{bmatrix}'$, $P_0=\mathrm{diag}(10^6,10^6,0.1,0.1)$ and $T=0.02$, the co-design optimization problem (6.24) with the same additional conditions to prevent $Q_\delta$ and $Q_\epsilon$ from becoming ill-conditioned yields:

$$K=\begin{bmatrix}-9.299 & -4.598\end{bmatrix} \quad Q_\epsilon=\begin{bmatrix}201.9 & -7.784 & 122.3\\ -7.784 & 44.37 & 11.15\\ 122.3 & 11.15 & 81.26\end{bmatrix} \quad Q_\delta=\begin{bmatrix}4.309 & 2.131\\ 2.131 & 1.054\end{bmatrix}$$

As mentioned in Remark 6.1, we can refine the results by solving the emulation optimization problem (6.20) with the gain $K=\begin{bmatrix}-9.299 & -4.598\end{bmatrix}$ obtained in the co-design. This yields the following results:

$$Q_\epsilon=\begin{bmatrix}63.14 & 1.518 & 37.73\\ 1.518 & 52.2 & 25.8\\ 37.73 & 25.8 & 36.2\end{bmatrix} \qquad Q_\delta=\begin{bmatrix}1.929 & 0.9537\\ 0.9537 & 0.4716\end{bmatrix}$$

The ellipses defined by the intersection between the plane $\hat{x}=0$ and the sets $\mathcal{L}_V(1)=\{x\in\mathbb{R}^{2n}:\ x'W^{-1}x=1\}$ for each $W$ obtained with the optimization problems above are shown in Figure 6.4 (in black lines), along with the intersection between the same plane and the border of $\mathcal{X}_0$ (in red lines). This figure also shows some trajectories that converge to the origin in blue and some divergent ones in magenta. The graphics at the bottom are zoomed views of the ones at the top. One can see that, in all cases, $\mathcal{L}_V(1)$ contains $\mathcal{X}_0$, as required by the optimization problems. It is also visible that the sets $\mathcal{L}_V(1)$ are contained in the region of attraction of the origin in each case and, therefore, can be used as estimates for it.

#### *6.5.1.2 Influence of $T$*

Table 6.1 shows the influence of $T$ in the results. It depicts the average number of control updates for simulations within the time interval $[0,10]$ seconds, considering 100 different initial plant states, distributed along the boundary of the respective $\mathcal{L}_V(1)$ set, for various values of $T$ and for each of the proposed design methods. The initial state of the observer is zero in all simulations. One can see that $T$ has an expressive impact

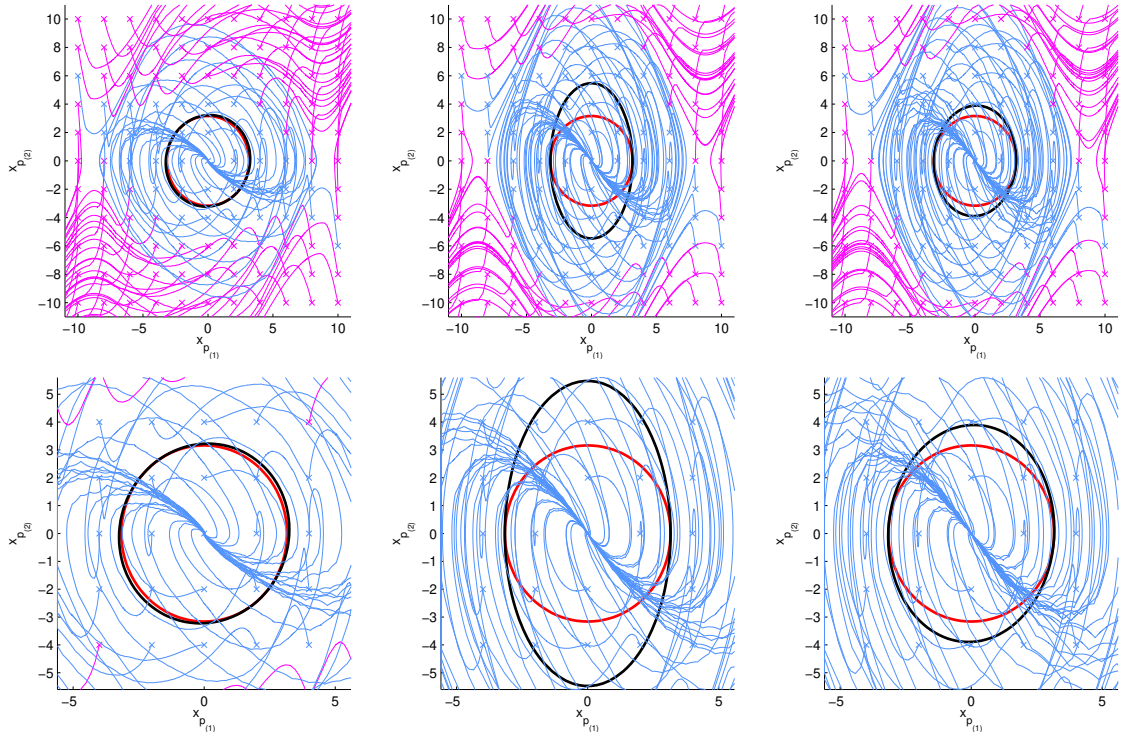


a) Emulation b) Co-design c) Co-design refinement

Figure 6.4: Example 1 – Phase portraits, $\mathcal{L}_V(1)$ (in black) and $\mathcal{X}_0$ ( in red).

on the number of events generated in the co-design and refinement cases, but not in the emulation case. In the emulation context, the impact of $T$ is highly dependent on the system characteristics and the chosen value of $K$. Different behaviors can occur for different choices of $K$. Moreover, notice that the co-design problem is not feasible for some values of $T$ where the emulation problem is. This can be expected since the co-design conditions are more restrictive than the emulation ones due to the structure imposed to $W$. It is also shown that the co-design leads to less events and that the refinements mentioned in Remark 6.1 reduce even more their number.

#### *6.5.1.3 Simulations*

Here we present simulations of the closed-loop systems designed with the help of optimization problems (6.20) and (6.24) and also with the co-design refinements proposed in Remark 6.1, considering two different values of $T$. In all simulations, the initial conditions for the plant and the observer are, respectively:

$$x_p(0) = \begin{bmatrix} -3 \\ 0 \end{bmatrix} \qquad \hat{x}(0) = \begin{bmatrix} 0 \\ 0 \end{bmatrix}$$

Figures 6.5 and 6.6 depict the plant and observer states in the top plots. It can be noticed that the observer states converge to the plant states, as expected, and also the convergence of the plant states to the origin. The middle plots show the control action. One can note that the value of the control is subject to a logarithmic quantization. The bottom plot depicts the event instants, with the sizes of the bars representing the inter-event times, i.e. the difference between the time of that event and the previous one. It can be seen that the triggering strategy effectively delays the event instants, yielding

Table 6.1: Example 1 – Average number of control updates for 100 different initial conditions.

| $T$ | Emulation | Co-design | Co-design refinement |
|---|---|---|---|
| 0.01 | 65.56 | 50.33 | 35.00 |
| 0.02 | 65.47 | 50.13 | 34.47 |
| 0.03 | 65.67 | 48.48 | 34.72 |
| 0.04 | 65.05 | 43.48 | 32.45 |
| 0.043 | 64.60 | 40.38 | 30.86 |
| 0.044 | 64.09 | 40.55 | 29.64 |
| 0.045 | 64.24 | unfeasible | – |
| 0.05 | 63.31 | unfeasible | – |
| 0.10 | 64.25 | unfeasible | – |
| 0.11 | unfeasible | unfeasible | – |

inter-event times larger than the dwell-time while ensuring the asymptotic stability of the closed-loop system. The figures also highlight that the co-design and refinement processes result in less events than the emulation.

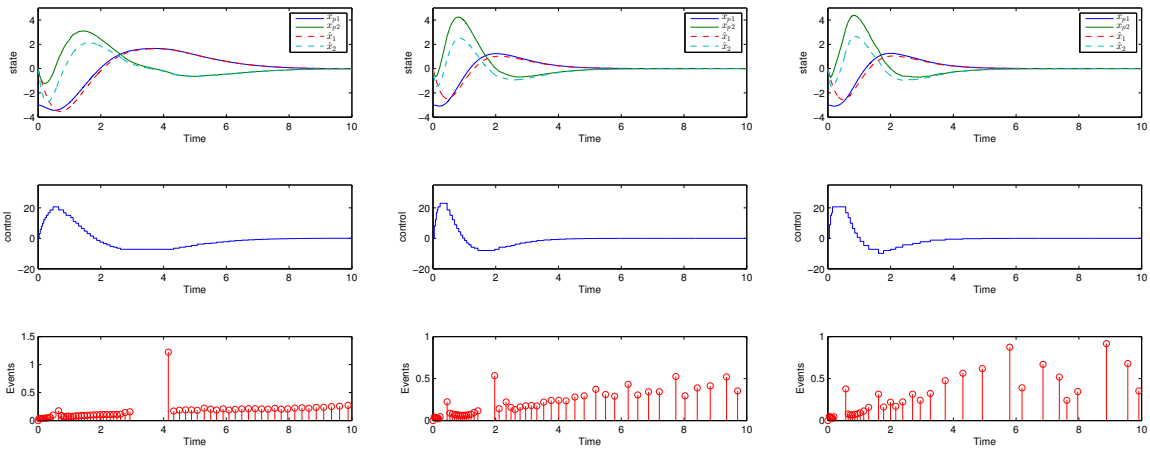


a) Emulation b) Co-design c) Co-design refinement

Figure 6.5: Example 1 – Simulations, $T = 0.02$.

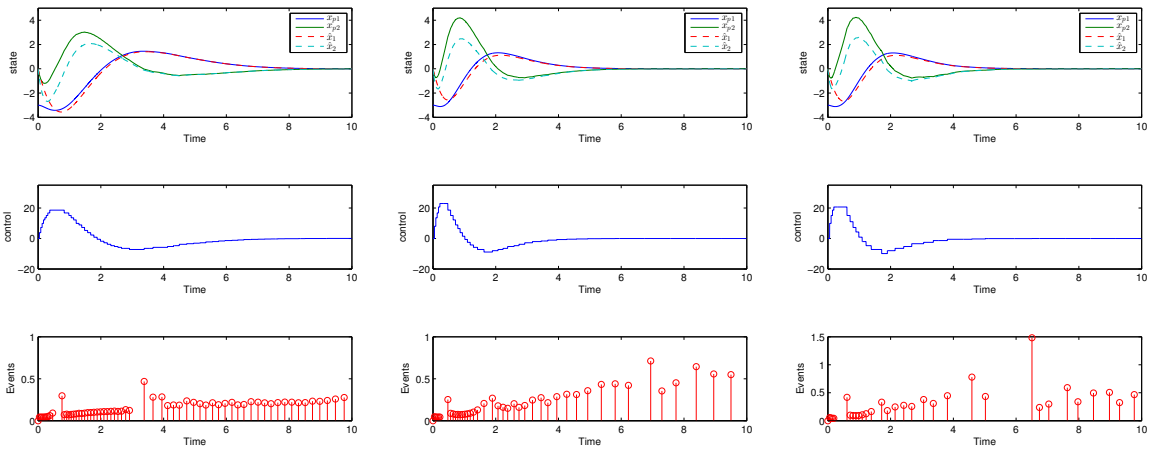


a) Emulation b) Co-design c) Co-design refinement

Figure 6.6: Example 1 – Simulations, $T = 0.043$.

### 6.5.2 Example 2 – Global stabilization

Now we consider the following stable plant:

$$\begin{cases} \dot{x}_p(t) = \begin{bmatrix} -1 & 2 \\ -2 & 0 \end{bmatrix} x_p(t) + \begin{bmatrix} 0 \\ 1 \end{bmatrix} \mathrm{sat}(u(t)) \\ y_p(t) = \begin{bmatrix} 1 & 0 \end{bmatrix} x_p(t) \end{cases} \tag{6.26}$$

where $\mathrm{sat}(\cdot)$ is a saturation function with saturation levels at $\pm 5$. Note that (6.26) can be re-written in the form (6.1) by assuming $f$ to be a dead-zone function, i.e. $f(u) = \mathrm{sat}(u) - u$, which satisfies condition (6.2) with $R = 1$ globally, i.e. $\forall u \in \mathbb{R}^m$ and the following matrices:

$$A_p = \begin{bmatrix} -1 & 2 \\ -2 & 0 \end{bmatrix} \qquad B_p = B_{pf} = \begin{bmatrix} 0 \\ 1 \end{bmatrix} \qquad C_p = \begin{bmatrix} 1 & 0 \end{bmatrix} \qquad D_{pf} = 0$$

#### 6.5.2.1 *Optimization results*

Consider first the emulation case with $K = \begin{bmatrix} 2 & -4 \end{bmatrix}$ and $L = \begin{bmatrix} -20 & -53 \end{bmatrix}'$. In this case, the eigenvalues of $A_p + B_p K$ are $-1$ and $-4$ and the eigenvalues of $A_p + LC_p$ are $-10$ and $-11$. Choosing a dwell-time $T = 0.1$, and solving the version of optimization problem (6.20) suitable for the global case, with modifications to impose a minimum exponential decay rate of $0.75$ so that the solution does not degenerate into open-loop [1], i.e. imposing $\dot{V}(x(t)) < -0.75V(x(t))$ and $V(x(t_k + T)) - V(x(t_k)) < (e^{-0.75T} - 1)V(x(t_k))$, one obtains the following results:

$$Q_\epsilon = \begin{bmatrix} 3.581 & 0.5562 & -0.001386 \\ 0.5562 & 2.715 & 0.008729 \\ -0.001386 & 0.008729 & 0.7225 \end{bmatrix} \qquad Q_\delta = \begin{bmatrix} 9.922 & -9.883 \\ -9.883 & 17.38 \end{bmatrix}$$

For the co-design case, considering the same values of $L = \begin{bmatrix} -20 & -53 \end{bmatrix}'$, $T = 0.1$ and the same additional conditions related to the conditioning of matrices and exponential decay rate, the solution of the version of optimization problem (6.24) suitable for the global case leads to:

$$K = \begin{bmatrix} 1.232 & -4.6503 \end{bmatrix}$$

$$Q_\epsilon = \begin{bmatrix} 1.067 & 0.1554 & 0.0005847 \\ 0.1554 & 1.058 & 0.002162 \\ 0.0005847 & 0.002162 & 0.1619 \end{bmatrix} \qquad Q_\delta = \begin{bmatrix} 6.266 & -5.72 \\ -5.72 & 16.92 \end{bmatrix}$$

Refining the event-trigger as mentioned in Remark 6.1, one obtains:

$$Q_\epsilon = \begin{bmatrix} 0.3437 & 0.04672 & 0.0003135 \\ 0.04672 & 0.3302 & 0.001317 \\ 0.0003135 & 0.001317 & 0.06555 \end{bmatrix} \qquad Q_\delta = \begin{bmatrix} 15.98 & -15.15 \\ -15.15 & 43.56 \end{bmatrix}$$

#### 6.5.2.2 *Influence of $T$*

Table 6.2 shows the influence of $T$ in the results. It depicts the average number of control updates for simulations considering 100 different initial plant states distributed along the unit circle and within the time interval $[0, 10]$ seconds for various values of $T$ and for each of the proposed design methods. The initial state of the observer is zero in all simulations. One can see that, for small values of $T$, the co-design leads again to less events and that the refinements mentioned in Remark 6.1 allow to further reduce the number of events. For larger values of $T$, on the other hand, all three methods give the same results. As it is going to be shown in the simulations, this is because, in the case presented here, when $T$ increases, the event-trigger mechanism becomes less effective and the triggering becomes periodic with period $T$. Table 6.2 also shows that, for this system and the particular value of $K$ considered in the emulation design, the co-design allows to choose a wider range of values for the dwell-time $T$. This illustrates again that, in the emulation case, the impact of $T$ is highly dependent on the system characteristics and the chosen value of $K$. In the example at hand, with the chosen $K = \begin{bmatrix} 2 & -4 \end{bmatrix}$, a periodic controller with a period greater than or equal to $0.5$ leads to a closed-loop system that is not asymptotically stable as can be seen in the simulations shown in Figure 6.7.

[1] Since the origin of the system is open-loop stable, if we impose just stability, the optimal event generator will be one that does not generate any events and the system will operate in open-loop.

Table 6.2: Example 2 – Average number of control updates for 100 different initial conditions.

| $T$ | Emulation | Co-design | Co-design refinement |
|---|---|---|---|
| 0.01 | 78.58 | 53.82 | 49.23 |
| 0.05 | 73.50 | 48.88 | 46.35 |
| 0.10 | 60.18 | 48.74 | 45.15 |
| 0.20 | 50.00 | 50.00 | 50.00 |
| 0.30 | 34.00 | 34.00 | 34.00 |
| 0.40 | 25.00 | 25.00 | 25.00 |
| 0.50 | unfeasible | 20.00 | 20.00 |
| 0.60 | unfeasible | 17.00 | 17.00 |

That explains why the emulation problem becomes unfeasible for $T \geq 0.5$. On the other hand, the co-design problem (which computes a different $K$) and the co-design refinement (which uses $K$ from the corresponding co-design) are still feasible for $T = 0.5$ and $T = 0.6$.

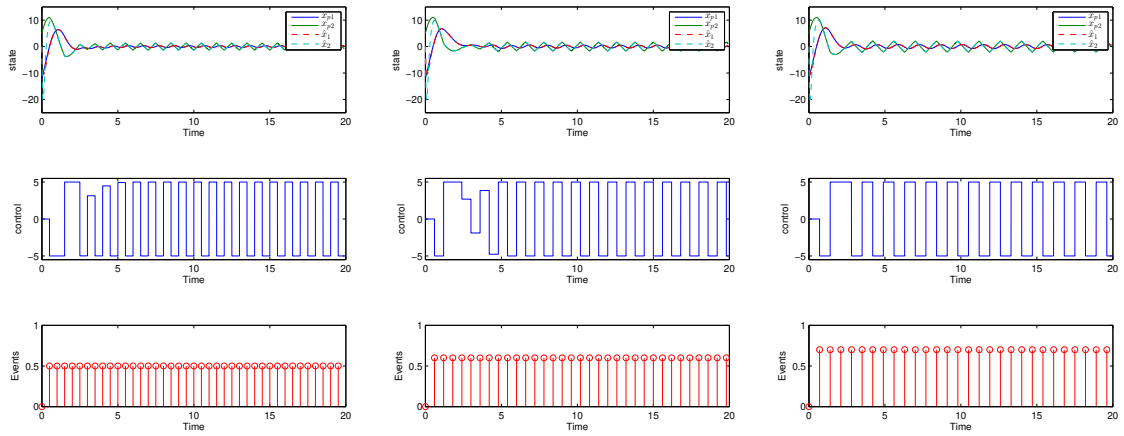


a) $T = 0.5$ b) $T = 0.6$ c) $T = 0.7$

Figure 6.7: Example 2 – Simulations of periodic implementation.

### *6.5.2.3 Simulations*

In this section, we present simulations of the closed-loop systems from an emulation and a co-design point of view for two different values of $T$. We also include simulations of the systems obtained with the refinements proposed in Remark 6.1. In all simulations, the initial conditions for the plant and the observer are, respectively:

$$x_p(0) = \begin{bmatrix} -12 \\ 5 \end{bmatrix} \qquad \hat{x}(0) = \begin{bmatrix} 0 \\ 0 \end{bmatrix}$$

Figures 6.8 and 6.9 depict the plant and observer states in the top plots. The observer states quickly converge to the plant states and the state converges to the origin, as expected. The middle plots show the control action, where one can note that it is indeed being limited at the values $\pm 5$ given by the saturation function. The bottom plot depicts

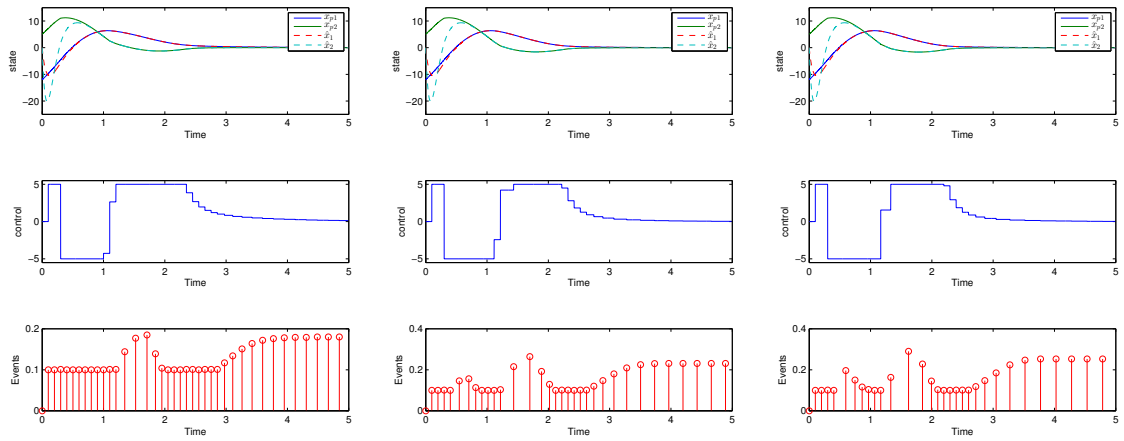


a) Emulation b) Co-design c) Co-design refinement

Figure 6.8: Example 2 – Simulations, $T = 0.1$.

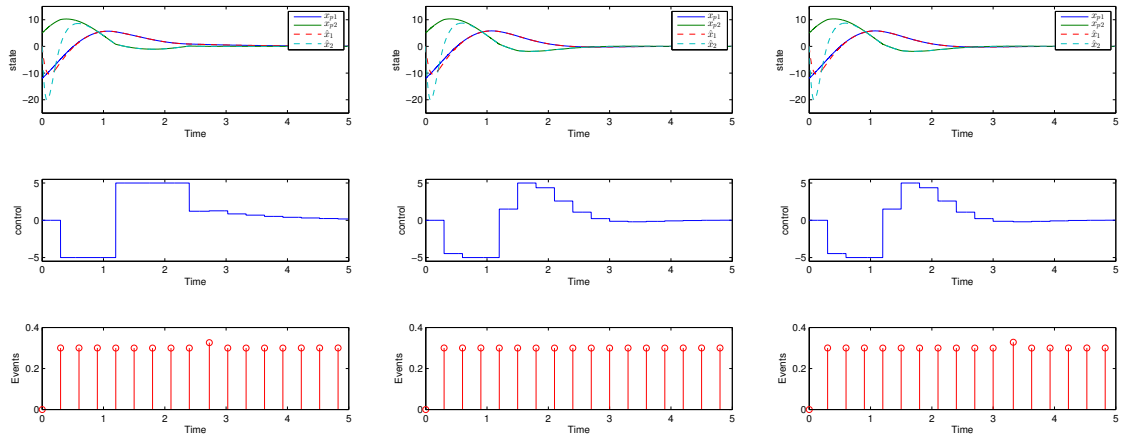


a) Emulation b) Co-design c) Co-design refinement

Figure 6.9: Example 2 – Simulations, $T = 0.3$.

the event instants, with the sizes of the bars representing the inter-event times. One can see that the triggering strategy effectively delays the event instants for low values of $T$. On the other hand, when $T$ increases, the event-trigger mechanism becomes less effective and the triggering becomes periodic.

## 6.6 Conclusion

In this chapter we addressed the design of event-triggered control for Lur'e type systems where the nonlinearities are sector-bounded and depend only on the system input. The triggering strategy uses only available information and an observer was proposed to recover the state variables that are not available.

Since this configuration is a type of output-based event-triggered control, it is generally impossible to eliminate the possibility Zeno behavior by the techniques employed in Part I of this thesis. Therefore, we imposed an explicit minimum inter-event time by

the use of a dwell-time $T$ in the trigger condition. The inclusion of a "discrete-time like" stability condition, derived from the solution of the system in the intervals $[t_k, t_k + T]$, allows to guarantee the asymptotic stability of the origin in the presence of the dwell-time. This approach is possible since the nonlinearity depends only on the system input, which is kept constant between any two consecutive events.

Emulation design and co-design of the event generator parameters and the controller gains have been addressed both for regional and global stabilization cases. Convex optimization problems were proposed as means to compute these parameters.

We ended the chapter with numerical examples showing some potential of the proposed methods and highlighting the superiority of results achievable in the co-design context with respect to the number of generated events. The examples also illustrated that solving the co-design problem to obtain a suitable control gain matrix $K$ and the subsequent use of this gain in an emulation context leads to a refinement in the event generator parameters and less events. This is explained by the fact that the linearization methods used to obtain the co-design stability conditions represent additional conservatism with respect to the stability conditions in the emulation context.

The results of this chapter were submitted for publication in (MOREIRA et al., 2018a) and a resumed congress version, encompassing the global stabilization case, was published in (TARBOURIECH et al., 2017). Besides that, (MOREIRA et al., 2017b) uses similar techniques, based on a dwell time and exact discretization of the system, to addresses the design of event-triggered PI controllers for systems subject to control input saturation.

An interesting related problem is the co-design including the observer gain $L$. It is difficult to be addressed with the methodology presented in this chapter due to the terms involving the exponential of $L$. Nevertheless, it can be elegantly addressed by the looped-functional approach that is going to be presented in Chapter 7.

# 7 LUR'E SYSTEMS WITH NONLINEARITIES DEPENDING ON THE STATE

In this chapter we address the design of event-triggered controllers for Lur'e systems where the nonlinearity depends on the plant's state. We assume again that the event generator and the controller do not have access to the entire state of the system and a nonlinear state observer is used to recover the missing information. This leads to an additional challenge since, in this case, the nonlinearity does not cancel out in the observation error dynamics. Thus, a different approach needs to be employed to cope with this fact.

A dwell-time is used, as in Chapter 6, to avoid Zeno behavior (MAZO; ANTA; TABUADA, 2010). In the case at hand, however, the exact discretization technique used in Chapter 6 to ensure the asymptotic stability in the presence of the dwell-time cannot be applied, since the value of the nonlinearity varies continuously. To overcome this issue, we consider a looped-functional approach (SEURET, 2012; BRIAT; SEURET, 2012) to ensure that the trajectories during the dwell-time are bounded and the total variation of a quadratic Lyapunov function over this time is strictly decreasing. As a side effect of the condition, the stability of the closed-loop nonlinear system under periodic sampled-data control, with period equal to the considered dwell time is also formally guaranteed.

Since the design of a continuous-time controller for the class of systems at hand can be carried out by the methods described e.g. in (CASTELAN; TARBOURIECH; QUEINNEC, 2008), we consider here the emulation case and the co-design of the observer and the event-generator. Nevertheless, the method can be extended to address the usual co-design of the event-generator and the controller gain as shown in Remark 7.1.

## 7.1 Addressed system

We consider a continuous-time plant represented by the following equations:

$$\begin{cases} \dot{x}_p(t) = A_p x_p(t) + B_p u(t) + B_{pf} f(H x_p(t)) \\ y_p(t) = C_p x_p(t) \end{cases} \tag{7.1}$$

where $x_p(t) \in \mathbb{R}^n$, $u(t) \in \mathbb{R}^m$, $y_p(t) \in \mathbb{R}^p$ are the state, the input and the output of the plant, respectively. The matrices $A_p$, $B_p$, $B_{pf}$, $C_p$ and $H$ are constant and of appropriate dimensions.

Function $f : \mathbb{R}^l \to \mathbb{R}^l$ is a sector-bounded, slope-restricted, decentralized nonlinearity, i.e., each component $f_{(i)} : \mathbb{R} \to \mathbb{R}, i \in \{1,...,l\}$ satisfies the assumptions:

(A1) $f_{(i)}(0) = 0$.

(A2) $f_{(i)}(v_i)\left(f_{(i)}(v_i) - \lambda_i v_i\right) \leq 0.$

(A3) $f_{(i)}(v_i)$ is continuous and differentiable by parts, satisfying

$$0 \leq \frac{df_{(i)}(v_i)}{dv_i} \leq \lambda_i; \qquad \lambda_i > 0, \forall v_i \in \mathbb{R}$$

Associated to the nonlinearity $f$, we can define a function $\rho : \mathbb{R}^l \times \mathbb{R}^l \to \mathbb{R}^l$ as follows:

$$\rho(a, b) = f(a + b) - f(b) \tag{7.2}$$

where $a$,$b \in \mathbb{R}^l$.

We consider the following observer-based state feedback controller to asymptotically stabilize the system (7.1):

$$\begin{cases} \dot{\hat{x}}(t) = A_p\hat{x}(t) + B_p u(t) + B_{pf} f(H\hat{x}(t)) - Le_y(t) \\ \hat{y}(t) = C_p\hat{x}(t) \\ u(t) = K\hat{x}(t) \end{cases} \tag{7.3}$$

where $\hat{x}(t) \in \mathbb{R}^n$ and $\hat{y}(t) \in \mathbb{R}^p$ are the state and the output of the observer, respectively, and $e_y(t) = y_p(t) - \hat{y}(t)$ is the output error. $L \in \mathbb{R}^{n\times p}$ and $K \in \mathbb{R}^{m\times n}$ are the observer and controller gains, respectively.

Considering an event-triggered control implementation, the actual control signal applied to the plant during the time interval $t \in [t_k, t_{k+1})$ is given by:

$$u(t) = K\hat{x}(t_k) \tag{7.4}$$

Now, taking (7.4) into consideration, defining the observation error $e(t) = x_p(t) - \hat{x}(t)$ and noticing that this implies $Hx_p(t) = He(t) + H\hat{x}(t)$, we can represent the dynamics of the closed-loop system with respect to the variables $\hat{x}(t)$ and $e(t)$ as follows:

$$\begin{cases} \dot{\hat{x}}(t) = A_p\hat{x}(t) + B_p u(t) + B_{pf} f(H\hat{x}(t)) - LC_p e(t) \\ \dot{e}(t) = (A_p + LC_p)e(t) + B_{pf}\left[f(Hx_p(t) - f(H\hat{x}(t))\right] \\ \qquad = (A_p + LC_p)e(t) + B_{pf}\left[f(He(t) + H\hat{x}(t)) - f(H\hat{x}(t))\right] \\ u(t) = K\hat{x}(t_k) \end{cases} \tag{7.5}$$

Then, from the definition of function $\rho$ in (7.2), it follows that $f(He(t) + H\hat{x}(t)) - f(H\hat{x}(t)) = \rho\left(He(t), H\hat{x}(t)\right)$ and (7.5) can be written as:

$$\begin{cases} \dot{\hat{x}}(t) = A_p\hat{x}(t) + B_p u(t) + B_{pf} f(H\hat{x}(t)) - LC_p e(t) \\ \dot{e}(t) = (A_p + LC_p)e(t) + B_{pf}\rho(He(t), H\hat{x}(t)) \\ u(t) = K\hat{x}(t_k) \end{cases} \tag{7.6}$$

Defining the augmented state vector $x(t) = \begin{bmatrix}\hat{x}'(t) & e'(t)\end{bmatrix}' \in \mathbb{R}^{2n}$, it follows that $H\hat{x}(t)) = \begin{bmatrix}H & 0\end{bmatrix} x$, $He(t) = \begin{bmatrix}0 & H\end{bmatrix} x$ and $K\hat{x}(t_k) = \begin{bmatrix}K & 0\end{bmatrix} x(t_k)$. Using these relations and defining the vector of information available to the event generator as $y_a(t) = \begin{bmatrix}\hat{x}'(t) & e_y'(t)\end{bmatrix}' \in \mathbb{R}^{2n+p}$, the closed-loop system can be represented, $\forall t \in [t_k, t_{k+1}), \forall k \in \mathbb{N}$, as follows:

$$\begin{cases} \dot{x}(t) = A_a x(t) + B_a u(t) + B_{af} f(H_1 x(t)) + B_{a\rho}\rho(H_2 x(t), H_1 x(t)) \\ u(t) = \begin{bmatrix}K & 0\end{bmatrix} x(t_k) \\ y_a(t) = C_a x(t) \end{cases} \tag{7.7}$$

with

$$H_1 = \begin{bmatrix} H & 0 \end{bmatrix} \qquad H_2 = \begin{bmatrix} 0 & H \end{bmatrix} \qquad A_a = \begin{bmatrix} A_p & -LC_p \\ 0 & A_p + LC_p \end{bmatrix}$$

$$B_a = \begin{bmatrix} B_p \\ 0 \end{bmatrix}, \qquad C_a = \begin{bmatrix} I & 0 \\ 0 & C_p \end{bmatrix} \qquad B_{af} = \begin{bmatrix} B_{pf} \\ 0 \end{bmatrix} \qquad B_{a\rho} = \begin{bmatrix} 0 \\ B_{pf} \end{bmatrix} \tag{7.8}$$

$$\rho(H_2 x(t), H_1 x(t)) = f(H_1 x(t) + H_2 x(t)) - f(H_1 x(t))$$

## 7.2 Event generator

Here, we consider the same event-triggering strategy used in the Chapter 6, i.e.:

$$t_{k+1} = \min\{t \geq t_k + T, \quad s.t. \quad \delta(t)' Q_\delta \delta(t) - \begin{bmatrix} \hat{x}(t) \\ e_y(t) \end{bmatrix}' Q_\epsilon^{-1} \begin{bmatrix} \hat{x}(t) \\ e_y(t) \end{bmatrix} \geq 0\} \tag{7.9}$$

where $Q_\delta$ and $Q_\epsilon$ are constant symmetric positive-definite matrices of appropriate dimensions, the dwell-time $T$ is a positive scalar and $\delta(t)$ is defined as follows:

$$\delta(t) = \hat{x}(t_k) - \hat{x}(t) \tag{7.10}$$

To simplify the notation in the exposition that follows, we are going to define the vector of information available to the event generator:

$$y_a(t) = \begin{bmatrix} \hat{x}(t) \\ e_y(t) \end{bmatrix} \in \mathbb{R}^{n+p} \tag{7.11}$$

and the triggering function:

$$g(\delta(t), y_a(t)) = \delta(t)' Q_\delta \delta(t) - \begin{bmatrix} \hat{x}(t) \\ e_y(t) \end{bmatrix}' Q_\epsilon^{-1} \begin{bmatrix} \hat{x}(t) \\ e_y(t) \end{bmatrix} \tag{7.12}$$

Considering (7.11) and (7.12), the trigger function can be written in the following compact form:

$$t_{k+1} = \min\{t \geq t_k + T, \quad s.t. \quad g(\delta(t), y_a(t)) \geq 0\}. \tag{7.13}$$

## 7.3 Instrumental tools

The following lemmas will be useful to derive the main results of this chapter. The first one is the classical sector condition (KHALIL, 1996):

**Lemma 7.1.** *If each component of $f$ satisfies the assumption (A2), then*

$$f'(v) S_f (f(v) - \Lambda v) \leq 0 \tag{7.14}$$

*where $\Lambda = \mathrm{diag}(\lambda_1, ..., \lambda_l)$ and $S_f \in \mathbb{R}^{l \times l}$ is any diagonal positive-definite matrix, is satisfied $\forall v \in \mathbb{R}^l$.*

*Proof.* It follows directly from (A2). □

To handle the nonlinearity $\rho(H_2x(t), H_1x(t))$ that appears from the use of the state observer, we derive the following lemma, inspired by Lemma 1 from (FISCHMANN; FLORES; GOMES DA SILVA JR., 2017):

**Lemma 7.2.** *Consider the nonlinearity $\rho$, derived from $f$ and defined in* (7.2)*, i.e.:*

$$\rho(v_1, v_0) = f(v_0 + v_1) - f(v_0) \tag{7.15}$$

*If each component of $f$ satisfies the assumptions (A1) - (A3), then*

$$\rho'(v_1, v_0)S_\rho(\rho(v_1,v_0) - \Lambda v_1) \leq 0 \tag{7.16}$$

*where $\Lambda = \mathrm{diag}(\lambda_1, ..., \lambda_l)$ and $S_\rho \in \mathbb{R}^{l\times l}$ is any diagonal positive-definite matrix, is satisfied $\forall v_1, v_0 \in \mathbb{R}^l$.*

*Proof.* Consider each component $\rho_{(i)}$ of $\rho$ and its corresponding arguments $v_{1i}$ and $v_{0i}$, which are scalars.

If $v_{1i} \geq 0$, the assumptions on the lower-bound of the derivative of $f_{(i)}$ imply that $f_{(i)}$ is monotonically crescent, i.e., $f_{(i)}(v_{0i} + v_{1i}) \geq f_{(i)}(v_{0i})$, or, equivalently, $f_{(i)}(v_{0i} + v_{1i}) - f_{(i)}(v_{0i}) \geq 0$, leading to $\rho_{(i)}(v_{1i},v_{0i}) \geq 0$. The upper-limit of the derivative leads, by applying the Mean Value Theorem, to $f_{(i)}(v_{0i}+v_{1i}) - f_{(i)}(v_{0i}) \leq \lambda_i v_{1i}$, i.e. $\rho_{(i)}(v_{1i}, v_{0i}) - \lambda_i v_{1i} \leq 0$. Thus (7.16) holds in this case.

If $v_{1i} < 0$, a similar analysis brings $\rho_{(i)}(v_{1i},v_{0i}) \leq 0$ and $\rho_{(i)}(v_{1i}, v_{0i}) - \lambda_i v_{1i} \geq 0$.

Hence, $\rho_{(i)}(v_{1i},v_{0i})\sigma_i(\rho_{(i)}(v_{1i},v_{0i}) - \lambda_i v_{1i}) \leq 0, \forall\sigma_i > 0$ and relation (7.16) follows directly with $S_\rho = \mathrm{diag}(\sigma_1, ..., \sigma_l)$.

□

To enable the use of a dwell-time in the triggering condition, we will use the following lemma, which is an adapted version of the Theorem 1 from (SEURET; GOMES DA SILVA JR., 2012).

**Lemma 7.3.** *Consider a positive scalar $T$, a differentiable function $\mathcal{X} \in \mathbb{F}^n_{[0,T]}$ and a differentiable positive definite function $V : \mathbb{R}^n \to \mathbb{R}$ such that there exist positive scalars $\mu_1$ and $\mu_2$ and a positive integer $p$ satisfying*

$$\mu_1\|x\|^p \leq V(x) \leq \mu_2\|x\|^p \tag{7.17}$$

*Then, the following statements are equivalent:*

*(i) The total variation of $V(\mathcal{X}(t))$ in the time interval $[0, T]$ is negative, i.e.:*

$$V(\mathcal{X}(T)) - V(\mathcal{X}(0)) < 0 \tag{7.18}$$

*(ii) There exist a continuous functional $V_0 : [0, T] \times \mathbb{F}^n_{[0,T]} \to \mathbb{R}$ such that:*

$$V_0(T, \mathcal{X}) = V_0(0, \mathcal{X}), \qquad \forall\mathcal{X} \in \mathbb{F}^n_{[0,T]} \tag{7.19}$$

$$\dot{W}(\tau, \mathcal{X}) = \frac{d}{d\tau}[V(\mathcal{X}(\tau)) + V_0(\tau,\mathcal{X})] < 0, \quad \forall\tau \in [0, T) \tag{7.20}$$

*Proof.* Assume that (i) is satisfied. Consider the functional $V_0(\tau, \mathcal{X}) = -V(\mathcal{X}(\tau)) + \frac{\tau}{T}[V(\mathcal{X}(T)) - V(\mathcal{X}(0))]$, with $\tau \in [0, T)$. It is easy to see that this functional satisfies (7.19) and that $\dot{W}(\tau, \mathcal{X}) = \frac{1}{T}[V(\mathcal{X}(T)) - V(\mathcal{X}(0))] < 0$, if (i) is satisfied.

Now assume that (ii) is satisfied, which means that (7.19) and (7.20) hold. Integrating (7.20) over $[0, T)$ leads to $V(\mathcal{X}(T)) - V(\mathcal{X}(0)) + V_0(T, \mathcal{X}) - V_0(0, \mathcal{X}) < 0$. Since (7.19) holds by assumption, relation (7.18) follows directly. □

## 7.4 Emulation case

In this section, the emulation case is addressed. The goal is to propose a way to design the parameters $Q_\delta$ and $Q_\epsilon$ of the event-triggering strategy (7.9) when the controller and observer gains, $K$ and $L$ respectively, are given *a priori*.

### 7.4.1 Stability conditions

The following theorem establishes sufficient conditions for the global asymptotic stabilization of the origin of the system (7.7) considering the event-triggering strategy (7.9).

The idea is basically the one adopted in Theorem 6.1: split the analysis in two intervals $[t_k, t_k + T)$ and $[t_k + T, t_{k+1})$. However, differently from Theorem 6.1, we employ a looped-functional approach instead of a exact discretization to cope with the stabilization issues imposed by the dwell time.

**Theorem 7.1.** *Considering $T$, $K$ and $L$ given, if there exist symmetric positive definite matrices $Q_\delta$, $Q_\epsilon$, $P$ and $R$, a symmetric matrix $F_1$, matrices $Y_1, Y_2, Y_{1c}, Y_{2c}$, $F_2$, $N$ and $X$ and positive definite diagonal matrices $S_f$, $S_\rho$, $S_{fc}$ and $S_{\rho c}$ satisfying:*

$$\Pi_1 + T(\Pi_2 + \Pi_3) < 0 \tag{7.21}$$

$$\begin{bmatrix} \Pi_1 - T\Pi_3 & TN \\ * & -TR \end{bmatrix} < 0 \tag{7.22}$$

$$\begin{bmatrix} \Pi_a & \Pi_b' \\ * & -Q_\epsilon \end{bmatrix} < 0 \tag{7.23}$$

*with* [1]*:*

$$\begin{aligned}
\Pi_1 &= \mathrm{He}\{M_1'PM_3 - NM_{12} - M_{12}'F_2M_2 + (M_1'Y_1' + M_3'Y_2')[A_aM_1 + B_a\begin{bmatrix} K & 0 \end{bmatrix} M_2 \\
&\quad - M_3 + B_{af}M_4 + B_{a\rho}M_5] - M_4'S_f(M_4 - \Lambda H_1M_1) - M_5'S_\rho(M_5 + \Lambda H_2M_1)\} \\
&\quad - M_{12}'F_1M_{12} \\
\Pi_2 &= \mathrm{He}\{M_3'(F_1M_{12} + F_2M_2)\} + M_3'RM_3 \\
\Pi_3 &= M_2'XM_2 \\
\Pi_a &= \mathrm{He}\{M_1'PM_2 - M_4'S_{fc}(M_4 - \Lambda H_1M_1) - M_5'S_{\rho c}(M_5 - \Lambda H_2M_1) \\
&\quad + (M_1'Y_{1c}' + M_2'Y_{2c}')[(A_a + B_a\begin{bmatrix} K & 0 \end{bmatrix})M_1 - M_2 + B_aKM_3 + B_{af}M_4 + B_{a\rho}M_5]\} \\
&\quad - M_3'Q_\delta M_3 \\
\Pi_b &= C_aM_1
\end{aligned}$$

*and*

$$\begin{gathered}
M_1 = \begin{bmatrix} I & 0 & 0 & 0 & 0 \end{bmatrix} \quad M_2 = \begin{bmatrix} 0 & I & 0 & 0 & 0 \end{bmatrix} \quad M_3 = \begin{bmatrix} 0 & 0 & I & 0 & 0 \end{bmatrix} \\
M_4 = \begin{bmatrix} 0 & 0 & 0 & I & 0 \end{bmatrix} \quad M_5 = \begin{bmatrix} 0 & 0 & 0 & 0 & I \end{bmatrix}
\end{gathered} \tag{7.24}$$

*Then the origin of system* (7.7) *with the trigger rule defined by* (7.9) *is globally asymptotic stable.*

*Proof.* Consider a quadratic function $V(x(t)) = x(t)'Px(t)$. The stability analysis is carried out considering two intervals, namely $[t_k, t_k + T)$ and $[t_k + T, t_{k+1})$. As in Theorem 6.1, we are going to show that conditions (7.21)-(7.23) ensure $V(x(t_k + T)) - V(x(t_k)) < 0, \forall k \in \mathbb{N}$ and $\dot{V}(x(t)) < 0$, $\forall t \in [t_k + T, t_{k+1})$, $\forall k \in \mathbb{N}$.

[1] Notice that the selector matrices $M_i$ in (7.21) and (7.22) differ from those in (7.23) in the dimensions of the third element, although they read the same in the notation used in this document.

For $t \in [t_k, t_k + T)$, we can represent the trajectories of (7.7) in a lifted domain (BRIAT; SEURET, 2012; SEURET, 2012; YAMAMOTO, 1990) by defining $\tau = t - t_k$, with $\tau \in [0, T)$, and denoting $\mathcal{X}_k(\tau) = x(t_k + \tau) = x(t)$. It follows that the dynamics of (7.7) in the interval $[t_k, t_k + T]$ can be equivalently described as follows:

$$\begin{aligned}\dot{\mathcal{X}}_k(\tau) = A_a\mathcal{X}_k(\tau) + B_a\begin{bmatrix}K & 0\end{bmatrix}\mathcal{X}_k(0) + B_{af}f(H_1\mathcal{X}_k(\tau)) \\ + B_{a\rho}\rho(H_2\mathcal{X}_k(\tau), H_1\mathcal{X}_k(\tau))\end{aligned} \qquad \forall\tau \in [0, T) \tag{7.25}$$

Moreover, for $t \in [t_k, t_k + T)$, we have:

$$V(x(t)) = V(\mathcal{X}_k(\tau)) = \mathcal{X}_k'(\tau)P\mathcal{X}_k(\tau) \qquad \tau \in [0, T) \tag{7.26}$$

Consider now the solution of (7.25) for $\tau \in [0, T]$ given by $\mathcal{X}_k \in \mathbb{F}^{2n}_{[0,T]}$ and define:

$$W(\tau, \mathcal{X}_k) = V(\mathcal{X}_k(\tau)) + V_0(\tau, \mathcal{X}_k) \tag{7.27}$$

with $V_0(\tau, \mathcal{X}_k) : [0, T] \to \mathbb{F}^{2n}_{[0,T]}$ being a functional defined as follows:

$$\begin{aligned}V_0(\tau, \mathcal{X}_k) = (T - \tau)(\mathcal{X}_k(\tau) - \mathcal{X}_k(0))'[F_1(\mathcal{X}_k(\tau) - \mathcal{X}_k(0)) + 2F_2\mathcal{X}_k(0)] \\ + (T - \tau)\tau\mathcal{X}_k'(0)X\mathcal{X}_k(0) + (T - \tau)\int_0^\tau \dot{\mathcal{X}}_k'(\theta)R\dot{\mathcal{X}}_k(\theta)d\theta\end{aligned} \tag{7.28}$$

Observe that $V_0(T, \mathcal{X}_k) = V_0(0, \mathcal{X}_k) = 0,\ \forall\mathcal{X}_k \in \mathbb{F}^{2n}_{[0,T]}$, meaning that condition (7.19) of Lemma 7.3 is satisfied. Besides that, we have:

$$\begin{aligned}\dot{W}(\tau, \mathcal{X}_k) = 2\mathcal{X}_k'(\tau)P\dot{\mathcal{X}}_k(\tau) \\ + (T - \tau)\dot{\mathcal{X}}_k'(\tau)[R\dot{\mathcal{X}}_k(\tau) + 2F_1(\mathcal{X}_k(\tau) - \mathcal{X}_k(0)) + 2F_2\mathcal{X}_k(0)] \\ - (\mathcal{X}_k(\tau) - \mathcal{X}_k(0))'[F_1(\mathcal{X}_k(\tau) - \mathcal{X}_k(0)) + 2F_2\mathcal{X}_k(0)] \\ + (T - 2\tau)\mathcal{X}_k'(0)X\mathcal{X}_k(0) - \int_0^\tau \dot{\mathcal{X}}_k'(\theta)R\dot{\mathcal{X}}_k(\theta)d\theta\end{aligned} \tag{7.29}$$

We show now that (7.21) and (7.22) imply that $\dot{W}(\tau, \mathcal{X}_k) < 0$. For this similar steps to those of Theorem 2 from (SEURET; GOMES DA SILVA JR., 2012) are taken. With this aim, consider the following augmented vector:

$$\xi_k(\tau) = \begin{bmatrix}\mathcal{X}_k'(\tau) & \mathcal{X}_k'(0) & \dot{\mathcal{X}}_k'(\tau) & f'(\tau) & \rho'(\tau)\end{bmatrix}' \tag{7.30}$$

where we are using the shortcuts $f(\tau) = f(H_1\mathcal{X}_k(\tau))$ and $\rho(\tau) = \rho(H_2\mathcal{X}_k(\tau), H_1\mathcal{X}_k(\tau))$ for clarity.

The coupling relation between the components of $\xi_k$ imposed by (7.25) leads to the following relation, valid for any matrices $Y_1$ and $Y_2$ of appropriate dimensions:

$$2(\mathcal{X}'(\tau)Y_1' + \dot{\mathcal{X}}_k'(\tau)Y_2')M_0\xi_k = 0 \tag{7.31}$$

with $M_0 = \begin{bmatrix}A_a & B_a\begin{bmatrix}K & 0\end{bmatrix} & -I & B_{af} & B_{a\rho}\end{bmatrix}$. Therefore, this null term can be added to the inequality (7.29). Combining (7.29), (7.31), taking into account that for any matrix $N$ of appropriate dimensions (SEURET; GOMES DA SILVA JR., 2012, Theorem 2), the inequality

$$\int_0^\tau \dot{\mathcal{X}}_k'(\theta)R\dot{\mathcal{X}}_k(\theta)d\theta \geq 2\xi_k'(\tau)N(\mathcal{X}_k(\tau) - \mathcal{X}_k(0)) - \tau\xi_k'(\tau)NR^{-1}N'\xi_k(\tau) \tag{7.32}$$

holds and that Lemma 7.1 and Lemma 7.2 ensure $f'(\tau)S_f(f'(\tau) - \Lambda H_1 \mathcal{X}_k(\tau)) < 0$ and $\rho'(\tau)S_\rho(\rho(\tau) - \Lambda H_2 \mathcal{X}_k(\tau)) < 0$, respectively, one obtains that:

$$\dot{W}(\tau, \mathcal{X}_k) \leq \xi_k'[\Pi_1 + (T-\tau)\Pi_2 + (T-2\tau)\Pi_3 + \tau N R^{-1} N']\xi_k \tag{7.33}$$

Hence, if the inequality

$$\Pi_1 + (T-\tau)\Pi_2 + (T-2\tau)\Pi_3 + \tau N R^{-1} N' < 0 \tag{7.34}$$

is satisfied, it follows from (7.33) that $\dot{W} < 0$.

Now, notice that (7.34) is affine with respect to $\tau$ with $\tau \in [0,T]$. Thus, by convexity, it suffices to ensure that it is satisfied for $\tau = 0$ and for $\tau = T$ to guarantee that it is satisfied for the entire interval $\tau \in [0,T]$. Applying these values leads to the following conditions:

$$\Pi_1 + T(\Pi_2 + \Pi_3) \leq 0 \tag{7.35}$$

$$\Pi_1 - T\Pi_3 + T N R^{-1} N' \leq 0 \tag{7.36}$$

Applying now the Schur complement to (7.36), one retrieves condition (7.22) and concludes that satisfaction of conditions (7.21) and (7.22) ensures $\dot{W}(\tau, \mathcal{X}_k) < 0$. Then, applying Lemma 7.3 allows to conclude that satisfaction of conditions (7.21) and (7.22) ensure that $V(x(t_k + T)) - V(x(t_k)) < 0, \forall k \in \mathbb{N}$.

For $t \in [t_k + T, t_{k+1})$, we can consider the signal $\delta(t)$, defined in (2.3) to re-write system (7.7) as follows:

$$\begin{aligned} \dot{x}(t) = (A_a + B_a \begin{bmatrix} K & 0 \end{bmatrix})x(t) + B_a K \delta(t) + B_{af} f(H_1 x(t)) \\ + B_{a\rho} \rho(H_2 x(t), H_1 x(t)) \end{aligned} \tag{7.37}$$

Consider now the following vector:

$$\xi(t) = \begin{bmatrix} x'(t) & \dot{x}'(t) & \delta'(t) & f'(t) & \rho'(t) \end{bmatrix}'$$

where the shortcuts $f(t) = f(H_1 x(t))$ and $\rho(t) = \rho(H_2 x(t), H_1 x(t))$ are used for simplicity.

Thus, considering the time derivative of $V$ along the trajectories of the system for any $t \in [t_k + T, t_{k+1})$ the following expression is obtained:

$$\begin{aligned} \Psi_c &= \dot{V}(x) - g(\delta(t), y_a(t)) - 2f'(t)S_{fc}(f(t) - \Lambda H_1 x(t)) \\ &\quad - 2\rho'(t)S_{\rho c}(\rho(t) + \Lambda H_2 x(t)) \\ &= \xi'(t)\big\{ \mathrm{He}\{M_1' P M_2 - M_3' Q_\delta M_3 + M_1' C_a' Q_\epsilon^{-1} C_a M_1 \\ &\quad - M_4' S_{fc}(M_4 - \Lambda H_1 M_1) - M_5' S_{\rho c}(M_5 + \Lambda H_2 M_1)\}\big\}\xi(t) \end{aligned} \tag{7.38}$$

Using the coupling between the components of $\xi$ imposed by (7.37), the following relation is satisfied for any matrices $Y_{c1}$ and $Y_{c2}$ of appropriate dimensions:

$$2(x'(t)Y_{1c}' + \dot{x}'(t)Y_{2c}')M_{0c}\xi(t) = 0 \tag{7.39}$$

with $M_{0c} = \begin{bmatrix} A_a + B_a \begin{bmatrix} K & 0 \end{bmatrix} & -I & B_a K & B_{af} & B_{a\rho} \end{bmatrix}$ and this term can be added to $\mathcal{L}_c$ without changing its value, i.e.:

$$\begin{aligned} \Psi_c &= \xi'(t)\big\{ \mathrm{He}\{M_1' P M_2 - M_3' Q_\delta M_3 + M_1' C_a' Q_\epsilon^{-1} C_a M_1 - \\ &\qquad M_4' S_{fc}(M_4 - \Lambda H_1 M_1) - M_5' S_{\rho c}(M_5 + \Lambda H_2 M_1) \\ &\qquad + (M_1' Y_{1c}' + M_2' Y_{2c}')M_{0c}\}\big\}\xi(t) \\ &= \xi'(t)(\Pi_a + \Pi_b' Q_\epsilon^{-1} \Pi_b)\xi(t) \end{aligned} \tag{7.40}$$

If we ensure $\Psi_c < 0$, relations (7.14) and (7.16) from lemmas 7.1 and 7.2, which are satisfied by hypothesis, and relation $g(\delta(t), y_a(t)) \leq 0$, which is ensured by the triggering condition (7.9) for any $t \in [t_k + T, t_{k+1})$, guarantee that $\dot{V}(x) < g(\delta(t), y_a(t)) - 2f'(t)S_f(f(t) - \Lambda H_1 x(t)) - 2\rho'(t)S_\rho(\rho(t) + \Lambda H_2 x(t))\} \leq 0$. Therefore, satisfying $(\Pi_a + \Pi_b' Q_\epsilon^{-1} \Pi_b) < 0$ ensures $\dot{V}(x) < 0$ when $g(\delta(t), y_a(t))$ is given as in (7.12). Applying the Schur complement to this last inequality, we recover (7.23). Hence, satisfaction of (7.23) effectively ensures that $\dot{V}(x) < 0 \; \forall t \in [t_k + T, t_{k+1})$.

To conclude the proof, we need to show that the trajectories of the system in the intervals $[t_k, t_k + T)$ are bounded and converge to the origin as $k \to \infty$. For this, define the set $\mathscr{S}_\theta = \{\begin{bmatrix}\theta_f' & \theta_\rho'\end{bmatrix}' \in \mathbb{R}^{2l} : \; 0 \leq \theta_{f(i)} \leq 1 \text{ and } 0 \leq \theta_{\rho(i)} \leq 1, i = 1, ..., l\}$, where $\theta_{f(i)}$ and $\theta_{\rho(i)}$ are the i-th components of $\theta_f$ and $\theta_\rho$, respectively. Since (7.14) and (7.16) are verified, note that there exists $\theta(t) = \begin{bmatrix}\theta_f' & \theta_\rho'\end{bmatrix}' \in \mathscr{S}_\theta$, such that

$$\begin{aligned} f_{(i)}(H_1 x(t)) &= \theta_{f(i)}(t)\Lambda H_1 x(t) \\ \rho_{(i)}(H_2 x(t), H_1 x(t)) &= \theta_{\rho(i)}(t)\Lambda H_2 x(t) \end{aligned} \qquad \forall i = 1, ..., l$$

Hence, the trajectories of the closed-loop system (7.7) can be represented by the following time-varying linear differential inclusion:

$$\dot{x}(t) = (A_a + B_{af}\Theta_f(t)\Lambda H_1 + B_{a\rho}\Theta_\rho(t)\Lambda H_2)x(t) + B_a \begin{bmatrix} K & 0 \end{bmatrix} x(t_k) \tag{7.41}$$

with $\Theta_f(t) = \text{diag}(\theta_{f1}(t), ..., \theta_{fl}(t))$ and $\Theta_\rho(t) = \text{diag}(\theta_{\rho 1}(t), ..., \theta_{\rho l}(t))$.

For each admissible function $\theta(t) \in \mathscr{S}_\theta$, since (7.41) is a linear time-varying system, we can define a transition matrix $\Psi_\theta(t, t_0)$ for the system (7.41). Defining $\Psi_{\theta_k}(\tau) = \Psi(t_k + \tau, t_k)$ as the restriction of function $\Psi_\theta(t, t_0)$ to the interval $[t_k, t_k + T]$, it follows that

$$\mathcal{X}_k(\tau) = \Psi_{\theta_k}(\tau)\mathcal{X}_k(0) + \int_0^\tau \Psi_{\theta_k}(s) ds B_a \begin{bmatrix} K & 0 \end{bmatrix} \mathcal{X}_k(0)$$

and thus we can write

$$\|\mathcal{X}_k(\tau)\| \leq \left( \|\Psi_{\theta_k}(\tau)\| + \left\| \int_0^\tau \Psi_{\theta_k}(s) ds \right\| \left\| B_a \begin{bmatrix} K & 0 \end{bmatrix} \right\| \right) \|\mathcal{X}_k(0)\|$$

Considering all the possible functions $\theta_k \in \mathbb{F}_{[0,T]}^{2l}$ such that $\theta_k(\tau) \in \Theta, \forall \tau \in [0, T]$, there exist a scalar

$$\mu_\Psi = \sup_{\theta_k \in \mathbb{F}_{[0,T]}^{2l}, \theta_k(\tau) \in \mathscr{S}_\theta} \left\{ \|\Psi_{\theta_k}(\tau)\| + \left\| \int_0^\tau \Psi_{\theta_k}(s) ds \right\| \left\| B_a \begin{bmatrix} K & 0 \end{bmatrix} \right\| \right\}$$

such that $\|\mathcal{X}_k(\tau)\| \leq \mu_\Psi \|\mathcal{X}_k(0)\|$.

Hence, since from (7.21) and (7.22) $\mathcal{X}_k(0) = x(t_k) \to 0$ as $k \to \infty$, it follows that $\mathcal{X}_k(\tau) = x(t) \to 0$ as $t \to \infty$.

□

Although the subject of this thesis regards event-triggered controllers, as a side effect of the conditions in Theorem 7.1, the asymptotic stability of the origin of the closed-loop system under periodic sampled control with a period equal to the dwell-time $T$ can be formally guaranteed. The following corollary addresses this.

**Corollary 7.1** (Periodic sampled control)**.** *Considering $T$, $K$ and $L$ given, if there exist symmetric positive definite matrices $P$ and $R$, a symmetric matrix $F_1$, matrices $Y_1$, $Y_2$, $Y_{1c}$, $Y_{2c}$, $F_2$, $N$ and $X$ and positive definite diagonal matrices $S_f$, $S_\rho$, $S_{fc}$ and $S_{\rho c}$ satisfying* (7.21) *and* (7.22)*, then the origin of system* (7.7) *is globally asymptotic stable when periodic sampling with period $T$ is considered, i.e. the sampling instants are given by $t_k = kT$, $\forall k \in \mathbb{N}$.*

*Proof.* It follows directly from Theorem 7.1. Just notice that for periodic sampling, one needs to consider only the time inteval $[t_k, t_k+T]$, therefore condition (7.23) is not needed. □

### 7.4.2 Optimization problem

Conditions in Theorem 7.1 are LMIs provided $K$, $L$ and $T$ are fixed. Thus, the following optimization problem is proposed as means to compute the parameters $Q_\delta$ and $Q_\epsilon$:

$$\begin{aligned} &\min(\mathrm{tr}(Q_\delta) + \mathrm{tr}(Q_\epsilon)) \\ &\quad \text{subject to:} \\ &\qquad (7.21), (7.22), (7.23), P > 0 \end{aligned} \tag{7.42}$$

The reasoning behind this optimization problem is again to get $Q_\delta$ and $Q_\epsilon$ as "small" as possible. Considering the definition of the trigger function (7.9), this means that the matrix $Q_\delta$ is "minimized" while the matrix $Q_\epsilon^{-1}$ is "maximized". Since an event is generated and the control input is updated only when the term $\delta(t)'Q_\delta\delta(t) - y_a'Q_\epsilon^{-1}y_a$ becomes positive, this optimization procedure aims at reducing the impact of the positive contribution of $Q_\delta > 0$, over the negative contribution, $-Q_\epsilon < 0$, which implies more time before a new event occurs.

The dwell-time parameter $T$ can be chosen according to the processing and network communication constraints, as stated in Section 6.3.2. That is, the designer can choose, for instance, the smallest dwell-time that is suitable given the infrastructure at hand or he can solve the optimization problems for various values of $T$ and choose the largest one that renders the optimization problem feasible.

## 7.5 Co-design

In this section, we assume that a stabilizing state feedback control law was previously designed using, for instance, the techniques presented in (CASTELAN; TARBOURIECH; QUEINNEC, 2008). From this starting point, the co-design of the observer gain $L$ and the event-trigger parameters is addressed.

### 7.5.1 Stability conditions

The following theorem establishes sufficient conditions for the global asymptotic stability of system (7.7) in the considered co-design case.

**Theorem 7.2.** *Considering $T$ and $K$ given, if there exist positive scalars $\epsilon_c, \epsilon_d, \gamma$, symmetric positive definite matrices $Q_\delta$, $Q_\epsilon$, $P$ and $R$, a non-singular matrix $Y_{11}$, a symmetric matrix $F_1$, matrices $U$, $F_2$, $N$ and $X$ and positive definite diagonal matrices $S_f$, $S_\rho$,$S_{fc}$*

*and $S_{\rho c}$ satisfying:*

$$\Pi_1 + T(\Pi_2 + \Pi_3) < 0 \tag{7.43}$$

$$\begin{bmatrix} \Pi_1 - T\Pi_3 & TN \\ * & -TR \end{bmatrix} < 0 \tag{7.44}$$

$$\begin{bmatrix} \Pi_a & \Pi_b' \\ * & -Q_\epsilon \end{bmatrix} < 0 \tag{7.45}$$

*with:*

$$\begin{aligned}
\Pi_1 &= \mathrm{He}\{M_1' P M_3 - N M_{12} - M_{12}' F_2 M_2 + (\epsilon_d M_1' + M_3')[(Y' A_{a1} + L_a) M_1 \\
&\quad + Y' B_a \begin{bmatrix} K & 0 \end{bmatrix} M_2 - Y' M_3 + Y' B_{af} M_4 + Y' B_{a\rho} M_5] \\
&\quad - M_4' S_f (M_4 - \Lambda H_1 M_1) - M_5' S_\rho (M_5 + \Lambda H_2 M_1)\} - M_{12}' F_1 M_{12} \\
\Pi_2 &= \mathrm{He}\{M_3'(F_1 M_{12} + F_2 M_2)\} + M_3' R M_3 \\
\Pi_3 &= M_2' X M_2 \\
\Pi_a &= \mathrm{He}\{M_1' P M_2 - M_4' S_{fc} (M_4 - \Lambda H_1 M_1) - M_5' S_{\rho c} (M_5 - \Lambda H_2 M_1) \\
&\quad + (\epsilon_c M_1' + M_2')[(Y' A_{a1} + L_a + Y' B_a \begin{bmatrix} K & 0 \end{bmatrix}) M_1 \\
&\quad - Y' M_2 + Y' B_a K M_3 + Y' B_{af} M_4 + Y' B_{a\rho} M_5]\} - M_3' Q_\delta M_3 \\
\Pi_b &= C_a M_1
\end{aligned}$$

$$A_{a1} = \begin{bmatrix} A_p & 0 \\ 0 & A_p \end{bmatrix} \qquad L_a = \begin{bmatrix} 0 & -UC_p \\ 0 & \gamma UC_p \end{bmatrix} \qquad Y = \begin{bmatrix} Y_{11} & 0 \\ 0 & \gamma Y_{11} \end{bmatrix}$$

*and $H_1$, $H_2$ and the matrices $M$ as defined in* (7.8) *and* (7.24)*, respectively.*

*Then the origin of system* (7.7) *with $L = (Y_{11}')^{-1} U$ is globally asymptotic stable.*

*Proof.* The proof follows the same steps as for Theorem 7.1. The differences arise from the fact that the conditions in Theorem 7.1 are not linear if $L$ is variable, due to the terms $2(\mathcal{X}'(\tau) Y_1' + \dot{\mathcal{X}}_k'(\tau) Y_2') M_0$ in (7.31) and $2(x'(t) Y_{1c}' + \dot{x}'(t) Y_{2c}') M_{0c}$ in (7.39). To linearize the conditions, one needs to isolate the terms depending on $L$ in $A_a$ and consider that

$$\begin{aligned}
Y_2 = Y_{2c} = Y &= \begin{bmatrix} Y_{11} & 0 \\ 0 & \gamma Y_{11} \end{bmatrix} \\
Y_1 &= \epsilon_d Y_2 \\
Y_{1c} &= \epsilon_c Y_{2c}
\end{aligned}$$

which readily leads to the conditions stated in the present theorem. □

**Remark 7.1** (Co-design of $K$, $Q_\delta$ and $Q_\epsilon$)**.** *If $L$ is given, but $K$ is a decision variable, conditions in Theorem 7.1 are not linear due to the terms $(M_1' Y_1' + M_3' Y_2') B_a \begin{bmatrix} K & 0 \end{bmatrix} M_2$ and $(M_1' Y_{1c}' + M_2' Y_{2c}') B_a \begin{bmatrix} K & 0 \end{bmatrix}) M_1$. Nevertheless they can be linearized considering:*

$$Y_2 = Y_{2c} = Y = \begin{bmatrix} Y_{11} & 0 \\ Y_{21} & Y_{22} \end{bmatrix}, \quad Y_1 = \epsilon_d Y, \quad Y_{1c} = \epsilon_c Y,$$

$$\bar{Y} = Y^{-1}, \quad \bar{Y}_{11} = Y_{11}^{-1}, \quad \bar{S}_f = S_f^{-1}, \quad \bar{S}_\rho = S_\rho^{-1}, \quad \bar{S}_{fc} = S_{fc}^{-1}, \quad \bar{S}_{\rho c} = S_{\rho c}^{-1}$$

*and applying congruence transformations with $\mathrm{diag}(\bar{Y}, \bar{Y}, \bar{Y}, \bar{S}_f, \bar{S}_\rho)$ and $\mathrm{diag}(\bar{Y}, \bar{Y}, \bar{Y}_{11}, \bar{S}_f, \bar{S}_\rho)$ to inequalities* (7.34) *and $(\Pi_a + \Pi_b' Q_\epsilon^{-1} \Pi_b) < 0$, respectively. Then, considering the variable changes $\bar{Q}_\delta = \bar{Y}' Q_\delta \bar{Y}$ and $\bar{K} = K \bar{Y}_{11}$ and*

*observing that* $\begin{bmatrix} K & 0 \end{bmatrix} \bar{Y} = \begin{bmatrix} \bar{K} & 0 \end{bmatrix}$*, one obtains the following stability conditions:*

$$\bar{\Pi}_1 + T(\bar{\Pi}_2 + \bar{\Pi}_3) < 0 \tag{7.46}$$

$$\begin{bmatrix} \bar{\Pi}_1 - T\bar{\Pi}_3 & TN \\ * & -TR \end{bmatrix} < 0 \tag{7.47}$$

$$\begin{bmatrix} \bar{\Pi}_a & \bar{\Pi}_b' \\ * & -Q_\epsilon \end{bmatrix} < 0 \tag{7.48}$$

*with*

$$\begin{aligned}
\bar{\Pi}_1 = \mathrm{He}\{&M_1' P M_3 - N M_{12} - M_{12}' F_2 M_2 + (\epsilon_d M_1' + M_3')[A_a \bar{Y} M_1 + B_a \begin{bmatrix} \bar{K} & 0 \end{bmatrix} M_2 \\
&- \bar{Y} M_3 + B_{af} \bar{S}_f M_4 + B_{a\rho} \bar{S}_\rho M_5] - M_4' \bar{S}_f (M_4 - \Lambda H_1 \bar{Y} M_1) - M_5' \bar{S}_\rho M_5 \\
&+ M_5' \Lambda H_2 \bar{Y} M_1\} - M_{12}' F_1 M_{12} \\
\bar{\Pi}_2 = \mathrm{He}\{&M_3'(F_1 M_{12} + F_2 M_2)\} + M_3' R M_3 \\
\bar{\Pi}_3 = &M_2' X M_2 \\
\bar{\Pi}_a = \mathrm{He}\{&M_1' P M_2 - M_4' \bar{S}_{fc} M_4 + M_4' \Lambda H_1 \bar{Y} M_1 - M_5' \bar{S}_{\rho c} M_5 - M_5' \Lambda H_2 \bar{Y} M_1 \\
&+ (\epsilon_c M_1' + M_2')[(A_a \bar{Y} + B_a \begin{bmatrix} \bar{K} & 0 \end{bmatrix}) M_1 - \bar{Y} M_2 + B_a \bar{K} M_3 + B_{af} \bar{S}_{fc} M_4 + \\
&B_{a\rho} \bar{S}_{a\rho} M_5]\} - M_3' \bar{Q}_\delta M_3 \\
\bar{\Pi}_b = &C_a \bar{Y} M_1
\end{aligned}$$

*which are linear with respect to the decision variables. Parameters* $K$ *and* $Q_\delta$ *can then be recovered as* $K = \bar{K} \bar{Y}_{11}^{-1}$ *and* $Q_\delta = (\bar{Y}')^{-1} \bar{Q}_\delta \bar{Y}^{-1}$*.*

*These conditions can be used as part of an interactive approach to set the system parameters. Starting from a given* $K$*, computed using the method presented in (CASTELAN; TARBOURIECH; QUEINNEC, 2008) for instance, solve the optimization problem for the co-design of* $L$*. Then, considering this value of* $L$*, use the conditions from this Remark to refine the values of* $K$*,* $Q_\delta$*,* $Q_\epsilon$*. Finally, a further step can be considered by solving the emulation problem using the values of* $K$ *and* $L$ *previously computed, which is analogous to the co-design refinement mentioned in Chapter 6. Notice, however, that in the case addressed in the present chapter, the improvements expected with this refinement are smaller since here the matrix structure for the co-design is imposed to the multipliers and not to the Lyapunov matrix as in Chapter 6.*

### 7.5.2 Optimization problem

Conditions in Theorem 7.2 are LMIs provided $K$, $T$, $\epsilon_c$, $\epsilon_d$ and $\gamma$ are fixed. Thus, the following optimization problem is proposed as means to compute the parameters $Q_\delta$ and $Q_\epsilon$:

$$\begin{aligned}
&\min(\mathrm{tr}(Q_\delta) + \mathrm{tr}(Q_\epsilon)) \\
&\quad \text{subject to:} \\
&\quad (7.43), (7.44), (7.45), P > 0
\end{aligned} \tag{7.49}$$

To select the scalars $\epsilon_c$, $\epsilon_d$ and $\gamma$, a grid search is proposed. $T$ is selected by the same criteria described in previous sections.

## 7.6 Numerical example

Consider the system (7.1) with:

$$A_p = \begin{bmatrix} 0 & 1 \\ 4 & 0 \end{bmatrix}, \quad B_p = \begin{bmatrix} 0 \\ 1 \end{bmatrix}, \quad B_{pf} = \begin{bmatrix} 0 \\ 0.5 \end{bmatrix}, \quad C_p = \begin{bmatrix} 1 & 0 \end{bmatrix}, \quad H = \begin{bmatrix} 0 & 1 \end{bmatrix}$$

and $f : \mathbb{R} \to \mathbb{R}$ being a logarithmic function with dead-zone (Figure 7.1):

$$f(v) = \begin{cases} 0, & \text{if } \|v\| \leq 1 \\ \ln(v), & \text{if } v > 1 \\ -\ln(-v), & \text{if } v < -1 \end{cases} \tag{7.50}$$

which leads to $\Lambda = 1$. We choose the controller gain $K = \begin{bmatrix} -6.102 & -3.915 \end{bmatrix}$, which stabilizes the origin of the system.

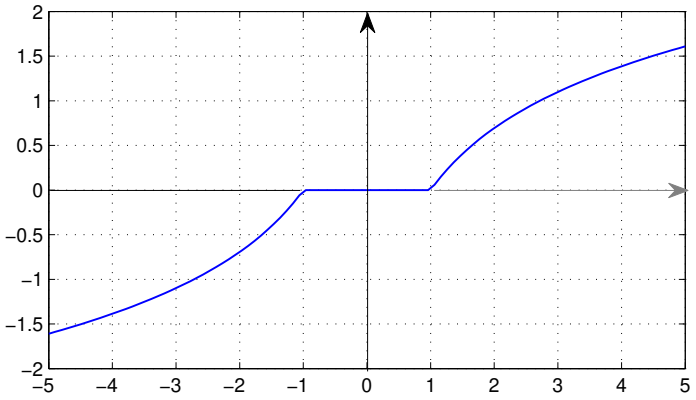


Figure 7.1: Logarithm function with dead-zone.

### 7.6.1 Emulation

Considering the dwell-time $T = 0.1$ and $L = \begin{bmatrix} -4 & -11 \end{bmatrix}'$, we solve the emulation optimization problem (7.42) with additional conditions $\lambda_{max}(Q_\delta) < 10^3 \lambda_{min}(Q_\delta)$ and $\lambda_{max}(Q_\epsilon) < 10^3 \lambda_{min}(Q_\epsilon)$ to prevent $Q_\delta$ and $Q_\epsilon$ from becoming ill-conditioned, obtaining the following results:

$$Q_\delta = \begin{bmatrix} 3.055 & 1.904 \\ 1.904 & 1.192 \end{bmatrix} \qquad Q_\epsilon = \begin{bmatrix} 2.63 & -1.231 \cdot 10^{-6} & 3.487 \cdot 10^{-7} \\ -1.231 \cdot 10^{-6} & 1.615 & 1.877 \cdot 10^{-7} \\ 3.487 \cdot 10^{-7} & 1.877 \cdot 10^{-7} & 0.00263 \end{bmatrix}$$

Figure 7.2 depicts the simulation results for $T = 0.1$, $T = 0.3$ and $T = 0.4$ considering the following initial condition:

$$x_p(0) = \begin{bmatrix} -4 \\ -3 \end{bmatrix} \qquad \hat{x}(0) = \begin{bmatrix} 0 \\ 0 \end{bmatrix}$$

For $T = 0.5$ the optimization problem becomes unfeasible. The upper plots in the figures depict the state of the plant and of the observer. One can see that the state of the closed-loop system effectively converges to the origin. The middle plots depict the control signal.

The bottom plots depict the instants where the events occurred. The heights of the bars in the bottom plot represent the inter-event times $t_k - t_{k-1}$ and the horizontal line represents the dwell-time $T$. One can see that the event-trigger mechanism effectively postpones the occurrence of events with respect to the dwell-time. The number of events generated in the time interval $[0, 10]$ seconds is 20, 19 and 16, respectively.

### 7.6.2 Co-design

Considering the dwell-time $T = 0.1$, we solve the co-design optimization problem (7.49) with additional conditions $\lambda_{max}(Q_\delta) < 10^3\lambda_{min}(Q_\delta)$ and $\lambda_{max}(Q_\epsilon) < 10^3\lambda_{min}(Q_\epsilon)$ to prevent $Q_\delta$ and $Q_\epsilon$ from becoming ill-conditioned, obtaining the following results:

$$L = \begin{bmatrix} -5.217 \\ -10.02 \end{bmatrix} \quad Q_\delta = \begin{bmatrix} 3.109 & 1.937 \\ 1.937 & 1.213 \end{bmatrix}$$

$$Q_\epsilon = \begin{bmatrix} 2.66 & 0.07092 & 2.442 \cdot 10^{-6} \\ 0.07092 & 1.659 & 1.01 \cdot 10^{-6} \\ 2.442 \cdot 10^{-6} & 1.01 \cdot 10^{-6} & 0.002665 \end{bmatrix}$$

Figure 7.3 depicts the simulation results for $T = 0.1$, $T = 0.3$ and $T = 0.4$ considering the following initial condition:

$$x_p(0) = \begin{bmatrix} -4 \\ -3 \end{bmatrix} \qquad \hat{x}(0) = \begin{bmatrix} 0 \\ 0 \end{bmatrix}$$

As in the emulation case, for $T = 0.5$ the optimization problem becomes unfeasible. The numbers of events generated in the time interval $[0, 10]$ seconds are 18, 17 and 15, respectively, representing a slight improvement with respect to the emulation case: an average reduction of around 9% in the number of events when the co-design is used.

## 7.7 Conclusion

In this chapter we addressed the design of observer-based event-triggered control for Lur'e systems with sector-bounded nonlinearities that depend on the system state. Emulation design and co-design of the event-trigger parameters and the observer gains have been addressed for global asymptotic stabilization. The proposed techniques use only available information and a state observer to recover the remaining plant state variables. Sufficient conditions in the form of LMIs associated to convex optimization problems have been proposed to design the observer and event-trigger parameters so that the asymptotic stability of the origin of the closed-loop system is ensured while aiming at reducing the number of events. The approach allows to design the event-trigger with a dwell time $T$ imposing a minimum inter-events time, which prevents the Zeno behavior occurrence. The stability analysis is carried out considering two intervals, the first one corresponding to the dwell time, i.e. $t \in [t_k, t_k + T)$, and the second one corresponding to the actual evaluation of the trigger condition, i.e $t \in [t_k + T, t_{k+1})$. During the dwell time, a looped-functional approach is used to certify that the total variation of an underlying Lyapunov function is negative, i.e. $V(x(t_k+T)) - V(x(t_k)) < 0$. Regarding the second interval, the trigger condition is designed to ensure that the time derivative of the Lyapunov function is negative, i.e. $\dot{V}(x(t)) < 0, \forall t \in [t_k + T, t_{k+1})$. The looped-functional approach also permits to derive conditions that guarantee the asymptotic stability of a periodic sampled implementation of the controller; a result that was presented as a corollary.

To the extent of the author's knowledge, the use of looped-functionals to address the design of observer-based event-triggered controllers for nonlinear systems is original. The most similar work in the literature seems to be (ZHANG; HAN, 2017), which addresses nonlinear systems and models the event-triggered closed-loop as a system with a time-varying delay, but does not use a looped-functional approach and assumes access to the entire state of the system. Besides that, (ZHANG; HAN; YU, 2016) presents a survey on networked control systems which also encompasses works that model the closed-loop as a system with a time-varying delay, but none of the referred works uses a looped-functional either.

Stability conditions that allow the co-design of the controller gain $K$ and the event-trigger parameters $Q_\delta$, $Q_\epsilon$ were also presented in this chapter. They can be used as part of an interactive approach to set the system parameters: Start from a given $K$, computed using the method presented in (CASTELAN; TARBOURIECH; QUEINNEC, 2008) for instance. Then solve the optimization problem proposed here for the co-design of $L$. Now, considering this value of $L$, use the conditions from Remark 7.1 to refine the values of $K$, $Q_\delta$, $Q_\epsilon$.

In this chapter, only global stabilization has been addressed. The regional stabilization imposes additional difficulties to ensure the sector condition for function $\rho(a, b) = f(a + b) - f(b)$ and the boundedness of the trajectories during the dwell-time. So far, these difficulties could not be overcome and the regional stabilization is still an open problem.

The full co-design, i.e. the co-design of $Q_\delta$, $Q_\epsilon$, $K$ and $L$ is still an open problem either. In fact, designing $K$ and $L$ simultaneously is an open problem even when linear plants and continuous-time control are considered.

We ended the chapter with a numerical example that illustrated the potential of the proposed methods and highlighted a slight superiority of results achievable in the co-design context with respect to the number of events generated.

The results presented in this chapter were submitted for publication as (MOREIRA et al., 2018b).

It is worth noticing that the looped-functional approach used here can also elegantly solve the problem of the co-design of the observer gain $L$ and the event-trigger parameters $Q_\delta$ and $Q_\epsilon$ in the context of Lur'e systems where the nonlinearity depends only on the plant input, that is, in the context of the problem addressed in Chapter 6. The main drawback in that case were the exponential terms involving $L$ that appear as a consequence of the exact discretization process. With the use of the looped-functional approach, there is no need of system discretization and one can follow the same steps presented in this chapter to obtain linear stability conditions considering the co-design of $L$ for the class of systems studied in Chapter 6.

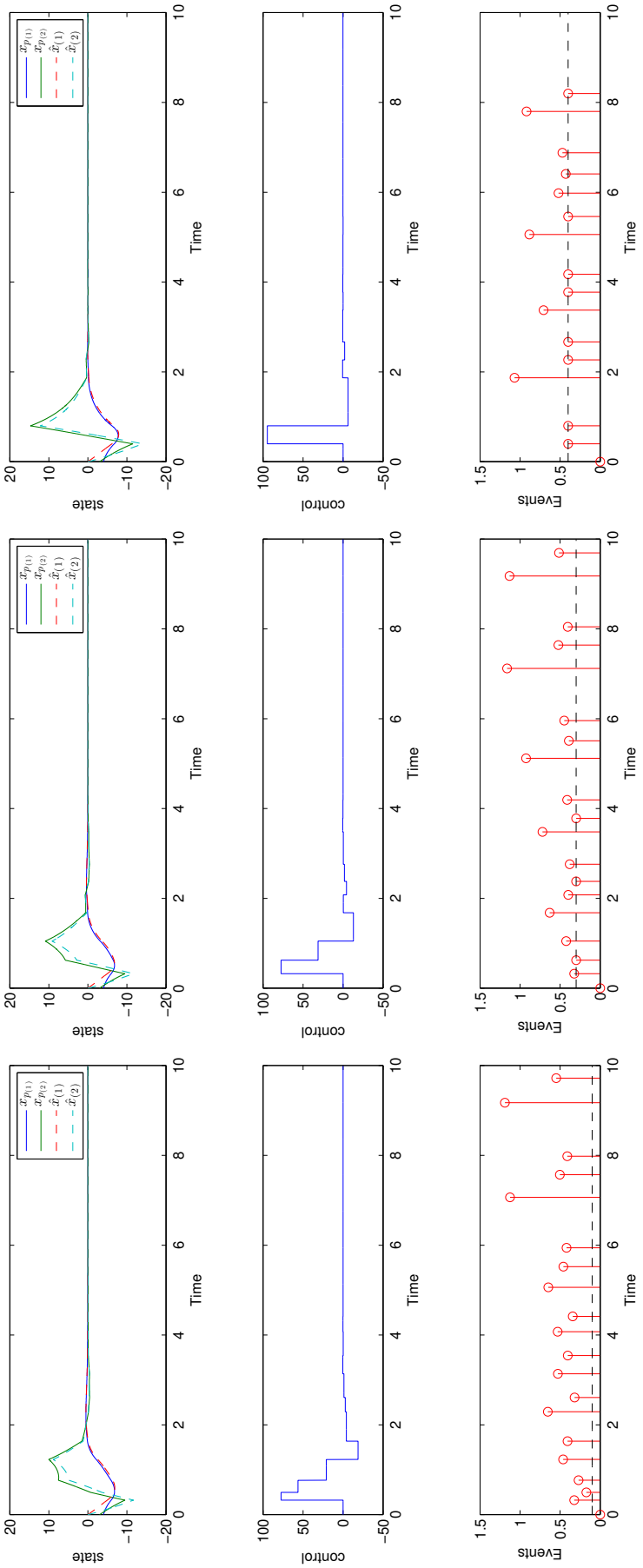


Figure 7.2: Emulation – Simulations for $T = 0.1$, $T = 0.3$ and $T = 0.4$.

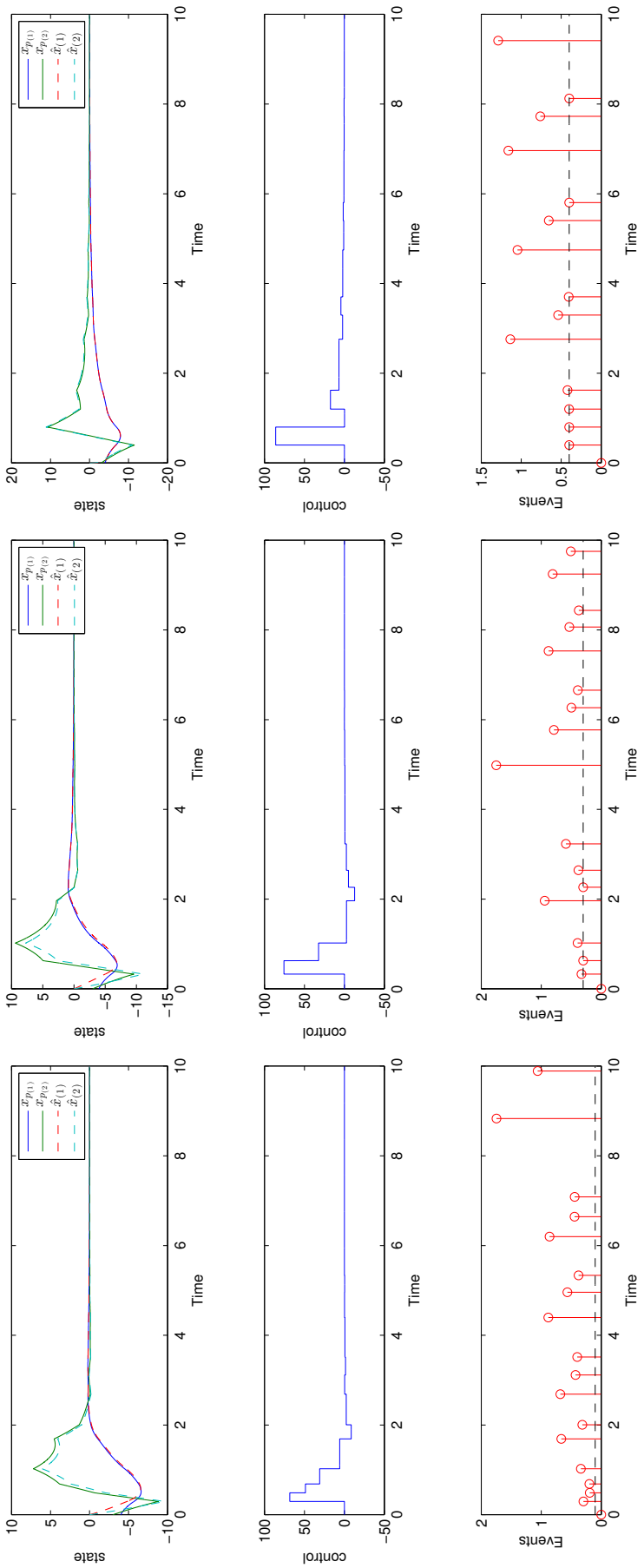


Figure 7.3: Co-design – Simulations for $T = 0.1$, $T = 0.3$ and $T = 0.4$.

# 8 FINAL REMARKS

## 8.1 Conclusions

In this thesis we studied the problems of designing event-trigger controllers in emulation and in co-design contexts for two different classes of nonlinear systems: rational systems and Lur'e type systems. For both cases, we proposed triggering strategies based on weighted relative error criteria and Lyapunov theory techniques were used to derive asymptotic stability conditions in LMI form. These conditions were then cast into convex optimization problems which allow the selection of the system parameters aiming at reducing the number of control updates needed. This reduction has the benefits of leading to fewer data transmissions in a NCS implementation and can also yield less actuator wear in some cases.

In the case of rational systems, we considered static state-feedback control and an event generator that has access to the entire plant state. Differential-algebraic representations (DARs) were used to obtain stability conditions in LMI form and this constitutes one of the contributions of this thesis. Indeed, the use of DARs in the event-triggered control field seems to be entirely new. Besides the use of DARs, approaches based on quasi-LPV, T-S fuzzy systems and LFRs could be used. These alternatives, however tend to lead to more conservative solutions. In the case of quasi-LPV and T-S, the relations among the varying parameter and the state are not taken into account, leading to additional conservatism. Moreover, for some rational plants these approaches lead to models which are not affine with respect to the parameter, leading to a more complex design methodology. The LFR can be seen as particular case of DAR (see (COUTINHO; GOMES DA SILVA JR., 2010)) and leads to one specific DAR for each plant, which does not allow to explore different representations, potentially leading to more conservative results.

Quadratic and rational underlying Lyapunov functions were considered in the stability conditions. It was illustrated that the use of more complex Lyapunov functions can lead to better results in terms of the number of events, but requires more calculation in design time and does not scale well when the order of the system increases. The size of the LMIs rapidly increases when more complex Lyapunov functions are considered. Moreover, even when considering relatively simple bi-quadratic Lyapunov functions, the number of variables involved increases with the order of the system, leading to large optimization problems, difficult to solve with available equipment even for third-order systems.

It was also shown that the triggering strategy proposed in this case has an implicit minimum inter-event time and, therefore, Zeno behavior is not an issue. On the other hand, if one considers, in the context of rational systems, event generators that have access only to the plant and controller outputs, it is not possible to exclude the possibility of Zeno behavior and the design of event-triggered controllers with these constraints for rational

systems is still an open problem.

In the case of Lur'e type systems, we addressed the problem of designing event-triggered controllers that have access only to the plant and controller outputs. In this case, a state observer was used to recover the missing information and a dwell time was introduced in the triggering strategy to avoid Zeno behavior. We considered systems where the nonlinearities depend only on the control input and systems where the nonlinearity depends on the state. In the first case, the exact time-discretization of the system is considered to ensure stability in the presence of the dwell time, while in the second case we employed a looped-functional approach. The application of looped-functionals in the context of event-triggered control is also a contribution of this thesis.

When compared to the existing literature on event-triggered control, the methodology proposed here has the following advantages:

- It is a systematic methodology for designing the event generator (in an emulation design context) or the event generator and the control gains or the observer gains (in a co-design context). The synthesis is systematically carried out by solving convex optimization problems and there is no need to choose arbitrary values for the parameters.

- It does not need *a priori* knowledge of a Lyapunov function for the system. The method computes a Lyapunov function implicitly while solving the optimization problems. Hence, it is potentially less conservative than methods which assume a fixed one.

- All event generator parameters are free (in the sense that they are not fixed *a priori*) and taken into account in the optimization process. Therefore, one can expect less conservative results than methods which consider parameter values that are fixed or that need to be arbitrated by the designer.

Finally, it is important to note that the co-design methodology proposed here can also be seen as a possible systematic solution to the problem of designing sampled-data control with certified stability. Recalling that, in general, exact discrete-time models of nonlinear systems cannot be obtained and approximated ones, generated by numerical approximations, are not always reliable when designing sampled-data control systems (NEŠIĆ; TEEL; KOKOTOVIĆ, 1999), as they can lead to unstable closed-loop systems even when the continuous-time corresponding closed-loop system is stable, the importance of this result becomes clear.

## 8.2 Future work perspectives

In this section we summarize the problems that remain open and present some additional potential future extensions for the research presented in this thesis.

- Consider, for rational plants, the case where the event generator does not have access to the entire state of the system. Both output-feedback and observer-based state-feedback could be addressed. The main challenge is to avoid Zeno behavior, which could potentially be handled by the use of dwell time and a looped-functional approach.

- In the cases where an observer is used, address the co-design of the event-trigger parameters, the control law and the observer gain. The main challenge in this case is to obtain convex stability conditions when all these parameters are variables. In fact, the simultaneous design of the control law and the observer gain is an open problem even when continuous-time controllers and linear systems are considered, that is, this is an open problem not only in the event-triggered control field.

- Address the regional stabilization case for Lur'e systems where the nonlinearity depends on the state. If the looped-functional approach is employed, the challenge is to ensure the boundedness of the trajectories during the dwell time so that the sector condition is valid during this period.

- Consider measurement errors and delays in the data processing/transmission. Practical implementations of the control systems discussed in this thesis will be affected by these imperfections. Therefore it is important to address them from a theoretical point of view.

- Consider state-dependent parameters in the event generators. Currently, the parameters $Q_x$, $Q_\epsilon$ and $Q_\delta$ are constant matrices. Relaxing this constraint so that they can be matrix functions of the system state could potentially lead to further reductions on the number of events.

- Use the looped-functional approach to address the co-design of the observer gain $L$ in the context of Lur'e systems where the nonlinearity depends on the input. This is a tough problem to address using exact discretization of the system due to the exponential terms involving the observer gain $L$. Nevertheless, this issue can be overcome by considering a looped-functional approach to ensure the overall decreasing of the Lyapunov function in the dwell time interval.

- Consider performance criteria in the design problems. Only stabilization has been considered so far. The inclusion of minimum exponential decay rate, for instance, could be coded as additional LMIs in the stability conditions. One could also consider $H_\infty$ optimization as performance criteria.

# REFERENCES

ABDELRAHIM, M. et al. Co-design of output feedback laws and event-triggering conditions for linear systems. In: IEEE CONFERENCE ON DECISION AND CONTROL, 2014, Los Angeles. **Proceedings...** New York: IEEE, 2014. p.3560–3565.

ABDELRAHIM, M. et al. Stabilization of nonlinear systems using event-triggered output feedback laws. In: INTERNATIONAL SYMPOSIUM ON MATHEMATICAL THEORY OF NETWORKS AND SYSTEMS, 2014, Groningen. **Proceedings...** Paris: HAL, 2014. p.p.CD–ROM.

ABDELRAHIM, M. et al. Input-to-state stabilization of nonlinear systems using event-triggered output feedback controllers. In: EUROPEAN CONTROL CONFERENCE, 2015, Linz. **Proceedings...** New York: IEEE, 2015. p.2180–2185.

ABDELRAHIM, M. et al. Stabilization of nonlinear systems using event-triggered output feedback controllers. **IEEE Transactions on Automatic Control**, New York, v.61, n.9, p.2682–2687, 2016.

AL-AREQI, S.; GÖRGES, D.; LIU, S. Event-based control and scheduling codesign subject to input and state constraints. In: EUROPEAN CONTROL CONFERENCE, 2015, Linz. **Proceedings...** New York: IEEE, 2015. p.1866–1871.

ANTONELLI, R. et al. Set-point regulation of an anaerobic digestion process with bounded output feedback. **IEEE Transactions on Control Systems Technology**, Piscataway, v.11, n.4, p.495–504, July 2003.

ARANDA-ESCOLÁSTICO, E. et al. Design of periodic event-triggered control for polynomial systems: a delay system approach. **IFAC-PapersOnLine**, Toulouse, v.50, n.1, p.7887–7892, 2017. 20th IFAC World Congress.

ARANDA-ESCOLASTICO, E.; GUINALDO, M.; DORMIDO, S. A novel approach for periodic event-triggering based on general quadratic functions. In: INTERNATIONAL CONFERENCE ON EVENT-BASED CONTROL, COMMUNICATION, AND SIGNAL PROCESSING, 2015, Krakow. **Proceedings...** New York: IEEE, 2015. p.1–6.

BESCHI, M. et al. Event-based PI controller with exponential thresholds. **IFAC Proceedings Volumes**, Cape Town, v.47, n.3, p.5766–5771, 2014. 19th IFAC World Congress.

BORGERS, D. P. N.; HEEMELS, W. P. M. H. M. Event-separation properties of event-triggered control systems. **IEEE Transactions on Automatic Control**, New York, v.59, n.10, p.2644–2656, Oct. 2014.

BOYD, S. et al. **Linear matrix inequalities in system and control theory**. Philadelphia, PA: SIAM, 1994. (Studies in Applied Mathematics, v.15).

BRIAT, C.; SEURET, A. A looped-functional approach for robust stability analysis of linear impulsive systems. **Systems & Control Letters**, Amsterdam, v.61, n.10, p.980–988, 2012.

CAMPESTRINI, L. et al. Identifiability analysis and prediction error identification of anaerobic batch bioreactors. **Journal of Control, Automation and Electrical Systems**, Campinas, v.25, n.4, p.438–447, 2014.

CASTELAN, E. B.; TARBOURIECH, S.; QUEINNEC, I. Control design for a class of nonlinear continuous-time systems. **Automatica**, Tarrytown, v.44, n.8, p.2034–2039, 2008.

COUTINHO, D. F. et al. Stability analysis and control of a class of differential-algebraic nonlinear systems. **International Journal of Robust and Nonlinear Control**, West Sussex, v.14, n.16, p.1301–1326, 2004.

COUTINHO, D. F.; GOMES DA SILVA JR., J. M. Computing estimates of the region of attraction for rational control systems with saturating actuators. **IET Control Theory Applications**, Hertford, v.4, n.3, p.315–325, Mar. 2010.

DE SOUZA, C. E.; COUTINHO, D.; FU, M. Stability analysis of finite-level quantized discrete-time linear control systems. **European Journal of Control**, London, v.16, n.3, p.258–271, 2010.

DONKERS, M. C. F.; HEEMELS, W. P. M. H. Output-based event-triggered control with guaranteed $\mathcal{L}_\infty$-gain and improved and decentralized event-triggering. **IEEE Transactions on Automatic Control**, New York, v.57, n.6, p.1362–1376, June 2012.

DURAND, S.; MARCHAND, N. Further results on event-based PID controller. In: EUROPEAN CONTROL CONFERENCE, 2009, Budapest. **Proceedings...** New York: IEEE, 2009. p.1979–1984.

DURAND, S.; MARCHAND, N. An event-based PID controller with low computational cost. In: INTERNATIONAL CONFERENCE ON SAMPLING THEORY AND APPLICATIONS, 2009, Marseille. **Proceedings...** New York: IEEE, 2009. Special session on Sampling and Industrial Applications.

FISCHMANN, M.; FLORES, J. V.; GOMES DA SILVA JR., J. M. Dynamic controller design for synchronization of Lur'e type systems subject to control saturation. **IFAC-PapersOnLine**, Toulouse, v.50, n.1, p.11853–11858, 2017. 20th IFAC World Congress.

FRIDMAN, E. Tutorial on Lyapunov-based methods for time-delay systems. **European Journal of Control**, London, v.20, n.6, p.271–283, 2014.

FU, M.; XIE, L. The sector bound approach to quantized feedback control. **IEEE Transactions on Automatic Control**, New York, v.50, n.11, p.1698–1711, 2005.

GAO, H.; CHEN, T. Stabilization of Nonlinear Systems Under Variable Sampling: a fuzzy control approach. **IEEE Transactions on Fuzzy Systems**, New York, v.15, n.5, p.972–983, Oct. 2007.

GENESIO, R.; TARTAGLIA, M.; VICINO, A. On the estimation of asymptotic stability regions: state of the art and new proposals. **IEEE Transactions on Automatic Control**, New York, v.30, n.8, p.747–755, 1985.

GHAOUI, L. E.; SCORLETTI, G. Control of rational systems using linear-fractional representations and linear matrix inequalities. **Automatica**, Tarrytown, v.32, n.9, p.1273–1284, 1996.

GHIGGI, I. F. M. et al. Stability analysis of nonlinear rational sampled-data control systems over communication networks. In: EUROPEAN CONTROL CONFERENCE, 2015, Linz. **Proceedings...** New York: IEEE, 2015. p.422–427.

GIRARD, A. Dynamic Triggering Mechanisms for Event-Triggered Control. **IEEE Transactions on Automatic Control**, New York, v.60, n.7, p.1992–1997, July 2015.

GOEBEL, R.; SANFELICE, R. G.; TEEL, A. R. **Hybrid dynamical systems**: modeling, stability, and robustness. New York: Princeton University Press, 2012.

GOMES DA SILVA JR., J. M. et al. Static anti-windup design for a class of nonlinear systems. **International Journal of Robust and Nonlinear Control**, West Sussex, v.24, n.5, p.793–810, 2014.

GOMES DA SILVA JR., J. M.; LAGES, W. F.; SBARBARO, D. G. Event-triggered PI control design. **IFAC Proceedings Volumes**, Cape Town, v.47, n.3, p.6947–6952, 2014. 19th IFAC World Congress.

GROFF, L. B. et al. Observer-based event-triggered control: a discrete-time approach. In: AMERICAN CONTROL CONFERENCE, 2016, Boston. **Proceedings...** New York: IEEE, 2016. p.4245–4250.

HEEMELS, W. P. M. H.; DONKERS, M. C. F.; TEEL, A. R. Periodic event-triggered control based on state feedback. In: IEEE CONFERENCE ON DECISION AND CONTROL AND EUROPEAN CONTROL CONFERENCE, 2011, Orlando. **Proceedings...** New York: IEEE, 2011. p.2571–2576.

HEEMELS, W. P. M. H.; JOHANSSON, K. H.; TABUADA, P. An introduction to event-triggered and self-triggered control. In: IEEE CONFERENCE ON DECISION AND CONTROL, 2012, Maui. **Proceedings...** New York: IEEE, 2012. p.3270–3285.

HEMATI, N. Strange attractors in brushless DC motors. **IEEE Transactions on Circuits and Systems I: Fundamental Theory and Applications**, New York, v.41, n.1, p.40–45, Jan. 1994.

HESPANHA, J. P.; NAGHSHTABRIZI, P.; XU, Y. A survey of recent results in networked control systems. **Proceedings of the IEEE**, Piscataway, v.95, n.1, p.138–162, Jan. 2007.

JAVAID, U.; DUJIĆ, D. Arbitrary order generalized state space average modeling of switching converters. In: IEEE ENERGY CONVERSION CONGRESS AND EXPOSITION, 2015, Montreal. **Proceedings...** New York: IEEE, 2015. p.6399–6406.

KHALIL, H. K. **Nonlinear systems**. 2.ed. Upper Saddle River: Prentice Hall, 1996.

KIENER, G.; LEHMANN, D.; JOHANSSON, K. Actuator saturation and anti-windup compensation in event-triggered control. **Discrete Event Dynamic Systems**, New York, v.24, n.2, p.173–197, 2014.

LEHMANN, D.; JOHANSSON, K. H. Event-triggered PI control subject to actuator saturation. **IFAC Proceedings Volumes**, Brescia, v.45, n.3, p.430–435, 2012. 2nd IFAC Conference on Advances in PID Control.

LEHMANN, D.; KIENER, G. A.; JOHANSSON, K. H. Event-triggered PI control: saturating actuators and anti-windup compensation. In: IEEE CONFERENCE ON DECISION AND CONTROL, 2012, Maui. **Proceedings...** New York: IEEE, 2012. p.6566–6571.

LEHMANN, D.; LUNZE, J. Extension and experimental evaluation of an event-based state-feedback approach. **Control Engineering Practice**, Oxford, v.19, n.2, p.101–112, 2011.

LI, S.; XU, B. Co-design of event generator and controller for event-triggered control system. In: CHINESE CONTROL CONFERENCE, 2011, Yantai. **Proceedings...** New York: IEEE, 2011. p.175–179.

LIU, T.; JIANG, Z. A Small-Gain Approach to Robust Event-Triggered Control of Nonlinear Systems. **IEEE Transactions on Automatic Control**, New York, v.60, n.8, p.2072–2085, Aug. 2015.

LORENZ, E. N. Deterministic nonperiodic flow. **Journal of Atmospheric Sciences**, Boston, v.20, p.130–141, 1963.

MAZO, M.; ANTA, A.; TABUADA, P. An ISS self-triggered implementation of linear controllers. **Automatica**, Tarrytown, v.46, n.8, p.1310–1314, 2010.

MOREIRA, L. G. et al. Event-triggered PI control for continuous plants with input saturation. In: AMERICAN CONTROL CONFERENCE, 2016, Boston. **Proceedings...** New York: IEEE, 2016. p.4251–4256.

MOREIRA, L. G. et al. Event-triggered control for nonlinear rational systems. **IFAC-PapersOnLine**, Toulouse, v.50, n.1, p.15307–15312, 2017a. 20th IFAC World Congress.

MOREIRA, L. G. et al. PI event-triggered control under saturating actuators. **International Journal of Control**, West Sussex, p.1–11, 2017b.

MOREIRA, L. G. et al. **Observer-based event-triggered control co-design in the presence of cone-bounded nonlinear inputs**. Submitted to Nonlinear Analysis: Hybrid Systems, 2018a.

MOREIRA, L. G. et al. **Observer-based event-triggered control for systems with sector-bounded nonlinearities**. Submitted to IEEE Transactions on Automatic Control, 2018b.

MOREIRA, L. G.; GROFF, L. B.; GOMES DA SILVA JR., J. M. Event-triggered state-feedback control for continuous-time plants subject to input saturation. **Journal of Control, Automation and Electrical Systems**, New York, v.27, n.5, p.473–484, Oct. 2016.

MOREIRA, L. G.; GROFF, L. B.; GOMES DA SILVA JR., J. M. Event-triggered control for rational plants. In: CONGRESSO BRASILEIRO DE AUTOMÁTICA, 2016, Vitória. **Anais...** Vitória: UFES, 2016.

NĚMCOVÁ, J. Structural identifiability of polynomial and rational systems. **Mathematical Biosciences**, New York, v.223, n.2, p.83–96, 2010.

NEŠIĆ, D.; TEEL, A.; KOKOTOVIĆ, P. Sufficient conditions for stabilization of sampled-data nonlinear systems via discrete-time approximations. **Systems & Control Letters**, Amsterdam, v.38, p.259–270, 1999.

OLIVEIRA, M. Z. **Estabilidade e estabilização de uma classe de sistemas não-lineares sujeitos a saturação**. 2012. 123 p. Thesis (Doutorado em Engenharia Elétrica) – Programa de Pós-Graduação em Engenharia Elétrica, Universidade Federal do Rio Grande do Sul, Porto Alegre, 2012.

OLIVEIRA, M. Z.; GOMES DA SILVA JR., J. M.; COUTINHO, D. State feedback design for rational nonlinear control systems with saturating inputs. In: AMERICAN CONTROL CONFERENCE, 2012, Montreal. **Proceedings...** New York: IEEE, 2012. p.2331–2336.

PALMEIRA, A. H. K.; GOMES DA SILVA JR., J. M.; FLORES, J. V. Regional Stability Analysis of Nonlinear Sampled-Data Control Systems: a quasi-LPV approach. In: EUROPEAN CONTROL CONFERENCE, 2018, Limassol. **Proceedings...** New York: IEEE, 2018.

POSTOYAN, R. et al. Periodic event-triggered control for nonlinear systems. In: IEEE CONFERENCE ON DECISION AND CONTROL, 2013, Florence. **Proceedings...** New York: IEEE, 2013. p.7397–7402.

POSTOYAN, R. et al. A framework for the event-triggered stabilization of nonlinear systems. **IEEE Transactions on Automatic Control**, New York, v.60, n.4, p.982–996, Apr. 2015.

REIMANN, S. et al. Stability analysis and PI control synthesis under event-triggered communication. In: EUROPEAN CONTROL CONFERENCE, 2015, Linz. **Proceedings...** New York: IEEE, 2015. p.2174–2179.

SASTRY, S. **Nonlinear systems**: analysis, stability, and control. New York: Springer, 1999. (Interdisciplinary Applied Mathematics).

SBARBARO, D.; TARBOURIECH, S.; GOMES DA SILVA JR., J. M. An event-triggered observer based control strategy for SISO systems. In: IEEE

CONFERENCE ON DECISION AND CONTROL, 2014, Los Angeles. **Proceedings...** New York: IEEE, 2014. p.2789–2794.

SELIVANOV, A.; FRIDMAN, E. Observer-based input-to-state stabilization of networked control systems with large uncertain delays. **Automatica**, Tarrytown, v.74, p.63–70, 2016.

SEURET, A. A novel stability analysis of linear systems under asynchronous samplings. **Automatica**, Tarrytown, v.48, n.1, p.177–182, 2012.

SEURET, A. et al. Event-triggered control with LQ optimality guarantees for saturated linear systems. In: IFAC SYMPOSIUM ON NONLINEAR CONTROL SYSTEMS, 2013, Toulouse. **Proceedings...** Toulouse: Elsevier, 2013.

SEURET, A.; GOMES DA SILVA JR., J. M. Taking into account period variations and actuators saturation in sampled-data systems. **Systems & Control Letters**, Amsterdam, v.61, n.12, p.1286–1293, Dec. 2012.

SIRA-RAMÍREZ, H.; SILVA-ORTIGOZA, R. **Control design techniques in power electronics devices**. New York: Springer Science & Business Media, 2006.

TABUADA, P. Event-triggered real-time scheduling of stabilizing control tasks. **IEEE Transactions on Automatic Control**, New York, v.52, n.9, p.1680–1685, Sept. 2007.

TALLAPRAGADA, P.; CHOPRA, N. Event-triggered dynamic output feedback control for LTI systems. In: IEEE CONFERENCE ON DECISION AND CONTROL, 2012, Maui. **Proceedings...** New York: IEEE, 2012. p.6597–6602.

TALLAPRAGADA, P.; CHOPRA, N. Decentralized Event-Triggering for Control of Nonlinear Systems. **IEEE Transactions on Automatic Control**, New York, v.59, n.12, p.3312–3324, Dec. 2014.

TARBOURIECH, S. et al. **Stability and stabilization of linear systems with saturating actuators**. London: Springer, 2011.

TARBOURIECH, S. et al. Observer-based event-triggered control co-design for linear systems. **IET Control Theory Applications**, London, v.10, n.18, p.2466–2473, 2016.

TARBOURIECH, S. et al. Observer-based event-triggered control for linear systems subject to cone-bounded nonlinearities. **IFAC-PapersOnLine**, Toulouse, v.50, n.1, p.7893–7898, 2017. 20th IFAC World Congress.

TIBERI, U.; ARAUJO, J.; JOHANSSON, K. H. On event-based PI control of first-order processes. In: IFAC CONFERENCE ON ADVANCES IN PID CONTROL, 2012, Brescia. **Proceedings...** Amsterdam: Elsevier, 2012. p.448–453.

TIBERI, U.; LINDBERG, C.-F.; ISAKSSON, A. J. Dead-band self-triggered PI control for processes with dead-time. In: IFAC CONFERENCE ON ADVANCES IN PID CONTROL, 2012, Brescia. **Proceedings...** Amsterdam: Elsevier, 2012. p.442–447.

TROFINO, A. Robust stability and domain of attraction of uncertain nonlinear systems. In: AMERICAN CONTROL CONFERENCE, 2000, Chicago. **Proceedings...** New York: IEEE, 2000. v.5, p.3707–3711.

TURNER, M.; HERRMANN, G. A non-square sector condition and its application in deferred-action anti-windup compensator design. **Automatica**, Tarrytown, v.50, n.1, p.268–276, 2014.

WU, F. X.; MU, L. Parameter estimation in rational models of molecular biological systems. In: ANNUAL INTERNATIONAL CONFERENCE OF THE IEEE ENGINEERING IN MEDICINE AND BIOLOGY SOCIETY, 2009, Minneapolis. **Proceedings...** New York: IEEE, 2009. p.3263–3266.

WU, W.; REIMANN, S.; LIU, S. Event-triggered control for linear systems subject to actuator saturation. **IFAC Proceedings Volumes**, Cape Town, v.47, n.3, p.9492–9497, 2014. 19th IFAC World Congress.

YAMAMOTO, Y. New approach to sampled-data control systems - a function space method. In: IEEE CONFERENCE ON DECISION AND CONTROL, 1990, Honolulu. **Proceedings...** New York: IEEE, 1990. p.1882–1887.

ZACCARIAN, L.; TEEL, A.-R. **Modern anti-windup synthesis**. New York: Princeton University Press, 2011.

ZHANG, X.; HAN, Q. Event-triggered $H_\infty$ control for a class of nonlinear networked control systems using novel integral inequalities. **International Journal of Robust and Nonlinear Control**, West Sussex, v.27, n.4, p.679–700, 2017.

ZHANG, X. M.; HAN, Q. L.; YU, X. Survey on recent advances in networked control systems. **IEEE Transactions on Industrial Informatics**, New York, v.12, n.5, p.1740–1752, Oct. 2016.

# APPENDIX A DYNAMICAL SYSTEMS STABILITY

One of the most fundamental requirements in control systems is stability. If the closed-loop system is not stable, other usual requirements as, for example, reference tracking, disturbance rejection, etc. cannot be fulfilled. Therefore, this appendix recalls some concepts and theorems related to the stability analysis of dynamical systems.

## A.1 Stability of an equilibrium point

Nonlinear systems, differently from the linear ones, can have many equilibrium points and even other types of critical elements, like periodic trajectories and chaotic attractors. Hence, when nonlinear systems are considered, stability is a concept related to the critical element and not to the entire system (KHALIL, 1996; SASTRY, 1999). In this thesis, only type of critical elements that we are interested in are the equilibrium points. As explained, for instance, in (KHALIL, 1996; SASTRY, 1999), we can study the stability of an arbitrary equilibrium point by applying a change of coordinates that translates the equilibrium of interest to the origin. Thus, we define:

**Definition 2.** *(KHALIL, 1996) Let the origin be an equilibrium point for system* $\dot{x} = f(x)$*, with* $f : \mathcal{D} \to \mathbb{R}^n$ *locally Lipschitz in a domain* $\mathcal{D} \subset \mathbb{R}^n$ *containing the origin. The origin is:*

- *Stable if, for each* $\epsilon > 0$*, there is a* $\delta > 0$ *such that* $||x(0)|| < \delta \implies ||x(t)|| < \epsilon, \forall t \geq 0$.
- *Unstable if it is not stable.*
- *Asymptotically stable if it is stable and* $\delta$ *can be chose such that* $||x(0)|| < \delta \implies \lim_{t\to\infty} x(t) = 0$.

Once one determines that an equilibrium is asymptotically stable, comes the question of how far from this equilibrium one can start a trajectory such that it converges to the equilibrium. This concept leads to the definition of region of attraction:

**Definition 3.** *(KHALIL, 1996) The region of attraction (RA) of the origin (assumed to be the equilibrium being addressed) is the set of all initial states* $x_0 \in \mathbb{R}^n$ *for which* $x(0) = x_0 \implies x(t) \to 0$ *when* $t \to \infty$.

The exact characterization of the region of attraction is, in general a complex task (KHALIL, 1996; GENESIO; TARTAGLIA; VICINO, 1985). Therefore, it is useful to approximate the region of attraction by sets which have analytical representations like ellipsoids and polyhedra (TARBOURIECH et al., 2011). Such sets can be used as estimates

of the region of attraction and are called Regions of Asymptotic Stability (RAS), formally defined as follows:

**Definition 4.** *(TARBOURIECH et al., 2011) A Region of Asymptotic Stability (RAS) of a equilibrium point is a region of the state space that contains the equilibrium and that is a subset of the region of attraction of that equilibrium.*

## A.2 Lyapunov stability criterion

A classical method to analyse the stability of equilibrium points is the direct Lyapunov method, summarized in the following theorem:

**Theorem A.1.** *(KHALIL, 1996) Let $x = 0$ be an equilibrium of system $\dot{x} = f(x)$, with $f : \mathcal{D} \to \mathbb{R}^n$ locally Lipschitz in a domain $\mathcal{D} \subset \mathbb{R}^n$ containing the origin. If there exists a function $V : \mathcal{B} \subset \mathcal{D} \to \mathbb{R}$ continuously differentiable such that:*

$$V(0) = 0; \qquad V(x) > 0, \quad \forall x \neq 0 \tag{A.1}$$

$$\dot{V}(x) < 0, \quad \forall x \neq 0 \tag{A.2}$$

*then $x = 0$ is a asymptotically stable equilibrium.*

A function $V$ that satisfies the conditions in Theorem A.1 is called a Lyapunov function. If $\mathcal{D} = \mathbb{R}^n$, both conditions of the theorem are valid in the entire state space and $V$ has bounded level surfaces [1], the origin is globally asymptotically stable, that is, its region of attraction is the entire state space.

If instead of ensuring (A.2), one can ensure only $\dot{V}(x) \leq 0, \quad \forall x \neq 0$, the origin is guaranteed to be stable. It can still be asymptotically stable and tools like LaSalle's invariance principle can be applied to such cases. More details regarding this topic can be found in (KHALIL, 1996) and (SASTRY, 1999).

## A.3 Regions of asymptotic stability associated to a Lyapunov function

In the context of regional stabilization, i.e. when one cannot ensure the global stability of the origin, estimates of the region of attraction can be obtained from the following criterion:

**Theorem A.2.** *(KHALIL, 1996) Consider a Lyapunov function $V(x)$ satisfying conditions of Theorem A.1 for all $x \in \mathcal{B}$. Then any bounded surface level of $V$, $\mathcal{L}_c = \{x \in \mathbb{R}^n : V(x) \leq c\}$, contained in $\mathcal{B}$ is a region of asymptotic stability of the origin and can be used as an estimate of its region of attraction.*

It is important to note that this estimates are, in general, conservative in the sense that they are smaller than the region of attraction. Moreover, different Lyapunov functions lead to different estimates, with different degrees of conservativeness (KHALIL, 1996).

[1] The level surfaces being limited is guaranteed if $V$ is radially unbounded, i.e., $||x|| \to \infty \implies V(x) \to \infty$.